OFF-ENERGY-SHELL NUCLEAR REACTION MATRIX

ON THE OFF-ENERGY-SHELL BEHAVIOUR OF THE NUCLEAR REACTION MATRIX

By

MAHENDRA KUMAR SRIVASTAVA, B.Sc., M.Sc.

A Thesis

Submitted to the School of Graduate Studies

in Partial Fulfilment of the Requirements

for the Degree

Doctor of Philosophy

McMaster University

March 1970

DOCTOR OF PHILOSOPHY (1970) McMASTER UNIVERSITY
(Physics) Hamilton, Ontario

TITLE: On the Off-energy-shell Behaviour of the Nuclear Reaction Matrix

AUTHOR: Mahendra Kumar Srivastava,
B.Sc., (Agra University)
M.Sc., Physics (Agra University)
M.Sc., Mathematics (Agra University)

SUPERVISOR: Professor D. W. L. Sprung

NUMBER OF PAGES: vi, 164

SCOPE AND CONTENTS:

Even with a good fit to nucleon-nucleon scattering data, there is considerable freedom in the off-energy-shell behaviour of the nuclear reaction matrix because of (1) the unavailability of the elastic scattering data in the high energy region and (2) the assumptions about the non-locality of the interaction. We have investigated off-energy shell behaviour by developing 'super' soft core potentials and several pairs of phase shift equivalent separable, local and momentum dependent potentials. Nuclear matter calculations were done using these potentials in order to study the sensitivity of the binding energy to the differences in the off-energy-shell behaviour. The effective range formula has been extended to the off-energy-shell case.

TO MY PARENTS

ACKNOWLEDGEMENTS

The advice and the guidance of Professor D. W. L. Sprung during the course of this work and throughout my studies at McMaster have been invaluable. Most of the work reported here was done in close cooperation with him.

I am indebted to Professor M. A. Preston for discussions at various stages of this work and for critically going through the manuscript. Thanks are also due to Professor R. K. Bhaduri for many helpful discussions during the course of this work.

I thank Mr. Yogeshwar Singh who helped me in several ways.

The numerical work in this investigation was carried out on the CDC-6400 computer of the McMaster Computing Centre. The cooperative and courteous service of the Computing Centre is highly appreciated.

I am grateful to the Government of Canada for support under the Commonwealth Scholarship and Fellowship Plan and the University of Roorkee, Roorkee, India, for the grant of leave of absence.

Miss Cathy Wivell has very capably and cheerfully typed the manuscript. I thank her very much for this.

Last, but by no means least, I would like to thank my wife for her continual encouragement and her patient endurance of neglect during the final stages of this work.

TABLE OF CONTENTS

		Page
CHAPTER I	INTRODUCTION	1
CHAPTER II	THE TWO BODY SCATTERING PROBLEM	9
CHAPTER III	INVERSE SCATTERING PROBLEM MARCHENKO METHOD	31
CHAPTER IV	SOFT CORE LOCAL POTENTIAL MODELS FOR $^1S_0$ NEUTRON-PROTON INTERACTION AND THEIR OFF-SHELL PROPERTIES	37
CHAPTER V	OFF-ENERGY-SHELL BEHAVIOUR OF PHASE SHIFT EQUIVALENT POTENTIALS	51
CHAPTER VI	SUMMARY AND COMMENTS	91
APPENDIX A	MODIFICATIONS IN THE METHOD OF CHAPTER III FOR THE CASE OF SECOND ORDER POLES	97
APPENDIX B	LOW ENERGY BEHAVIOUR OF OFF-SHELL REACTION MATRIX ELEMENTS	101
REFERENCES		107
FIGURE CAPTIONS		112
FIGURES		120

LIST OF TABLES

		Page
Table 1	Parameters Defining the Potentials SSC and SSC-NP-2	40
Table 2	Perturbation Theory Calculations in Nuclear Matter	46
Table 3	Numerical Values of the Parameters in eq. (V-3.1) for the case I	61
Table 4	Numerical Values of the Parameters in eq. (V-3.2) for the cases II and III	62
Table 5	Parameters Defining the Potentials I-a and I-b	77
Table 6	Parameters Defining the Potentials HJ-a, b, c and d	77
Table 7	Occupied State Energy Spectrum Parameters Δ and m*	82

CHAPTER I

INTRODUCTION

I-1. Any problem in nuclear physics involving three or more particles requires off-energy-shell elements of the nuclear reaction matrix K, i.e., of $\langle \underset{\sim}{p}_1, \underset{\sim}{p}_2 | K | \underset{\sim}{p}'_1, \underset{\sim}{p}'_2 \rangle$ where $E = \frac{p_1^2}{2m} + \frac{p_2^2}{2m} \neq E' = \frac{p_1'^2}{2m} + \frac{p_2'^2}{2m}$. These can be determined uniquely only if the nuclear potential is fully known. Our present information about it comes mainly from the properties of the deuteron and the analysis of the two particle elastic scattering data. Since there are about 1000 items of data, differential cross-section measurements, polarisation, correlation and triple scattering measurements at various energies and angles, it is clear that these data are quite detailed. Nevertheless the data determine the partial wave scattering amplitudes up to only about 350 MeV laboratory energy. Equivalently one can say that they determine the on-energy-shell reaction matrix (E=E') or the phase shifts in the same range. Beyond this, in the high energy region, the data are incomplete and largely inaccurate. Furthermore, analysis becomes difficult because of a large number of partial waves taking part in the scattering process and because of the diffraction effects due to pion production. Therefore in practice the available information about the scattering

parameters is phenomenologically extrapolated to the high energy region by imposing various model constraints. This introduces uncertainty in the nuclear forces particularly at small distances.

Even if the data were determined unambiguously at all energies by high precision elastic scattering experiments, the interaction can be determined uniquely (in the absence of any bound state) only if it is assumed to be local or having a specified form of non-locality. There can be infinitely many types of non-locality of the interaction which correspond to the different off-energy-shell extensions of the K-matrix, even if on-energy-shell they are all equivalent, i.e., correspond to the same phase shifts. If a particular nuclear process involves matrix elements which are strongly off-energy-shell, then theoretical predictions for that process will be strongly dependent on the potential model used in the calculation.

We have studied how far these two limitations (1) the absence of the data in the high energy region and (2) the assumptions about the non-locality of the interaction, affect the off-energy-shell behaviour of the reaction matrix elements and to what extent the differences in this behaviour are reflected in the physical properties.

In the next section we review the procedures used to investigate the off-shell* behaviour for various types of

---

* For ease of writing we shall speak of on-energy-shell and off-energy-shell matrix elements as on-shell and off-shell matrix elements respectively.

interactions. We also indicate in what respects our attempt differs from others. Section I-3 gives the general plan followed in the thesis.

I-2. In principle, inelastic experiments such as electron-deuteron scattering, deuteron photo-disintegration, neutron-deuteron scattering, proton-proton bremsstrahlung, etc. which depend on the off-shell behaviour could serve as a starting point to determine the various features of the nuclear interaction. But these experiments have been performed only at very few energies and are not far off-shell. There is another difficulty in attempting an explicit parameterization of the reaction matrix based on its off-shell behaviour: the analytic properties of the off-shell reaction matrix are not fully known.

One, therefore, follows the alternative of choosing a potential which provides a good description of the available nucleon-nucleon data and then calculates the off-shell matrix elements via the Lippmann Schwinger equation. These matrix elements are then used in calculations involving off-shell behaviour in an attempt to distinguish between different potentials and find criteria for favouring a particular one. This approach can be supplemented by theoretical guidance as to the terms to be included[1-5] in the potential, for example at large distances it must agree with the one pion exchange potential (OPEP). This

procedure naturally has inherent limitations, since it seeks to generate a function of two variables (the initial momentum k_i and the final momentum k_f, $k_i \neq k_f$) starting from its values on a part of the $k_i=k_f$ line in the $k_i k_f$-plane. As a result, many potentials[6-12] have been proposed. They differ, partly, in the assumption they make about the on-shell matrix elements at high energies where the data do not exist (e.g. hard core, Yukawa core and finite square core local potentials) and partly in the form of non-local interaction assumed (purely local or momentum dependent). Separable potentials[13-21] have also been used because of the simplicity they bring to the calculations. They have the additional advantage that the reaction matrix elements can sometimes be written as specific functions of the potential parameters rather than only occuring as numbers in the computer output. The requirements of time reversal invariance, off-shell unitarity and the condition of reduction to on-shell analytic properties of the partial wave scattering amplitude can be easily satisfied and do not put any significant restrictions on the form of the potential.

A number of calculations[22-26] involving off-shell matrix elements have been done using different potentials. These calculations are difficult enough so that when two potentials are compared one does not know whether to ascribe the different results to different approximations in the calculation, to different on-shell behaviour, or to different

forms of non-locality (and therefore different off-shell extensions). This realization has prompted a direct comparison of the off-shell reaction matrix elements.

Laughlin and Scott[27] have studied some local potentials in the $\ell=0$ state to see the effect of the hard core. These potentials were designed to fit only the low energy data (up to about 10 MeV laboratory energy).

In order to compare potentials which may not agree on the energy shell it has been proposed to use the Kowalski-Noyes[28,29] half-shell function $f_\ell(p,k) = t_\ell(p,k;k^2)/t_\ell(k,k;k^2)$ instead of $t_\ell(p,k;k^2)$. The differences in on-shell behaviour are thereby compensated. Mongan[30] used this function for comparing several potentials.

We have developed very soft local potentials for the neutron-proton scattering in the $^1S_0$ state. These are based on a high energy phase shift extrapolation radically different from that of the other local potentials. We studied their off-shell properties and their implications in relation to other local and non-local potential models.

In these comparisons it is difficult to identify a particular feature with the high energy on-shell behaviour of the model assumed or with its off-shell properties. The former can be isolated from the latter if the potentials used correspond to precisely the same S-matrix at all energies. That infinitely many such potentials exist was pointed out by H. Ekstein[31]. Three practical methods have

been proposed to construct phase shift equivalent potentials. In the one proposed by Fiedeldey[32], a set of equivalent second rank separable potentials is obtained by choosing, rather arbitrarily, one of the form factors and calculating the other from the on-shell data. Another approach has been followed by Coester[33] et. al. They have chosen the unitary operator of Ekstein to be an operator of rank two. Starting from a local potential, this produces a short range non-locality. A third method is to construct a family of equivalent* p^2-dependent potentials generated by isometric point transformations**[34-36]. In this method one picks a fairly arbitrary function $v_2(r)$ and constructs a corresponding function $v_1(r)$ such that

$$v(r) = v_1(r) + p^2 v_2(r) + v_2(r) p^2$$

reproduces the phase shift of a given static potential. Different choices of $v_2(r)$ give different equivalent potentials. Such potentials have been used in nuclear matter[33,37,38], proton-proton bremsstrahlung[38] and deuteron photo-disintegration[39] studies, but no systematic comparison of their off-shell behaviour has been done so far. We study this behaviour in relation to the equivalent local potential and as a function of the strength and the range

---

* phase shift (or on-shell) equivalent.

** These are unitary transformations induced by the distortions of the radial scale. Details are given in Section V-5.

of the p^2-dependent term.

In addition we have followed a different procedure of obtaining equivalent potentials. Starting with a specified S-matrix, we analytically construct pairs of non-local separable and local interactions. This method generates only one pair of equivalent potentials, but because the separable force is in a sense "very" non-local it is an interesting comparison. By combining our procedure with that of the isometric point transformations and the method proposed by Fiedeldey, one can generate and compare the off-shell behaviour of a family of separable potentials, a local potential and a family of p^2-dependent potentials; all being equivalent on the energy shell. Such comparisons, naturally, are useful only in conjunction with many-body calculations, so that one can discover what sort of off-shell properties lead to particular physical effects.

I-3. In Chapter II we outline the two body scattering theory, enumerate the analytic properties of the Jost functions, the scattering amplitude etc. for the case of local and non-local (separable) potentials, discuss the separable approximation of Noyes to the off-shell transition matrix and present the method used to calculate the off-shell reaction matrix elements. Chapter III contains explicit details of Marchenko's method for constructing a local potential from a rational S-matrix having simple poles in the upper half k-plane. Generalization for the case of higher

order poles is given in Appendix A. These two chapters present the necessary apparatus which is used in Chapters IV and V. In Chapter IV we construct two soft potentials for n-p scattering in the $^1S_0$ state and discuss the possible implications of the differences in their off-shell properties. In Chapter V we present a procedure to obtain in the $^1S_0$ state a local potential which corresponds to precisely the same S-matrix as a given separable potential. We also use isometric point transformations to construct p^2-dependent potentials. The off-shell properties of such equivalent potentials are then studied. Chapter VI contains the summary and general comments.

In Appendix B we have presented a detailed investigation of the low energy behaviour of off-shell reaction matrix elements.

CHAPTER II

THE TWO BODY SCATTERING PROBLEM

This chapter is devoted to the basic ground work. In Sections II-1 and II-2 we briefly review the ordinary scattering theory and give the analytic properties of the scattering matrix, etc. In Sections II-3 and II-4 we define the off-shell transition and reaction matrices, give their analytic structure and introduce the separable approximation of Noyes. In Section II-5 we present the method used to calculate the off-shell reaction matrix elements for the local and p^2-dependent interactions.

II-1. Introduction

The two particle Schroedinger equation, in the centre of mass system, may be written as

$$(\nabla^2+k^2)\ \Psi_{\underset{\sim}{k}}(\underset{\sim}{r}) = \int \langle \underset{\sim}{r}|V|\underset{\sim}{r}'\rangle\ \Psi_{\underset{\sim}{k}}(\underset{\sim}{r}')d\underset{\sim}{r}' \qquad ,(II1.1)$$

where $\underset{\sim}{r}$ and $\underset{\sim}{r}'$ are the relative coordinates. The potential times $m/\hbar^2$ is V and $2\hbar^2k^2/m$ is the energy of the incident particle in the laboratory frame. The nucleon mass or more precisely twice the reduced mass of the nucleon pair is m. In momentum space, absorbing factors of 2π into the

potential, eq. (II-1.1) can be written as

$$(\underset{\sim}{k}^2-\underset{\sim}{p}^2)\ \Psi_{\underset{\sim}{k}}(\underset{\sim}{p}) = \int \langle \underset{\sim}{p}|V|\underset{\sim}{p}'\rangle\ \Psi_{\underset{\sim}{k}}(\underset{\sim}{p}')\,d\underset{\sim}{p}' \qquad .(II\text{-}1.2)$$

For the purpose of scattering theory it is convenient to replace this by the Lippmann Schwinger integral equation, which incorporates the boundary condition that at large distances the wave function consists of a plane wave plus an outgoing spherical wave

$$|\Psi_{\underset{\sim}{k}}^{(+)}\rangle = |\underset{\sim}{k}\rangle + (k^2-H_0+i\varepsilon)^{-1}\ V|\Psi_{\underset{\sim}{k}}^{(+)}\rangle \qquad .(II\text{-}1.3)$$

H_0 is the kinetic energy in units of $m/\hbar^2$. The superscript '+' on Ψ indicates an outgoing solution. The usual definitions[40] of the S-matrix and the transition matrix T are

$$\langle \underset{\sim}{p}|S|\underset{\sim}{k}\rangle = \langle \Psi_{\underset{\sim}{p}}^{(-)}|\Psi_{\underset{\sim}{k}}^{(+)}\rangle$$

$$= \langle \underset{\sim}{p}|\underset{\sim}{k}\rangle - 2\pi i\delta(p^2-k^2)\ \langle \underset{\sim}{p}|T|\underset{\sim}{k}\rangle, |\underset{\sim}{p}| = |\underset{\sim}{k}| \qquad (II\text{-}1.4)$$

with

$$\langle \underset{\sim}{p}|T|\underset{\sim}{k}\rangle = \langle \underset{\sim}{p}|V|\Psi_{\underset{\sim}{k}}^{(+)}\rangle$$

$$= \langle \underset{\sim}{p}|V|\underset{\sim}{k}\rangle + \langle \underset{\sim}{p}|V\ \frac{1}{k^2-H_0+i\varepsilon}\ V|\Psi_{\underset{\sim}{k}}^{(+)}\rangle \qquad .(II\text{-}1.5)$$

For a spherically symmetric potential, Ψ and T have partial

wave expansions. Ignoring the possible tensor force , we get*

$$\langle \underset{\sim}{r}|\underset{\sim}{k}\rangle = \sum_{\ell=0}^{\infty} i^{\ell}\,(2\ell+1)\,\frac{\mathcal{J}_{\ell}(kr)}{kr}\,P_{\ell}(\cos\theta_{kr}) \qquad \text{(II-1.6)}$$

$$\langle \underset{\sim}{r}|\Psi_{\underset{\sim}{k}}^{(+)}\rangle = \sum_{\ell=0}^{\infty} i^{\ell}\,(2\ell+1)\,\frac{\psi_{\ell}^{(+)}(k,r)}{kr}\,P_{\ell}(\cos\theta_{kr}) \qquad \text{(II-1.7)}$$

$$\langle \underset{\sim}{p}|T|\underset{\sim}{k}\rangle = \frac{1}{2\pi^2}\sum_{\ell=0}^{\infty}(2\ell+1)\,t_{\ell}(p,k;k^2)\,P_{\ell}(\cos\theta_{pk}) \qquad \text{(II-1.8)}$$

where $\mathcal{J}_{\ell}(z)$, the Ricatti Bessel function of the first kind, is given by

$$\mathcal{J}_{\ell}(z) = z\,j_{\ell}(z) = \sqrt{\frac{\pi z}{2}}\,J_{\ell+\frac{1}{2}}(z) \quad ,$$

and

$$t_{\ell}(p,k;k^2) = \frac{1}{pk}\int_0^{\infty}\mathcal{J}_{\ell}(kr)\,V\,\psi_{\ell}^{(+)}(k,r)\,dr \quad .$$

Asymptotically,

$$\mathcal{J}_{\ell}(kr) \rightarrow \sin(kr-\ell\pi/2)$$

$$\psi_{\ell}^{(+)}(k,r) \rightarrow \sin(kr-\ell\pi/2) + e^{i\delta_{\ell}(k)}\sin\delta_{\ell}(k)\,e^{i(kr-\ell\pi/2)} \qquad \text{(II-1.9)}$$

---

* The factor $\frac{1}{2\pi^2}$ in the expansion for $\langle \underset{\sim}{p}|T|\underset{\sim}{k}\rangle$ sets our normalization such that the on-shell t_{ℓ}-matrix

$$t_{\ell}(k,k;k^2) = -\,e^{i\delta_{\ell}(k)}\sin\delta_{\ell}(k)/k.$$

The partial wave Lippmann Schwinger equation is

$$\psi_\ell^{(+)}(k,r) = \mathcal{J}_\ell(kr) + \frac{2}{\pi}\int_0^\infty \frac{\mathcal{J}_\ell(qr)\ t_\ell(q,k;k^2)}{k^2-q^2+i\varepsilon}\, q^2 dq \quad .(II\text{-}1.10)$$

Although T was introduced only for $|\underset{\sim}{p}| = |\underset{\sim}{k}|$ in eq. (II-1.4), it is convenient to define it for $|\underset{\sim}{p}| \neq |\underset{\sim}{k}|$ also, so that eq. (II-1.5) can be written as

$$\langle \underset{\sim}{p}|T(\omega)|\underset{\sim}{k}\rangle = \langle \underset{\sim}{p}|V|\underset{\sim}{k}\rangle + \langle \underset{\sim}{p}|V\,\frac{1}{\omega-H_0}\,T(\omega)|\underset{\sim}{k}\rangle \quad .(II\text{-}1.11)$$

The on-shell T matrix required in eq. (II-1.5) is obtained when $\omega \to k^2+i\varepsilon$. This is why the partial wave t_ℓ-matrix has been given three parameters.

The scattering state wave function $\psi_\ell^{(+)}(k,r)$ can be expressed in terms of the so called Jost solutions:

$$\psi_\ell^{(+)}(k,r) = \frac{e^{\ell\pi i/2}}{2i\ f_\ell(-k)}\,(f_\ell(k)\ f_\ell(-k,r) - f_\ell(-k)\ f_\ell(k,r)) \quad .(II\text{-}1.12)$$

The Jost solutions $f_\ell(\pm k,r)$ are the solutions of the radial Schroedinger equation

$$u''(r) + \left(k^2 - \frac{\ell(\ell+1)}{r^2} - V(r)\right) u(r) = 0 \quad ,(II\text{-}1.13)$$

with simple exponential behaviour at large r, i.e.,

$$\lim_{r\to\infty} e^{\pm ikr}\ f_\ell(\pm k,r) = 1 \quad ,(II\text{-}1.14)$$

and the Jost functions $f_\ell(\pm k)$ are defined by the Wronskian $W(f_\ell, \phi_\ell)$

$$f_\ell(\pm k) = W(f_\ell(\pm k,r),\ \phi_\ell(k,r))$$

$$= f_\ell(\pm k,r)\ \phi'_\ell(k,r) - f'_\ell(\pm k,r)\ \phi_\ell(k,r)$$

$$= (2\ell+1) \lim_{r\to 0} r^\ell\ f_\ell(\pm k,r) \qquad ,(II\text{-}1.15)$$

where $\phi_\ell(k,r)$ is another solution of eq. (II-1.13) defined by the boundary condition at the origin

$$\phi_\ell(k,r) \xrightarrow{r=0} r^{\ell+1} \qquad .(II\text{-}1.16)$$

It can be shown[41] that the Jost function $f_\ell(-k)$ is the Fredholm determinant of the Lippmann Schwinger equation for the ℓth partial wave.

From eqs. (II-1.9), (II-1.12) and (II-1.14) the phase shift is given by

$$S_\ell(k) = \frac{f_\ell(k)}{f_\ell(-k)}\ e^{i\ell\pi} = e^{2i\delta_\ell(k)}$$

since

$$\psi_\ell^{(+)}(k,r) \to \frac{1}{2i}(S(k)\ e^{i(kr-\ell\pi/2)} - e^{-i(kr-\ell\pi/2)}) \text{ as } r\to\infty \qquad .(II\text{-}1.17)$$

The usual scattering amplitude is then

$$F(k, \cos\theta) = -\sum_{\ell=0}^{\infty} (2\ell+1)\ t_\ell(k,k;k^2)\ P_\ell(\cos\theta) \qquad ,(II\text{-}1.18)$$

with

$$t_\ell(k,k;k^2) = \frac{1}{2ik}(1-S(k))$$

$$= -\frac{1}{k} e^{i\delta_\ell(k)} \sin \delta_\ell(k) \qquad \text{(II-1.19)}$$

being the on-shell t_ℓ-matrix element.

When $\langle \underset{\sim}{r}|V|\underset{\sim}{r}'\rangle$ is a separable potential the Lippmann Schwinger equation can be solved explicitly. We write the potential in the rotationally invariant form

$$\langle \underset{\sim}{p}|V|\underset{\sim}{k}\rangle = \frac{\hbar^2}{m} \frac{1}{2\pi^2} \sum_{\ell=0}^{\infty} (2\ell+1) \sum_{i=1}^{N_\ell} \sigma_{i\ell}\, g_{i\ell}(p)\, g_{i\ell}(k)\, P_\ell(\cos\theta_{pk}) \qquad \text{(II-1.20)}$$

The sign factor $\sigma_{i\ell}$ is -1 for an attractive component and +1 for a repulsive component. The Lippmann Schwinger equation for the ℓth partial wave becomes (k is initial momentum)

$$\psi_\ell^{(+)}(k,p) = \delta(p-k) + \frac{2}{\pi} \int_0^\infty dq\, pq \sum_{i=1}^{N_\ell} \frac{\sigma_{i\ell}\, g_{i\ell}(p)\, g_{i\ell}(q)}{k^2-p^2+i\varepsilon} \psi_\ell^{(+)}(k,q) \qquad \text{(II-1.21)}$$

Dropping now the index ℓ, we define

$$G_{ij}^{(+)}(k) = -\frac{2}{\pi} \int_0^\infty \frac{\sqrt{\sigma_i}\,\sqrt{\sigma_j}\, g_i(q)\, g_j(q)}{k^2-q^2+i\varepsilon} q^2 dq \qquad \text{(II-1.22)}$$

The solution of eq. (II-1.21) can now be written as

$$\psi_\ell^{(+)}(k,p) = \delta(p-k) + [\det|\delta_{ij} + G_{ij}^{(+)}(k)|]^{-1}$$

$$\times \sum_{i,j=1}^{N_\ell} \frac{\sqrt{\sigma_i}\,\sqrt{\sigma_j}\; g_i(p)\; g_j(k)}{k^2-p^2+i\varepsilon}\; pk\; d\binom{j}{i} \quad , \text{(II-1.23)}$$

where $d\binom{j}{i}$ is cofactor of the element $\delta_{ji} + G_{ji}^{(+)}(k)$ in the determinant $|\delta_{ij} + G_{ij}^{(+)}(k)|$. Noting that the scattered wave in momentum space is $t_\ell(p,k;k^2)/(k^2-p^2+i\varepsilon)$, we see

$$t_\ell(p,k;k^2) = \sum_{i,j=1}^{N_\ell} \frac{\sqrt{\sigma_{i\ell}}\,\sqrt{\sigma_{j\ell}}\; g_{i\ell}(p)\; g_{j\ell}(k)}{\det|\delta_{ij} + G_{ij,\ell}^{(+)}(k)|}\; d\binom{j}{i}_\ell \quad . \text{(II-1.24)}$$

Fully off-shell t_ℓ-matrix element is given by

$$t_\ell(p,q;k^2) = \sum_{i,j=1}^{N_\ell} \frac{\sqrt{\sigma_{i\ell}}\,\sqrt{\sigma_{j\ell}}\; g_{i\ell}(p)\; g_{j\ell}(q)}{\det\,|\,\delta_{ij} + G_{ij,\ell}^{(+)}(k)\,|}\; d\binom{j}{i}_\ell \qquad \text{(II-1.25)}$$

and the Jost function by

$$f_\ell(-k) = \det|\delta_{ij} + G_{ij,\ell}^{(+)}(k)| \quad . \text{(II-1.26)}$$

For a single term separable potential eq. (II-1.25) reduce to:

$$t_\ell(p,q;k^2) = \sigma_\ell g_\ell(p)\; g_\ell(q)/[1 + \frac{2\sigma_\ell}{\pi}\int_0^\infty \frac{g_\ell^2(k')}{k'^2-k^2-i\varepsilon}\; k'^2 dk'] \qquad \text{(II-1.27)}$$

II-2. Analytic Properties

The Jost function $f_\ell(k)$, the S-matrix and the partial wave t_ℓ-matrix elements can be considered as functions of complex variables. Their analytic properties naturally depend upon the nature of the potential, and have been studied in detail for local forces[42]. We here summarise the well known results which have been proved.

Consider the on-shell partial wave scattering amplitude $t_\ell(\omega=k^2) = \frac{1}{2ik}(1-S(k))$, in the absence of bound states. In the complex ω-plane it (i) has a branch cut of order two from $\omega=0$ to $+\infty$, the physical value being the one on the upper edge of the cut, and (ii) tends to zero as $\omega\to\infty$ except for hard core potentials. "Driving singularities", representing the interaction, exist on the lower or unphysical sheet of the cut ω-plane. For example, for a Yukawa potential of range μ^{-1}, there is a branch cut $-\infty<\omega<-\mu^2/4$ while for a potential which is expressed as a finite sum of exponentials the dynamical left hand cut degenerates into a sequence of poles commencing at $-\mu^2/4$.The Jost function $f_\ell(-k)$ is analytic in the upper half k-plane. A zero of $f_\ell(-k)$ on the positive imaginary axis would represent a bound state. The singularities of $f_\ell(-k)$ in the lower half k-plane are the potential or driving singularities.

The potentials we will consider, the extended Bargmann class, have a rational S-matrix. The Jost function $f_\ell(-k)$ is meromorphic in the lower half k-plane. In general, the

range of the potential is determined by the smallest imaginary part of one of the potential singularities as in the exponential example. The analytic properties of $f_\ell(k)$ follow from the reflection relation

$$f_\ell(k^*) = f_\ell^*(-k) \qquad \text{(II-2.1)}$$

From this it follows that zeros of $f_\ell(k)$ on the real axis make $f_\ell(-k)$ vanish as well, giveing $S(k)$ the indeterminate form 0/0. This property was exploited by Tabakin[17] to form his single term separable potential, our case III below. The wave function and half-shell t_ℓ-matrix are well behaved in such a case. If Im $f_\ell(k)$ has an m^{th} order zero and Re $f_\ell(k)$ an n^{th} order zero at some real $k=k_c$ value, $t_\ell(k)$ will pass through zero at $k=k_c$ if $m>n$ and the phase shift will 'change sign' if $m-n$ is odd. This corresponds, however, to having a bound state in the continuum[43].

Gutkowski and Scalia[44] have studied analytic properties for the case of a separable potential. They showed that the Jost function $f_\ell(-k)$, given by $\det|\delta_{ij}+G^{(+)}_{ij,\ell}(k)|$, is again analytic in the upper half k-plane, has no zeros there in the absence of bound states, can be considered as the Fredholm determinant of the Lippmann Schwinger equation, is meromorphic in the lower half k-plane and satisfies the relationship eq. (II-2.1), provided (i) the form factors $g_{i\ell}(p)$ are nonsingular and real for real p (ii) there exists a unique analytic continuation of $g_{i\ell}(p)$ into the complex

p-plane, such continuation being an even meromorphic function of p, and (iii)

$$\lim_{|\bar{k}|\to\infty} \int_C g_{i\ell}(k)\, g_{j\ell}(k)\, dk = 0 \qquad \text{(II-2.2)}$$

along a semi-circle C of radius $\bar{k}$ is the upper half k-plane. The separable potentials we study here belong to this class, as do any others of which we are aware.

II-3. The Off-Shell Reaction Matrix

The off-shell T operator was defined by the equation

$$T(z) = V + V(z-H_o+i\varepsilon)^{-1}\, T(z)\ , \qquad \text{(II-3.1)}$$

whose formal solution is

$$T(z) = V + V(z-H+i\varepsilon)^{-1}\, V\ , \qquad \text{(II-3.2)}$$

where $H = H_o+V$. In the partial wave representation of Section II-1, these relations become

$$T\ (p,k;z) = v_\ell(p,k) + \frac{2}{\pi}\int_o^\infty \frac{v_\ell(p,q)\ t_\ell(q,k;z)}{z - q^2 + i\varepsilon}\, q^2dq \qquad \text{(II-3.3)}$$

$$= v_\ell(p,k) + \frac{2}{\pi}\int_o^\infty \frac{t_\ell(p,q;q^2)\ t_\ell^*(k,q;q^2)}{z - q^2 + i\varepsilon}\, q^2dq \qquad \text{(II-3.4)}$$

In eq. (II-3.4) we have assumed that there is no bound state in the ℓ th partial wave. For a fixed z and for a hermitian

potential, t_ℓ is symmetric in p and k. It is real for $z<0$ and satisfies the off-shell unitarity relation

$$\text{Im } t_\ell(p,q;k^2) = -kt_\ell(p,k;k^2)\ t^*_\ell(q,k;k^2)\ ,\ k^2>0 \qquad \text{(II-3.5)}$$

The phase shifts are related to the on-shell value by the relation

$$t_\ell(k,k;k^2) = -e^{i\delta_\ell(k)} \sin\delta_\ell(k)/k \equiv t_\ell(k) \qquad \text{(II-3.6)}$$

In a practical calculation it is more convenient to calculate the reaction matrix $K_\ell(p,k;z)$ which is defined for real z by the corresponding equation with a principal value integral

$$K_\ell(p,k;z) = v_\ell(p,k) + \frac{2}{\pi} P \int_0^\infty \frac{v_\ell(p,q)\ K_\ell(q,k;z)}{z - q^2}\, q^2dq \qquad \text{(II-3.7)}$$

One can then find t_ℓ from the Heitler damping equation*

$$t_\ell(p,q;k^2) = K_\ell(p,q;k^2) - ik\theta(k^2)\ K_\ell(p,k;k^2)\ t_\ell(q,k;k^2)$$

giving[45] (II-3.8)

$$t_\ell(p,q;k^2) = K_\ell(p,q;k^2) - \frac{ik\theta(k^2)\ K_\ell(p,k;k^2)\ K_\ell(q,k;k^2)}{1 + ik\ K_\ell(k,k;k^2)} \qquad \text{(II-3.9)}$$

The inverse relation is

$$K_\ell(p,q,k^2) = t_\ell(p,q;k^2) + \frac{ik\theta(k^2)\ t_\ell(p,k;k^2)\ t_\ell(q,k;k^2)}{i - ik\ t_\ell(k,k;k^2)} \qquad \text{(II-3.10)}$$

---

* The symbol $\theta(x)$ defines the step function $\frac{1}{2}(1 + x/|x|)$.

Eqs. (II-3.9) and (II-3.10) are the generalizations of the on-shell relation

$$t_\ell(k,k;k^2) = \frac{K_\ell(k,k;k^2)}{1+ik\,K_\ell(k,k;k^2)} \qquad \text{(II-3.11)}$$

and show that K_ℓ will be separable in initial and final momenta if t_ℓ is so. It also follows from them that the half-shell matrix elements $t_\ell(p,k;k^2)$ have a common phase factor $e^{i\delta_\ell(k)}$.

The reaction matrix is real and hermitian and its on-shell value is related to the phase shifts by

$$K_\ell(k,k;k^2) = -\tan\delta_\ell(k)/k \equiv K_\ell(k) \qquad \text{(II-3.12)}$$

$K_\ell(k)$ has no cut from 0 to $+\infty$ along the real axis in the z $(=k^2)$ plane and has poles in z at the actual position of resonances and not on the unphysical sheet as is the case with $t_\ell(k)$ [46].

The fully off-shell t_ℓ-matrix elements can be expressed in terms of the half-shell ones. This follows at once from eq. (II-3.4) by considering one half-shell and one off-shell case:

$$t_\ell(p,q;k^2) = t_\ell(p,q;q^2) + \frac{2}{\pi}\int_0^\infty t_\ell(p,h;h^2)\; t_\ell^*(q,h;h^2)$$

$$\times\left(\frac{1}{k^2-h^2+i\varepsilon} - \frac{1}{q^2-h^2+i\varepsilon}\right)h^2dh \qquad \text{(II-3.13)}$$

Such a relation is not surprising because according to eq. (II-1.10) the half-shell matrix elements completely determine the scattering wave function at each energy, which should constitute a complete knowledge of the system in the absence of any bound state.

II-4. Separable Approximation

The calculations become much easier if the matrix elements $K_\ell(p,k;z)$ are separable in the initial and final momenta p,k. For example the kernel of the Faddeev equations becomes separable. In this section we consider the possibility of approximating the K_ℓ-matrix by a factorable form. Several different factorable forms[47-50] have been studied with a view to practical applications. If the potential is separable, the reaction matrix obtained from it has this characteristic. For a single term separable potential, it is of the form $g(p)\ D(z)\ g(k)$.

Noyes[29] has proposed a simple approximation t_ℓ^N for the t_ℓ-matrix of a local potential. It may be derived by using the unitarity relation (eq. (II-3.5)) in eq. (II-3.13) as follows: We write the factor $h\ t_\ell(p,h;h^2)\ t_\ell^*(q,h;h^2)$ on the R.H.S. of eq. (II-3.13) as

$$h\ t_\ell(p,h;h^2)\ t_\ell^*(q,h;h^2) = h\ f_\ell(p,h)\ f_\ell(q,h)\ |t_\ell(h)|^2$$

$$= -\ f_\ell(p,h)\ f_\ell(q,h)\ \mathrm{Im}\ t_\ell(h)$$

$$= -\frac{1}{2i} f_\ell(p,h)\ f_\ell(q,h)[t_\ell(h)-t^*_\ell(h)]$$

$$= -\frac{1}{2i} f_\ell(p,h)\ f_\ell(q,h)[t_\ell(h)-t_\ell(-h)]$$

$$= -\frac{1}{2i}[f_\ell(p,h)\ f_\ell(q,h)\ t_\ell(h)$$

$$- f_\ell(p,-h)\ f_\ell(q,-h)\ t_\ell(-h)]$$

to obtain

$$t_\ell(p,q;k^2) = t_\ell(p,q;q^2) + \frac{1}{\pi i}\int_{-\infty}^{\infty} f_\ell(p,h)\ f_\ell(q,h)\ t_\ell(h)$$

$$\times \left(\frac{1}{q^2-h^2+i\varepsilon} - \frac{1}{k^2-h^2+i\varepsilon}\right)hdh$$

$$= t_\ell(p,q;q^2) + \frac{1}{\pi i}\int_{-\infty}^{\infty} \frac{t_\ell(p,h;h^2)\ t_\ell(q,h;h^2)}{t_\ell(h,h;h^2)}$$

$$\times \left(\frac{1}{q^2-h^2+i\varepsilon} - \frac{1}{k^2-h^2+i\varepsilon}\right)hdh \qquad .(II-4.1)$$

In the above we have used[29]

$$f_\ell(p,h) = (-1)^\ell f_\ell(p,-h) \qquad (II-4.2)$$

and

$$t^*_\ell(k) = t_\ell(-k) \qquad .$$

In eq. (II-4.1), if we consider only the δ-function contributions from the poles at $h=k+i\varepsilon$ and $h=q+i\varepsilon$, we get the

Noyes approximation

$$t_\ell(p,q;k^2) \simeq t_\ell^N(p,q;k^2) = \frac{t_\ell(p,k;k^2)\ t_\ell(q,k;k^2)}{t_\ell(k,k;k^2)} \quad .(II-4.3)$$

Noyes showed that the exact t_ℓ may be written as this plus a term which vanishes when either p or q takes the value k. As an approximation, it has the virtue of being unitary and is trivially correct for half-shell matrix elements. It is exact at poles on the negative real z ($=k^2$) axis and at resonances on the unphysical sheet.

II-5. Calculation of Off-shell Reaction Matrix Elements

A. Local Potential

We solve the equation

$$K(z) = v + v\,\frac{P}{z-H_0}\,K(z) \qquad (II-5.1)$$

in the coordinate space. Introducing a wave function $|\Psi_{\underset{\sim}{k}z}\rangle$ such that

$$K(z)\,|\underset{\sim}{k}\rangle = v|\Psi_{\underset{\sim}{k}z}\rangle \quad ,(II-5.2)$$

we get

$$|\Psi_{\underset{\sim}{k}z}\rangle = |\underset{\sim}{k}\rangle + \frac{P}{z-H_0}\,v|\Psi_{\underset{\sim}{k}z}\rangle \quad ,(II-5.3)$$

$$(H_0+v-z)\,|\Psi_{\underset{\sim}{k}z}\rangle = (H_0-z)\,|\underset{\sim}{k}\rangle = (k^2-z)\,|\underset{\sim}{k}\rangle \quad .(II-5.4)$$

In the coordinate space, it is

$$(-\nabla^2+v-z)\ \Psi_{\underset{\sim}{k}z}(\underset{\sim}{r}) = (k^2-z)e^{i\underset{\sim}{k}\cdot\underset{\sim}{r}} \qquad .(II-5.5)$$

Using the partial wave expansion (II-1.6), we write, ignoring the tensor force

$$\Psi_{\underset{\sim}{k}z}(\underset{\sim}{r}) = \sum_{\ell=0}^{\infty} i^{\ell}(2\ell+1)\ \frac{\psi_{\ell}(k,z,r)}{kr}\ P_{\ell}(\cos\theta_{kr}) \qquad (II-5.6)$$

$$\langle \underset{\sim}{p}|K(z)|\underset{\sim}{k}\rangle = \frac{1}{2\pi^2}\sum_{\ell=0}^{\infty}(2\ell+1)\ K_{\ell}(p,k;z)\ P_{\ell}(\cos\theta_{pk}), \qquad (II-5.7)$$

where

$$K_{\ell}(p,k;z) = \frac{1}{p\ k}\int_0^{\infty} \mathcal{J}_{\ell}(pr)\ v(r)\ \psi_{\ell}(k,z,r)\,dr \qquad (II-5.8)$$

and the wave function $\psi_{\ell}(k,z,r)$ satisfies

$$\left(\frac{d^2}{dr^2} + z - v(r) - \frac{\ell(\ell+1)}{r^2}\right)\ \psi_{\ell}(k,z,r) = (z-k^2)\ \mathcal{J}_{\ell}(kr). \qquad (II-5.9)$$

At the origin, or inside a hard core, ψ_{ℓ} vanishes. At large r the behaviour is determined by the fact that the principal value operator in eq. (II-5.3) is half the sum of incoming and outgoing waves. This implies

$$\lim_{r\to\infty}\psi_{\ell}(k,z,r) = \mathcal{J}_{\ell}(kr) - A_{\ell}(k,\tau)\ \eta_{\ell}(\tau r), \quad z=\tau^2>0 \qquad (II-5.10)$$

where A is a constant determined by the equation and η_{ℓ}

is the RicattiBessel function of the second kind. The boundary conditions on ψ_ℓ suggest defining the wave defect

$$\chi_\ell(k,z,r) = \mathcal{J}_\ell(kr) - \psi_\ell(k,z,r) \quad ,(II\text{-}5.11)$$

satisfying the equation

$$\left(\frac{d^2}{dr^2} + z - v(r) - \frac{\ell(\ell+1)}{r^2}\right) \chi_\ell(k,z,r) = -v(r)\, \mathcal{J}_\ell(kr) \quad ,(II\text{-}5.12)$$

with the boundary conditions

$$\chi_\ell(k,z,r=c) = \mathcal{J}_\ell(kc) \quad \text{at the hard core edge}$$

or

$$\chi_\ell(k,z,r=0) = 0 \quad \text{if there is no hard core} \qquad (II\text{-}5.13)$$

and

$$\chi_\ell(k,z,r\to\infty) = A_\ell(k,\tau)\ \eta_\ell(\tau r) \quad .(II\text{-}5.14)$$

In the case $z<0$, it is well known that χ_ℓ decays exponentially at large r.

Eqs. (II-5.12-14) represent a two point boundary value problem of the type

$$\left(\frac{d^2}{dr^2} + f(r)\right)\chi(r) = g(r) \qquad (II\text{-}5.15)$$

$$\chi(c) = \mathcal{J}_\ell(kc) \qquad (II\text{-}5.16)$$

$$\chi'(b) + \beta\chi(b) = B \qquad (II\text{-}5.17)$$

over an interval c<r<b. The outer radius b can be chosen between 10 and 20 fm. These equations can be solved in several ways[51]. For z<0 it was shown by Bhargava and Sprung[22] that the Ridley method[52] is very convenient and efficient. The same applies for positive z, but with some additional complications.

In the ordinary Ridley method, one factorizes the L.H.S. of eq. (II-5.15), reducing the problem to the solution of three first order equations

$$\frac{ds}{dr} - s^2 = f \qquad \text{(II-5.18)}$$

$$\frac{dw}{dr} - sw = g \qquad \text{(II-5.19)}$$

$$\frac{d\chi}{dr} + s\chi = w \qquad \text{,(II-5.20)}$$

where

$$f(r) = z - v(r) - \frac{\ell(\ell+1)}{r^2}$$

$$g(r) = -v(r)\, j_\ell(kr) \qquad .$$

Starting at the outer radius b, where eqs. (II-5.14) and (II-5.17) imply $\beta = -\tau \tan \tau b$ and B=0, we put $s(b)=\beta$ and $w(b)=B$. The two eqs. (II-5.18-19) can be solved in to r=c and then eq. (II-5.20) solved back out to r=b generating the desired solution. There is no danger of building any spurious solution of $\chi(r)$ on the outward integration because

a first order equation is being solved.

The complication, when $z>0$, arises because over most of the interval in question, we have

$$f(r) = (z-v(r) - \frac{\ell(\ell+1)}{r^2})>0 \qquad \text{(II-5.21)}$$

which causes $s(r)$ to have poles. This does not happen when the energy parameter z is negative. For example if $f(r)=C^2$, a constant, the solution would be $s(r)=C \tan Cr$, which has poles. If we had $f(r)=-C^2$, we would have $s(r)=C \tanh Cr$, which is well behaved. This problem is overcome by introducing the 'Ridley-alternate' method where we have three new functions

$$S = \frac{1}{s} \quad , \quad W = \frac{w}{s} \quad , \quad Z = w-s\chi$$

or

$$s = \frac{1}{S} \quad , \quad w = \frac{W}{S} \quad , \quad \chi = W-SZ \qquad \text{(II-5.22)}$$

which satisfy

$$\frac{dS}{dr} = -1 - S\, f(r) S \qquad \text{(II-5.23)}$$

$$\frac{dW}{dr} = S(g(r) - f(r)W) \qquad \text{(II-5.24)}$$

$$\frac{dZ}{dr} = g(r) - f(r)\ (W-SZ) \qquad \text{(II-5.25)}$$

Whenever the solution $s(r)$ begins to grow, say at $|s|=2$, we switch over to the alternate method. Since the operation eq. (II-5.22) is reflexive this is very convenient on the

computer; one needs only to keep a record of the step at which a flip-flop was performed, so that on the reverse integration for χ (or Z) the corresponding operation is effected. Eqs. (II-5.22-25) apply equally well to the case of coupled partial waves, where f, g, s, S, w, W, χ and Z become 2x2 matrices. Since s and S are symmetric, only three of their four elements need be solved.

If it were desired to start the integration process at the origin (or core radius) where the boundary condition is $\chi_\ell(c)=\mathcal{J}_\ell(kc)$, it would be necessary to begin in the 'variant mode' with $S(c)=0$, $W(c)=\mathcal{J}_\ell(kc)$. At negative z this is convenient only when one is looking for the Moszkowski-Scott separation distance[53], determined by the first zero of W(r).

Once $\chi_\ell(k,z,r)$, and therefore the wave function $\psi_\ell(k,z,r)=\mathcal{J}_\ell(kr) - \chi_\ell(k,z,r)$, has been calculated, the matrix element $K_\ell(p,k;z)$ can be obtained from eq. (II-5.8).

For soft core potentials it is probably easier to evaluate the K_ℓ-matrix elements in momentum space, but for hard core forces the coordinate space solution is necessary.

B. Momentum Dependent Potential

The Ridley equations (II-5.18-20) get slightly modified in the case of a p^2-dependent potential. For a Hamiltonian of the form $H = v_1(r)p^2\ v_1(r) + v_2(r)$, eq. (II-5.12) satisfied by the wave defect $\chi_\ell(k,z,r)$, changes

to*

$$\{v_1(r)\ (-\frac{d^2}{dr^2} + \frac{\ell(\ell+1)}{r^2})\ v_1(r) + v_2(r) - z\}\ \chi_\ell(k,z,r)$$

$$= \{v_1(r)\ (-\frac{d^2}{dr^2} + \frac{\ell(\ell+1)}{r^2})\ v_1(r) + v_2(r) - (-\frac{d^2}{dr^2} + \frac{\ell(\ell+1)}{r^2})\}$$

$$x\, \mathcal{J}_\ell(kr)$$

or

$$(\frac{d^2}{dr^2} + \frac{2v_1'(r)}{v_1(r)}\frac{d}{dr} + \frac{v_1''(r)}{v_1(r)} - \frac{\ell(\ell+1)}{r^2} - \frac{v_2(r)}{v_1^2(r)} + \frac{z}{v_1^2(r)})\chi_\ell(k,z,r)$$

$$= (1 - \frac{1}{v_1^2(r)})\,\mathcal{J}_\ell''(kr) + \frac{v_1'(r)}{v_1(r)}\mathcal{J}_\ell'(kr)$$

$$+ \{\frac{v_1''(r)}{v_1(r)} - (1 - \frac{1}{v_1^2(r)})\ \frac{\ell(\ell+1)}{r^2} - \frac{v_2(r)}{v_1^2(r)}\}\mathcal{J}_\ell(kr)$$

or

$$(\frac{d^2}{dr^2} + h\,\frac{d}{dr} + f)\chi_\ell = g \qquad \text{(II-5.26)}$$

where

$$h(r) = \frac{2v_1'(r)}{v_1(r)}$$

$$f(r) = \frac{v_1''(r)}{v_1(r)} - \frac{\ell(\ell+1)}{r^2} - \frac{v_2(r)}{v_1^2(r)} + \frac{z}{v_1^2(r)}$$

---

* We have used $p^2 \equiv -\frac{1}{r}\frac{d^2}{dr^2}\,r + \frac{\hat{\ell}^2}{r^2}$, where $\hat{\ell}$ is the orbital angular momentum operator.

$$g(r) = (1 - \frac{1}{v_1^2(r)})\mathcal{J}_\ell''(kr) + \frac{v_1'(r)}{v_1(r)}\mathcal{J}_\ell'(kr) + \{\frac{v_1''(r)}{v(r)}$$

$$- (1 - \frac{1}{v_1^2(r)})\frac{\ell(\ell+1)}{r^2} - \frac{v_2(r)}{v_1^2(r)}\}\mathcal{J}_\ell(kr) \qquad \text{(II-5.27)}$$

and the prime over v_1 and $\mathcal{J}$ indicates differentiation with respect to r. There is no change in the boundary conditions if $v_1(r)$ has a finite range. For a local potential $v_1(r)=1$ and the eq. (II-5.26) reduces to eq. (II-5.15). The Ridley method can again be used giving the following three first order equations

$$\frac{ds}{dr} + (h-s)s = f$$

$$\frac{dw}{dr} + (h-s)w = g$$

$$\frac{d\chi}{dr} + s\chi = w \qquad \text{(II-5.28)}$$

These equations can be solved for $\chi_\ell(k,z,r)$ as indicated earlier. Eq. (II-5.8) then gives the reaction matrix elements.

CHAPTER III

INVERSE SCATTERING PROBLEM
MARCHENKO METHOD

III-1. Introduction

The inverse scattering problem aims at obtaining the interparticle potential from the phase shifts or the S-matrix. Starting from any given S-matrix, a local potential can be constructed by using the Gel'fand and Levitan[54] or Marchenko[55] equations, and a one term separable potential by the methods proposed by Omnes[56], Bolsterli and Mackenzie[57] and Tabakin[58]. In both cases the potentials are unique in the absence of any bound state. Another inversion procedure valid only for Yukawian potentials has been proposed by Martin[59].

We are interested in obtaining a local potential from a rational S-matrix. The general construction procedure using the Gel'fand and Levitan equations for such an S-matrix has been given by a number of workers[60-63]. Here we follow the Marchenko scheme which seems much easier. It is applicable only to the $\ell=0$ case but can be modified for the higher partial waves also[64].

III-2. Method

In this method one forms a kernel

$$F(x) = \frac{1}{2\pi}\int_{-\infty}^{\infty}\{S(k) - 1\}e^{ikx}dk, \qquad \text{(III-2.1)}$$

from the S-matrix and solves the Fredholm equation

$$A(t,x) = F(t+x) + \int_{t}^{\infty}A(t,y)F(y+x)dy, \qquad \text{(III-2.2)}$$

for the kernel $A(t,x)$. If bound states are present, eq. (III-2.2) still holds in the same form provided $F(x)$ is defined as

$$F(x) = \frac{1}{2\pi}\int_{-\infty}^{\infty}\{S(k) - 1\}e^{ikx}dk + \sum_{n} iS_n e^{-\xi_n x}.$$

Here $\xi_n{}^2$ are the binding energies of the bound states and S_n are the residues of the S-matrix at bound state poles. This kernel is square integrable in the range (t,∞) in x and is related to the Jost solution by

$$F(\pm k,x) = e^{\mp ikx} + \int_{x}^{\infty}A(x,y)e^{\mp iky}dy. \qquad \text{(III-2.3)}$$

The potential is given by

$$V(x) = -2\frac{d}{dx}A(x,x) \qquad \text{(III-2.4)}$$

All the potentials which we have considered correspond to a rational S-matrix of the form

$$S(k) = \prod_{m=1}^{n_\alpha}\left(\frac{k-i\alpha_m}{k+i\alpha_m}\right)\prod_{n=1}^{n_\beta}\left(\frac{k+i\beta_n}{k-i\beta_n}\right) \qquad \text{(III-2.5)}$$

where Re $\alpha_m>0$ and Re $\beta_n>0$ for all m and n. The poles at

$k = -i\alpha_m$, correspond to antibound states (α_m real) or resonances while those at $k = i\beta_n$ are the, so called,'redundant poles' or 'potential singularities'. The phase shift follows immediately from eq. (III-2.5)

$$\delta(k) = \sum_{n=1}^{n_\beta} \tan^{-1}\left(\frac{\beta_n}{k}\right) - \sum_{n=1}^{n_\alpha} \tan^{-1}\left(\frac{\alpha_n}{k}\right) \qquad \text{(III-2.6)}$$

For $n_\alpha = n_\beta$, the phase shift will vanish both at k=0 and k=∞.

If the S-matrix has only simple poles in the upper half k-plane, the kernel F(x+y) can be evaluated by closing the contour in the upper half k-plane. Only the poles at $k = i\beta_r$ contribute, so that

$$\begin{aligned} F(x+y) &= -2 \sum_{r=1}^{n_\beta} \left[\frac{(k-i\beta_r)\,\mathrm{Im}\, f(k)}{f(-k)}\right]_{k=i\beta_r} e^{-\beta_r(x+y)} \\ &= \sum_{r=1}^{n_\beta} b_r e^{-\beta_r(x+y)} \\ &= \sum_{r=1}^{n_\beta} F_r(x) F_r(y) \end{aligned} \qquad \text{(III-2.7)}$$

is separable and the eq. (III-2.2) can therefore be solved by standard methods giving

$$A(t,x) = \sum_{i=1}^{n_\beta} M_i(t) e^{-\beta_i x} \qquad \text{(III-2.8)}$$

with

$$M_i(t) = -\frac{b_i e^{-\beta_i t}}{\Delta(t)} \left[1 + \sum_{n=1}^{n=n_\beta} \sum_{j_1 \neq j_2 \neq \ldots j_{n-1} \neq i}^{n_\beta} \cdots \sum^{n_\beta} b_{j_1} b_{j_2} \cdots b_{j_{n-1}} \right.$$

$$\left. q^{(n)}_{i;j_1,j_2,\ldots j_{n-1}} \exp\{-2(\beta_{j_1}+\beta_{j_2}+\ldots\beta_{j_{n-1}})t\} \right]$$

(III-2.9)

and

$$\Delta(t) = \left[1 + \sum_{n=1}^{n=n_\beta} \sum_{j_1 \neq j_2 \neq} \cdots \sum_{j_n} b_{j_1} b_{j_2} \cdots b_{j_n} \right.$$

$$\left. p^{(n)}_{j_1,j_2 \cdots j_n} \exp\{-2(\beta_{j_1}+\beta_{j_2}+\ldots\beta_{j_n})t\} \right]$$

$$= \det \left| \delta_{ij} + \frac{b_i}{\beta_i+\beta_j} e^{-2\beta_i x} \right| \qquad \text{(III-2.10)}$$

where

$$p^{(n)}_{j_1,j_2 \cdots j_n} = \begin{vmatrix} \frac{1}{2\beta_{j_1}} & \frac{1}{\beta_{j_1}+\beta_{j_2}} & \cdots & \frac{1}{\beta_{j_1}+\beta_{j_n}} \\ \frac{1}{\beta_{j_2}+\beta_{j_1}} & \frac{1}{2\beta_{j_2}} & \cdots & \frac{1}{\beta_{j_2}+\beta_{j_n}} \\ \cdot & \cdot & \cdots & \cdot \\ \cdot & \cdot & \cdots & \cdot \\ \frac{1}{\beta_{j_n}+\beta_{j_1}} & \frac{1}{\beta_{j_n}+\beta_{j_2}} & \cdots & \frac{1}{2\beta_{j_n}} \end{vmatrix}$$

$$= \frac{2^{-n}}{\beta_{j_1}\beta_{j_2}\cdots\beta_{j_n}} \prod_{r<s}^{n} \left(\frac{\beta_{j_r}-\beta_{j_s}}{\beta_{j_r}+\beta_{j_s}} \right)^2 \qquad \text{(III-2.11)}$$

$$q^{(n)}_{j_1;j_2,j_3,\cdots j_n} = \begin{vmatrix} 1 & \frac{1}{\beta_{j_1}+\beta_{j_2}} & \cdots & \frac{1}{\beta_{j_1}+\beta_{j_n}} \\ 1 & \frac{1}{2\beta_{j_2}} & \cdots & \frac{1}{\beta_{j_2}+\beta_{j_n}} \\ \cdot & \cdot & \cdots & \cdot \\ \cdot & \cdot & \cdots & \cdot \\ \cdot & \cdot & \cdots & \cdot \\ 1 & \frac{1}{\beta_{j_n}+\beta_{j_2}} & \cdots & \frac{1}{2\beta_{j_n}} \end{vmatrix}$$

$$= \frac{2^{-(n-1)}}{\beta_{j_2}\beta_{j_3}\cdots\beta_{j_n}} \prod_{m\neq 1}^{n} \left(\frac{\beta_{j_1}-\beta_{j_m}}{\beta_{j_1}+\beta_{j_m}}\right) \prod_{\substack{r<s \\ r,s\neq 1}}^{n} \left(\frac{\beta_{j_r}-\beta_{j_s}}{\beta_{j_r}+\beta_{j_s}}\right)^2 \qquad \text{(III-2.12)}$$

For t=x, the expression for A(t,x) simplifies to

$$A(x,x) = \frac{d}{dx}\{\log\Delta(x)\} \qquad \text{(III-2.13)}$$

which is sufficient to obtain the potential. The scattering wave function asymptotic to $\sin(kx+\delta)$ has the simple expression

$$\psi_0(x) = \left(1 + \sum_{i=1}^{n_\beta} \frac{\beta_i M_i(x)}{\beta_i^2 + k^2} e^{-\beta_i x}\right)\sin(kx+\delta)$$

$$+ \left(\sum_{i=1}^{n_\beta} \frac{k\, M_i(x)}{\beta_i^2 + k^2} e^{-\beta_i x}\right)\cos(kx+\delta) \qquad \text{(III-2.14)}$$

III-3 Generalisation for the Case of Higher Order Poles

If the S-matrix has higher order poles the solution becomes considerably more complicated. We have not been able to express it in a simple explicit form as above. A general procedure for handling several poles of second order is outlined in Appendix A. If $i\beta$ is a double pole, we replace it by a pair of simple poles at $i\beta(1\pm\varepsilon)$ and take the limit $\varepsilon \to 0$ of the solution $A(t,x)$. Even easier, for $\varepsilon = 0.001$, the CDC computer would give an accurate construction of the potential using the above formulae for simple poles. In view of eq. (III-2.6) the error in the phase shift is of order $\beta\varepsilon^2/k$ and is important only at the lowest energies (of order one eV).

CHAPTER IV

SOFT CORE LOCAL POTENTIAL MODELS FOR $^1S_0$ NEUTRON-PROTON INTERACTION AND THEIR OFF-SHELL PROPERTIES

IV-1. Introduction

Local potential models for the nucleon-nucleon interaction in the $^1S_0$ state have usually included very strong repulsive cores[6-9]. Even the relatively soft potential of Bressel, Kerman and Rouben[10] has a repulsive core of 670 MeV. It has been widely believed that the existing experimental data require the use of very strong repulsive cores in the case of local potentials. We wish to investigate whether the existing experimental data (more precisely the phase shifts) do require a substantial repulsion at small distances, and if not, what differences are produced in the off-shell behaviour. Following Bargmann[65], we make an ansatz that the S-matrix is of rational form (eq. (IV-2.1)). This implies that at infinite energy the phase shift will go to zero, ruling out the infinite hard core but little else. In principle this is little different than assuming, as for example Reid does, that the core shall be a Yukawa of certain range because the latter statement also implies the asymptotic behaviour of the phase shifts.

In Section IV-2 we describe the construction of the

potentials and point out their special features. In Section IV-3 we compare Noyes-Kowalski half-shell function* $f_\ell(p,k) = K_\ell(p,k;k^2)/K_\ell(k,k;k^2)$ for our potentials with those obtained from other local and non-local potential models. In Section IV-4 some implications of the existence of such soft potentials and the difference in their off-shell properties are considered. Section IV-5 gives our conclusions.

IV-2. Construction of the Potentials

We write

$$S(k) = e^{2i\delta(k)} = \prod_{r=1}^{N} \left(\frac{k+i\beta_r}{k-i\beta_r}\right)\left(\frac{k-i\alpha_r}{k+i\alpha_r}\right) \qquad \text{(IV-2.1)}$$

and consider N=3. At least N=2 terms are required (see Section II-2) in order that the phase shift can change sign. We find it convenient to require that $\sum_i \alpha_i = \sum_i \beta_i$, which allows only one change of sign of the phase shift (Im f(k) vanishes for only one real value of k).

The parameters α_r, β_r were fitted to the 40 $^1S_0$ n-p phase shifts of MacGregor et.al.[66] in the energy range 1 to 460 MeV, giving a χ^2 value of 12.2. This fit is superior to any other potential model. The positions of the zeros and the poles of the S-matrix are shown in Fig. 1. There

---

* This definition is completely equivalent to the usual one involving transition matrix elements.

are three redundant poles in the upper half k-plane. In the lower half there is the $^1S_0$ antibound state pole near the origin and a pair of 'resonances' of very large width. The precise positions of these are very much model dependent, so are not to be taken seriously. Once our S-matrix has been fitted to the data, the potential is completely determined and is calculated by using the method described in Chapter III.

As a practical matter, in fitting the potential we introduced the following five real parameters

C_1: scattering length

C_2: effective range

C_3: energy at which phase shift changes sign

C_4: phase shift at an arbitrary energy C_6

C_5: governs asymptotic behaviour $\delta(E\to\infty) \simeq -C_5/E^{3/2}$.

The parameters α_r, β_r are the roots of a polynomial related to these new parameters by the following relations:

$$\prod_{r=1}^{3} (k-i\beta_r)\ (k+i\alpha_r) = a + bk^2 + ck^4 + k^6 - iek(f-k^2) \qquad \text{(IV-2.2)}$$

where

$$e = C_5\left(\frac{m}{2\hbar^2}\right)^{3/2}$$

$$f = C_3\left(\frac{m}{2\hbar^2}\right)$$

$$a = -ef/C_1 = -\left(\frac{m}{2\hbar^2}\right)^{5/2} C_3C_5/C_1$$

$$b = \frac{1}{2} efC_2 - a/f = \left(C_2C_3 \frac{C_5 m}{4\hbar^2} + \frac{C_5}{C_1}\right) \left(\frac{m}{2\hbar^2}\right)^{3/2}$$

$$c = [es(f-s^2) \cot (C_4) - a - bs^2 - s^6]/s^4; \quad s^2 \equiv \frac{mC_6}{2\hbar^2}$$

.(IV-2.3)

We have used $\hbar^2/m = 41.47$ MeV fm^2. The fact that there are only five parameters reflects the constraint on the sum of α's and β's. C_1 and C_2 are well known, although a slightly better overall fit was achieved by letting these readjust slightly.

The parameters C_1 to C_6 which define the potential are given in Table 1. In Fig. 2 our phase shifts are compared against those of Reid[9] (who fitted p-p data, not n-p data) and the Livermore group[66]. We are everywhere within a standard deviation.

In Fig. 3 our potential (called SSC) is plotted alongside Reid Soft Core potential. The repulsive core in our case is of nearly the same radius (half height radius) but achieves a height of only 87 MeV. The narrow attractive pocket at the origin does not support a bound or resonant state and indeed has no significance. If the potential were cut off flat at its maximum the high energy phases would become only a few percent more repulsive (0.5° at 300 MeV). At large r our potential oscillates. We believe this is

TABLE 1

PARAMETERS DEFINING THE POTENTIALS SSC AND SSC-NP-2

Parameter	SSC	SSC-NP-2
C_1(fm)	-23.5518	-6.4719
C_2(fm)	2.4653	2.3271
C_3(MeV)	261.2205	263.3857
C_4	-0.1007	-0.11089
C_5($MeV^{3/2}$)	3144.58	6353.98
C_6(MeV)	335.0	325.0
Joining Radius(fm)	-	1.86775

because the potentials of Bargmann class decay exponentially; the data, however, favour the OPEP Yukawa tail and this more rapid decay is simulated by the oscillations.

In order to accommodate the OPEP tail, which is well established, we fitted a hybrid potential defined to have the functional form of SSC at small r, and to be equal to OPEP at large r (beyond about 1.8 fm). The precise joining radius was selected so as to make the potential continuous, but with a discontinuity in slope. To avoid introducing further adjustable parameter we defined the tail potential following Reid[9]

$$V_{TAIL}(r) = -10.463\ e^{-\mu r}/\mu r \text{ MeV} \quad ,$$

$$\mu = 0.7 \text{ fm}^{-1} \quad .(IV-2.4)$$

Of course, simply replacing the large distance part of SSC by OPEP would make the potential more attractive, so the parameters C_1 - C_5 defining the short range force were treated as adjustable parameters and again chosen to secure a best fit. This removes any direct physical significance of these parameters; in particular the S-matrix of the hybrid potential is very different from eq. (IV-2.1). The phase shifts in the combined potential were determined by numerically integrating the Schrödinger equation. Since the long range potential was fixed, considerable time was saved by integrating through it only once. At each stage in the

search procedure, one needs only to integrate through the short range potential. To see this, let $M_\ell(r)$ and $P_\ell(r)$ be solutions in the potential V_{TAIL} with asymptotic forms

$$M_\ell(r) \to \sin(kr - \ell\pi/2)$$

$$P_\ell(r) \to \cos(kr - \ell\pi/2) \qquad .(IV\text{-}2.5)$$

If d is the joining radius between the short distance and tail potentials (or any greater distance), a solution $\Psi(r)$ in the interior region can be matched at r=d to

$$\Psi(r) = A\cos(\delta)[M_\ell(r) + \tan(\delta)P_\ell(r)]_{r=d}$$

$$\to A\sin(kr + \delta - \ell\pi/2) \text{ as } r\to\infty \qquad .(IV\text{-}2.6)$$

Thus, δ can be determined at the point d, provided that one has previously evaluated two independent solutions in the tail potential and has available their boundary values. Since for our potential, d is about 1.8 fm, this procedure made for a great saving in effort.

The searches were carried out by a computer programme MINI2 following the Powell[67] method. χ^2 for the phase shifts at 20 energies (from 1 to 400 meV) was minimized. The best solution found, called SSC-NP-2*, gave χ^2=3.9 with constants C_1 to C_6 as in Table 1. The quality of the fit

---

* Another solution called SSC-NP-1 was discarded in favour of SSC-NP-2.

is superior to the pure SSC, which is consistent with the introduction of a new parameter.

The high energy phase shifts are completely different from those of the Reid or Hamada-Johnston potentials. For SSC-NP-2 there is a minimum of about -12° at 635 MeV; thereafter they tend to zero. In Fig. 4 the high energy phases for a number of potentials are compared. Strongly repulsive cores behave essentially like a hard core, for which $\delta_0 = -kc$, over an energy range up to several BeV.

The means by which such a weakly repulsive potential can produce a reversal of sign in the phase shift is best illustrated in Figs.5(i-v) where we show the radial wave function normalized to be asymptotically sin $(kr + \delta)$, at a number of energies. In contrast to strongly repulsive cores which make the short range Ψ very rigid, we see that Ψ changes considerably with energy. Between E = 20 and 60 MeV, our Ψ is rather rigid inside 1 fm, but as the energy becomes comparable with the core height Ψ begins to penetrate in towards the origin just as the Bessel function does. The wave function is just stiff enough to give the required negative phase shifts above 250 MeV.

IV-3. Off-Shell Properties

In Figs. 6(i-iv) we compare the behaviour of the half-shell functions f(p,k) of our potentials with those obtained from the well known Reid Soft Core[9], Hamada-Johnston[7]

and Mongan[16] (separable) potentials. At p=k, this function is equal to one. Initial state energies k^2 corresponding to laboratory energies of 20, 60, 140 and 360 MeV were chosen as illustrating the overall behaviour. The final state momentum p runs up to 10 fm^{-1}, corresponding to 8 BeV.

There is noted a steady progression in behaviour from the SSC potentials through Reid to Hamada-Johnston, evidently reflecting the hardening of the core. At very high p, the Hamada-Johnston curve seems to be oscillating wildly due to its infinite hard core. Reid's potential seems to have gone about half way in softening of the core; we would expect potentials of intermediate softness to give intermediate results. Finally we see in every case that the separable potential of Mongan (his case 2) has a very different behaviour than any of the local potential examples, particularly as $p \to 0$ or at $p \gtrsim 4$ fm^{-1}. At high momenta his off-shell matrix elements are much more repulsive than those for any local potential. It is noted, however, that not only do all potentials agree in f(k,k)=1 but that $[\frac{\partial f(p,k)}{\partial p}]_{p=k}$ is very nearly the same for all of them. For processes in which one does not go far off the energy shell, all of these should give nearly the same result, separable potentials included.

IV-4. Other Implications

The existence of such 'super' soft core local

potentials raises a number of questions e.g. the use of perturbation theory in nuclear structure calculations, the evidence for an L^2-dependent potential, etc.

The chief barrier to use of perturbation theory in nuclear structure calculations is the existence of the strong tensor force in the $^3S_1 - {}^3D_1$ wave, causing a substantial second order contribution but none at all in first order. However, even in the $^1S_0$ state the second order term has far overwhelmed the leading order for all previous local potential models; even for the moderately strong core potential of Bressel Kerman and Rouben[10]. Table 2 summarizes the results of perturbation calculations in nuclear matter for the SSC potentials considered here.

TABLE 2

Perturbation theory, calculations* in nuclear matter at k_F=1.4 fm^{-1}, for the potentials SSC and SSC-NP-2, $^1S_0$ only considered. V_1 and V_2 are the first and second order potential energy per particle.

Potential	$-V_1$	$-V_2$	V_2/V_1 %
SSC	19.97	2.48	12.4
SSC-NP-2	19.74	2.85	14.4

* If an effective mass m* were considered, V_2 would be further reduced, proportional to m*.

The ratio of second to first order terms is 12 - 14%. The potential energy at normal density in first order is close to the results of nuclear matter reaction matrix calculations with the same potential; the second order term makes the result too large. It is unlikely that SSC type potentials will improve the applicability of perturbation theory in the $^3S_1$ state.

One of the most striking evidences for the non-static character of the nuclear force is the fact that the potentials fitted to the $^1S_0$ data give a $^1D_2$ phase shift twice too large at high energies. Reid[9] in Fig. 5 of his paper makes the point that the potential inside 1 fm (at which point the centrifugal barrier reaches 250 MeV height) is irrelevant. His $^1D_2$ potential is 40 MeV deep at 1 fm while his $^1S_0$ potential is 80 MeV at the same point. Though our potentials have shallower attraction as well as less repulsion, we still find that the $^1D_2$ phase shifts would require a weaker potential than our $^1S_0$ force. Hence, there is still evidence for an L^2-dependent potential although the non-static part is weaker than in the past. This would have implications for nuclear matter calculation at very high density, as considered by Razavy[68].

Nuclear matter calculations* were carried out using

---

* These calculations were done by Dr. P. K. Banerjee using the self-consistent method of Kallio and Day[69].

our potentials in the $^1S_0$ state and Reid Soft Core potential in all others. Because Reid's potential is fitted independently to each partial wave, this is a reasonable procedure. A gain of up to 1.1 MeV in binding energy per particle was observed. This gain can be associated with a reduction of the "wound integral", which was .02 for the Reid potential, to about .006 for the potentials of SSC type. Little further gain can thus be expected in this state. However, there is every indication that an equal or greater increase in binding can be secured in the $^3S_1$ state from a similar softening of the repulsive core. Thus there is a good likelihood of achieving agreement with 'experiment' in nuclear matter calculations without being forced to admit non-local nucleon-nucleon forces.

For finite nucleus calculations, the matrix elements $\langle n\ ^1S_0|v|n\ ^1S_0\rangle$ for our two n-p potentials between oscillator wave functions are of interest. These are shown as a function of oscillator size parameter $b = \sqrt{\frac{\hbar}{mw}}$ in Fig. 7, where we compare them with the "Sussex matrix elements" of Elliott et. al.[70]. For the lower principal quantum numbers (n=0,1,2) the agreement is quite good. Even for n=0, where the result is very sensitive to oscillator size, there is little to choose between the various sets. For the higher principal quantum numbers, where high energy phase shifts are given greater weight, there is a rather different trend, with our SSC-NP-2 values turning up

(saturating) as the oscillator size parameter increases. Assuming that perturbation theory would converge sufficiently well in finite nuclei, the Sussex matrix elements would give results very similar to those obtained with our potential. It is therefore quite possible that their prescription for fitting these matrix elements is related to the existence of SSC type potentials.

IV-5. Conclusion

Two local potentials containing very soft repulsive cores have been developed*. One of them is of the Bargmann class; in the other the short range behaviour is of the Bargmann type while the long range form agrees with OPEP. The existence of these very soft core potentials indicates that infinite or very strong repulsive cores are not essential requirements of a potential model which fits the data. Theoretical considerations allow the existence of very strong cores but cancellations are possible and in any case strong cores are not required by theory.

The half-off-energy-shell properties of our potentials have been studied and found to be consistent with a natural progression from very hard core potentials through strong soft cores to our weak core potentials. All potentials

---

* Similar potentials for the $^1S_0$ proton-proton case have also been obtained[71].

studied show close agreement in the vicinity of the on-energy-shell point in the ratio f(p,k); substantial differences are noted however as $p \to 0$ and for $p \gtrsim 4$ fm^{-1}. The differences probably have scant effect on bremsstrahlung calculations but could be important in nuclear matter. Mongan's separable potential shows radically different behaviour at both large and small momenta; it cannot be considered as qualitatively similar to a soft local potential.

The results of nuclear matter calculations are slightly improved by use of our potentials in preference to Yukawa core potentials. Our finite nucleus matrix elements are strikingly similar to those of Elliott et. al., and the existence of such weak local potentials may well be related to the success of their prescription for evaluating matrix elements directly from the phase shifts. As an alternative to the Sussex group's procedure, we propose to determine $\ell=0$ matrix elements from SSC type potentials, and $\ell\neq 0$ matrix elements from a phase shift approximation with correction terms[72].

CHAPTER V

OFF-ENERGY-SHELL BEHAVIOUR OF PHASE SHIFT EQUIVALENT POTENTIALS

V-1. Introduction

In this chapter we make a comparative study of the off-shell behaviour of phase shift equivalent potentials. In Sections V-2,3 and 4 we consider pairs of equivalent separable and local potentials, while in Sections V-5 and 6, we compare equivalent local and p^2-dependent potentials. For simplicity, only $^1S_0$ state is considered. A nuclear matter binding energy calculation has been done using each of the potentials. In Section V-7, we give the details of these calculations and in Section V-8, the results. Section V-9 gives our conclusions.

We have chosen three separable potentials. These are (i) the two term separable potential of Mongan[16] (his case 2), (ii) the two term separable potential of Tabakin[14] and (iii) the one term separable potential of Tabakin[17]. This choice covers a reasonably wide range of the available separable potentials. The potential used by Lee[19] and Hammann and Ho-kim[21] is of the same form as Mongan's while the one proposed by Naqvi[13] is similar to Tabakin's two term separable potential (they differ slightly in the repulsive form factor). The earlier models proposed by Mitra[73] and

Yamaguchi[74] are good only for the low energy region. We have therefore not included them in our study. For each of the above three potentials an equivalent local potential has been constructed by first obtaining the corresponding S-matrix and then using the method given in Chapter III

$$\begin{matrix}\text{Separable} \\ \text{Potential}\end{matrix} \longrightarrow \text{S-matrix} \xrightarrow[\text{Method}]{\text{Marchenko}} \begin{matrix}\text{Local} \\ \text{Potential}\end{matrix} \qquad \text{.(V-1.1)}$$

We compare the half-shell $K_\ell(p,k;k^2)$ and fully off-shell $K_\ell(p,q;s)$ matrix elements for both positive and negative s. We have preferred to use the reaction matrix K over the transition matrix T because the former is real and more directly used in nuclear reaction theory and nuclear structure calculations.

For positive s we have studied the validity of the Noyes separable approximation[29] to the reaction matrix*. Reiner[75] has compared this approximation with others[47] for a square well potential. He found it to be much better than other approximations over the entire energy range studied but he did not consider it sufficiently accurate to be

---

* Noyes separable approximation applied to the K_ℓ-matrix is completely equivalent to applying it to the t_ℓ-matrix. In both cases, it implies that the phase of the fully off-shell t_ℓ-matrix element $t_\ell(p,q;k^2)$ is the same as the phase of the on-shell matrix element $t_\ell(k)$, $e^{i\delta_\ell(k)}$.

useful. Since the validity of the approximation depends on the potential, we feel it is interesting to consider several local potentials which agree with nucleon-nucleon scattering data and to compare the results with those from equivalent separable potentials for which the non-separable term in the reaction matrix is identically zero.

Recently Baranger et. al.[76] have pointed out the usefulness of studying the symmetric part of the half-shell transition matrix. For simplicity they consider the half-shell t_ℓ-matrix elements with the phase factor $e^{i\delta_\ell(k)}$ removed:

$$\hat{t}_\ell(p,k) = e^{-i\delta_\ell(k)}\, t_\ell(p,k;k^2)$$

$$= \cos\,\delta_\ell(k)\; K_\ell(p,k;k^2) \qquad .(V\text{-}1.2)$$

Considering

$$\hat{t}_\ell(p,k) = \hat{s}_\ell(p,k) + \hat{a}_\ell(p,k) \qquad ,(V\text{-}1.3)$$

a symmetric and antisymmetric part, they show how the unitarity (in the absence of any bound state) of the Möller wave operator determines $\hat{a}_\ell(p,k)$ algebraically once $\hat{s}_\ell(p,k)$ is specified. They propose to eliminate consideration of potentials by specifying $\hat{s}_\ell(p,k)$ arbitrarily (except $\hat{s}_\ell(k,k) = -\sin\,\delta_\ell(k)/k$). The hermiticity of $K_\ell(p,q;k^2)$ is no advantage here since it applies for fixed k^2 and the

whole idea is to deal only with the half-shell matrix elements in a convenient way. We have therefore included a study of the symmetric part for our pairs of equivalent potentials.

Starting from (i) the local potential equivalent to the Mongan's separable potential[16] (his case 2) and (ii) the Hamada-Johnston potential[7], we have obtained equivalent p^2-dependent potentials by using the isometric point transformations (Section V-5). Their half-shell $K_\ell(p,k;k^2)$ and fully off-shell $K_\ell(p,q;s)$ reaction matrix elements are compared as before.

Finally we have used all these equivalent potentials in nuclear matter binding energy calculations (Sections V-7 and 8) to see how the differences in the off-shell behaviour are reflected in the results. In other words we seek to discover whether some systematic effects are introduced by replacing the local potential by its equivalent separable or p^2-dependent potential. We have chosen nuclear matter calculations for this purpose because they seem to be a more sensitive indicator than, for example, proton-proton bremsstrahlung or neutron-neutron scattering length predictions[38]. We feel that this comparison is of interest both as a test of the effects of non-locality and because separable potentials are widely used in the three body calculations.

V-2. The Separable Potentials

In the following we give details of the separable

potentials and obtain S-matrices corresponding to them.

Case I: The separable potential of Mongan[16], his case 2, is a two term separable potential

$$\langle k|V|k'\rangle = \frac{\hbar^2}{m}\frac{1}{2\pi^2}\left[-g_1(k)\, g_1(k') + g_2(k)\, g_2(k')\right] \quad .(V\text{-}2.1)$$

Both form factors are of Yamaguchi form[74]

$$g_i(k) = \frac{\rho_i}{k^2+a_i^2} \quad ,$$

$$\rho_1 = 5.319\ \text{fm}^{-3/2} \qquad a_1 = 1.786\ \text{fm}^{-1}$$

$$\rho_2 = 58.776\ \text{fm}^{-3/2} \qquad a_2 = 6.157\ \text{fm}^{-1} \quad .(V\text{-}2.2)$$

The Jost function* is

$$f(-k) = \left[\{(k+ia_2)^2 - \rho_2^2/2a_2\}\{(k+ia_1)^2 + \rho_1^2/2a_1\} + \left(\frac{\rho_1\rho_2}{a_1+a_2}\right)^2\right]$$

$$\times \{(k+ia_1)(k+ia_2)\}^{-2} \quad .(V\text{-}2.3)$$

The S-matrix has therefore two double poles in the upper half k-plane at $k=i\beta_j$, where

$$\beta_1 = 1.7860 \quad , \quad \beta_2 = 6.1570 \qquad (V\text{-}2.4)$$

and four simple poles in the lower half at $k=-i\alpha_j$, where

---

* See eqs. (II-1.22) and (II-1.26).

$$\alpha_1 = 0.0400$$
$$\alpha_2 = 3.3816$$
$$\alpha_{3,4} = 6.2322 \pm 16.6157i \qquad .(V\text{-}2.5)$$

Case II: The two term separable potential of Tabakin[14] is again of the form eq. (V-2.1). The attractive form factor is of Yamaguchi form

$$g_1(k) = \frac{\rho_1}{k^2+a^2} \quad , \quad a = 1.1990 \text{ fm}^{-1} \quad , \quad \rho_1 = 1.8306 \text{ fm}^{-3/2},$$

while

$$g_2(k) = \frac{\rho_2 \, k^2}{\{(k-d)^2+b^2\}\ \{(k+d)^2+b^2\}}$$

$$b = 1.2484 \text{ fm}^{-1} \quad , \quad d = 1.4409 \text{ fm}^{-1} \quad , \quad \rho_2 = 2.6632 \text{ fm}^{-3/2}.$$

The Jost function is

$$f(-k) = (1 + G_{11}^{(+)}(k))\ (1 + G_{22}^{(+)}(k)) - G_{12}^{(+)}(k)^2 \qquad (V\text{-}2.6)$$

with

$$G_{11}^{(+)}(k) = (\frac{k^2-a^2}{2a} - ik)\ g_1^2(k)$$

$$G_{22}^{(+)}(k) = [\{\frac{(5b^6-3d^6+7b^4d^2-d^4b^2)}{k^2} + \frac{(b^2+d^2)^4}{k^4} - k^2(5b^2+d^2)$$

$$+ 3d^4+15b^4+2d^2b^2\}/16b^3+ik]\ g_2^2(k)$$

$$G_{12}^{(+)}(k) = [\{(\frac{a^2(d^2+b^2)^2}{k^2} + (d^2+b^2)^2 + a(2b-a)\ (d^2+b^2)$$

$$+ 4a^2b^2-k^2(d^2+b^2+2ab))/2b(d^2+(a+b)^2)\}i - k]$$

$$x\ g_1(k).g_2(k) \qquad .(V\text{-}2.7)$$

The S-matrix has three double poles in the upper half k-plane at $i\beta_j$, where

$$\beta_1 = 1.1990$$

$$\beta_{2,3} = 1.2484 \mp 1.4409i \qquad (V\text{-}2.8)$$

and six simple poles in the lower half at $-i\alpha_j$, where

$$\alpha_1 = 0.0441$$

$$\alpha_2 = 2.1740$$

$$\alpha_{3,4} = 1.1912 \pm 1.1270i$$

$$\alpha_{5,6} = 1.3957 \pm 2.2157i \qquad .(V\text{-}2.9)$$

Case III: Tabakin[17] has recently proposed a single term separable potential which contains, in a sense[43], both attraction and repulsion. The form factor is

$$g(k) = \rho(k_c^2-k^2)\ \frac{(k^2+d^2)}{(k^4+a^4)\ (k^2+b^2)} \quad ,$$

$\rho^2 = 400.8434\ fm^{-3}$, $k_c = 1.7\ fm^{-1}$, $a = 4.05\ fm^{-1}$,

$b = 1.08548\ fm^{-1}$ and $d = 1.683\ fm^{-1}$.

It should be noted that this form factor vanishes at $k=k_c$. The S-matrix has three double poles in the upper half plane. The calculations are simpler if we use the slightly generalized form factor

$$g_{mod}(k) = \rho(k_c^2-k^2)\ \frac{(k^2+d^2)}{[(k^4+a_1^4)\ (k^4+a_2^4)\ (k^2+b_1^2)\ (k^2+b_2^2)]^{\frac{1}{2}}} \quad ,(V\text{-}2.10)$$

with

$$a_{1,2} = a \pm .005\ ,\ b_{1,2} = b \pm .005 \text{ and } \rho^2 = 400.840543.$$

The six simple S-matrix poles in the upper half plane lie at $i\beta_j$, where

$$\begin{aligned} \beta_1 &= 1.0805 \\ \beta_2 &= 1.0905 \\ \beta_{3,4} &= 2.8602(1\mp i) \\ \beta_{5,6} &= 2.8673(1\mp i) \end{aligned} \qquad (V\text{-}2.11)$$

while the four simple poles in the lower half plane are at $-i\alpha_j$, where

$$\begin{aligned} \alpha_1 &= 0.0400 \\ \alpha_2 &= 1.4677 \\ \alpha_3 &= 2.1026 \\ \alpha_4 &= 10.0157 \end{aligned} \qquad .(V\text{-}2.12)$$

Because there are more β's than α's, the phase shift starting from zero and taken continuous at $k=k_c$ will tend to $-\pi$ at large k.

V-3. The Equivalent Local Potentials

The equivalent local potentials are obtained by using the above S-matrices in the method described in Chapter III. We find the following expressions for $\Delta(x)$*, which are sufficient to determine the potential by differentiation

$$V(x) = -2 \frac{d^2}{dx^2} \{\log\Delta(x)\} \quad .$$

When the β's are all real the potential decays exponentially; for complex β's which occur in conjugate pairs the long range behaviour is damped oscillatory.

Case I:

$$\Delta(x) = 1 + (c_1+c_2x)\, e^{-2\beta_1 x} + (c_3+c_4x)\, e^{-2\beta_2 x} + c_5\, e^{-4\beta_1 x} + c_6\, e^{-4\beta_2 x} + (c_7+c_8x+c_9x^2)\, e^{-2(\beta_1+\beta_2)x} + (c_{10}+c_{11}x)\, e^{-2(2\beta_1+\beta_2)x} + (c_{12}+c_{13}x)\, e^{-2(\beta_1+2\beta_2)x} + c_{14}\, e^{-4(\beta_1+\beta_2)x} \quad . \text{(V-3.1)}$$

---

* See eq. (III-2.10).

The S-matrix has two double poles on the positive imaginary axis, $\beta_1 = 1.7860\ \text{fm}^{-1}$ and $\beta_2 = 6.1570\ \text{fm}^{-1}$. The coefficients c_i are given in Table 3, while the potential is plotted in Fig. 8. It is quite similar to the Reid Soft Core potential which is included for comparison.

Cases II and III: In both cases we have modified the S-matrix by replacing the three double poles in the upper half plane by six simple poles as suggested earlier. Then

$$\Delta(x) = 1 + \sum_{i=1}^{6} a_i\, e^{-2\beta_i x} + \sum_{i<j}^{6} b_{ij}\, e^{-2(\beta_i+\beta_j)x}$$
$$+ \sum_{i<j<k}^{6} c_{ijk}\, e^{-2(\beta_i+\beta_j+\beta_k)x} + \sum_{i<j}^{6} d_{ij}\, e^{-2(\Sigma\beta-\beta_i-\beta_j)x}$$
$$+ \sum_{i}^{6} e_i\, e^{-2(\Sigma\beta-\beta_i)x} + f\, e^{-2(\Sigma\beta)x} \qquad \text{(V-3.2)}$$

where $\Sigma\beta$ indicates the sum of all six β's. In case II,

$$\beta_1 = 1.2000$$
$$\beta_2 = 1.1980$$
$$\beta_{3,4} = 1.2494 \mp 1.4411i$$
$$\beta_{5,6} = 1.2474 \mp 1.4411i \qquad \text{(V-3.3)}$$

For case III the β's are given in eq. (V-2.11). The coefficients a .... f are in Table 4 and the potentials are plotted in Figs. 8 and 9.

The potential of case II, equivalent to Tabakin's two term separable potential, has a weak repulsive core

TABLE 3

NUMERICAL VALUES OF THE PARAMETERS IN EQ. (V-3.1) FOR THE CASE I

Parameter	Value
C_1	0.493110
C_2	6.053838
C_3	- 0.048046
C_4	-15.011616
C_5	- 0.718093
C_6	- 0.371532
C_7	0.258126
C_8	- 9.259147
C_9	-27.520224
C_{10}	- 0.200245
C_{11}	0.988543
C_{12}	- 0.163112
C_{13}	- 0.206260
C_{14}	0.002244

TABLE 4

NUMERICAL VALUES OF THE PARAMETERS IN EQ. (V-3.2) FOR THE CASES II AND III

Parameter	Case II		Case III	
	Real Part	Imaginary Part	Real Part	Imaginary Part
a_1	-3.756761 +2	0.0	3.451541 +1	0.0
a_2	3.765379 +2	0.0	-3.344541 +1	0.0
a_3	1.349527 +1	5.255720 +1	-3.095750 +2	-1.269441 +1
a_4	a_3^*		a_3^*	
a_5	-1.358397 +1	-5.253018 +1	3.094329 +2	1.214725 +1
a_6	a_5^*		a_5^*	
b_{12}	-9.774074 -2	0.0	-2.449323 -2	0.0
b_{13}	-4.046166 +3	3.340244 +3	-3.808427 +3	3.419870 +3
b_{14}	b_{13}^*		b_{13}^*	
b_{15}	4.037832 +3	-3.358981 +3	3.813791 +3	-3.423040 +3
b_{16}	b_{15}^*		b_{15}^*	
b_{23}	4.072374 +3	-3.338150 +3	3.641963 +3	-3.319780 +3
b_{24}	b_{23}^*		b_{23}^*	

TABLE 4 - CONTINUED

Parameter	Case II		Case III	
	Real Part	Imaginary Part	Real Part	Imaginary Part
b_{25}	-4.064064 +3	3.356967 +3	-3.647220 +3	3.322839 +3
b_{26}	b^*_{25}		b^*_{25}	
b_{34}	-3.915986 +3	0.0	-9.599783 +4	0.0
b_{35}	2.799282 -4	7.601045 -4	-1.457682 -1	-1.171859 -2
b_{36}	3.921977 +3	1.211275 +1	9.594656 +4	-3.062266 +2
b_{45}	b^*_{36}		b^*_{36}	
b_{46}	b^*_{35}		b^*_{35}	
b_{56}	-3.928017 +3	0.0	-9.589630 +4	0.0
c_{123}	3.174869 -1	1.515587 -1	1.017967 -1	-1.724350 0
c_{124}	c^*_{123}		c^*_{123}	
c_{125}	-3.190577 -1	-1.500371 -1	-1.059779 -1	1.729172 0
c_{126}	c^*_{125}		c^*_{125}	
c_{134}	9.745833 +4	0.0	-7.590705 +5	0.0
c_{135}	1.903767 -2	6.698608 -3	-1.244482 -1	1.151619 0

TABLE 4 - CONTINUED

Parameter	Case II		Case III	
	Real Part	Imaginary Part	Real Part	Imaginary Part
c_{136}	-9.771690 +4	-5.025020 +2	7.599662 +5	-3.934644 +3
c_{145}	c^*_{136}		c^*_{136}	
c_{146}	c^*_{135}		c^*_{135}	
c_{156}	-9.797877 +4	0.0	-7.608834 +5	0.0
c_{234}	-9.793739 +4	0.0	7.261035 +5	0.0
c_{235}	-1.908393 -2	-6.864338 -3	1.026247 -1	-1.103269 0
c_{236}	9.819690 +4	5.048611 +2	-7.269698 +5	3.778693 +3
c_{245}	c^*_{236}		c^*_{236}	
c_{246}	c^*_{235}		c^*_{235}	
c_{256}	-9.845972 +4	0.0	7.278568 +5	0.0
c_{345}	7.745994 -2	-7.998936 -3	4.526561 +1	2.000900 0
c_{346}	c^*_{345}		c^*_{345}	
c_{356}	-7.773877 -2	7.676729 -3	-4.525643 +1	-1.631969 0
c_{456}	c^*_{356}		c^*_{356}	

TABLE 4 - CONTINUED

Parameter	Case II				Case III			
	Real Part		Imaginary Part		Real Part		Imaginary Part	
d_{12}	2.066158	-6	0.0		2.138569	-2	0.0	
d_{13}	2.567335	-1	-4.344502	-1	1.202570	+2	1.107107	+2
d_{14}	d_{13}^*				d_{13}^*			
d_{15}	-2.584563	-1	4.309236	-1	-1.212267	+2	-1.093542	+2
d_{16}	d_{15}^*				d_{15}^*			
d_{23}	-2.566448	-1	4.308745	-1	-1.273929	+2	-1.155370	+2
d_{24}	d_{23}^*				d_{23}^*			
d_{25}	2.583444	-1	-4.273620	-1	1.284019	+2	1.141063	+2
d_{26}	d_{25}^*				d_{25}^*			
d_{34}	1.696956	0	0.0		1.225346	+2	0.0	
d_{35}	0.0		0.0		-1.848729	-4	2.232529	-5
d_{36}	-1.690495	0	1.216371	-2	-1.221732	+2	-8.776514	-1
d_{45}	d_{36}^*				d_{36}^*			
d_{46}	d_{35}^*				d_{35}^*			

TABLE 4 - CONTINUED

Parameter	Case II				Case III			
	Real Part		Imaginary Part		Real Part		Imaginary Part	
d_{56}	1.684146	0	0.0		1.218192	+2	0.0	
e_1	3.439914	-6	0.0		-3.670860	-2	0.0	
e_2	-3.414180	-6	0.0		3.887291	-2	0.0	
e_3	-1.260843	-6	-1.849740	-6	7.112685	-4	1.315192	-2
e_4			e_3^*				e_3^*	
e_5	1.238232		1.850472	-6	-8.680922	-4	-1.310391	-2
e_6			e_5^*				e_5^*	
f	0.0		0.0		-1.415755	-6	0.0	

[1]Each entry is followed by its exponent to the base 10. The values less than 10^{-6} have been put equal to zero. The asterisk indicates the complex conjugate.

about .7 fm wide and maximum height 95 MeV outside a narrow attractive pocket (140 MeV deep and .11 fm wide). The outer attraction reaches a depth of about 45 MeV at 1.3 fm. In all respects this potential is similar to the SSC potentials considered in Chapter IV. In contrast the case I potential has a strong repulsive core, $\sim$7.5 BeV at 0.1 fm. Thus there is a very great difference in the strength of the force engendered by the choice of the repulsive form factor. Tabakin[14] emphasized that he chose this form factor so as to make the off-shell extension of his matrix elements smooth. The case III potential differs from both of these. It has a very strong repulsive core ($\sim$ 100 BeV) followed by a deep attraction ($\sim$ 220 MeV) at about 0.9 fm where Reid Soft Core, for example, has a maximum depth of only 120 MeV. The potential then shows oscillations in strength. The solid line in Fig. 9 is the attractive part of the Hamada-Johnston potential, whose hard core is the left hand axis.

V-4. Discussion of the Off-Shell Behaviour of Equivalent Separable and Local Potentials

We first discuss the behaviour of the half-shell reaction matrix elements $K_\ell(p,k;k^2)$. Initial state energies k^2 corresponding to 60, 200 and 360 MeV in the laboratory frame were chosen as illustrating the overall behaviour. The final state momentum p runs from 0 to 10 fm^{-1}, corresponding to about 8 BeV. Figs. 10, 11 and 12 contain the matrix elements for our three potential pairs. For $k^2 \lesssim 1.5$ fm^{-2}

(120 MeV lab.) and over a range in p of about 2 fm^{-1}, the separable force and its equivalent local potential give very similar off-shell matrix elements. The agreement is best in case I. For larger p the local potential values oscillate, those for the separable force are more constant and more repulsive at higher p. The local potentials show a repulsive hump at $p \sim 3$ fm^{-1}, reflecting the repulsive core at r of order .5 fm. The height of this hump is correlated with the strength of the repulsion, being 0.32 fm in case II, 0.5 fm in case I and 0.73 fm in case III (referring to the 60 MeV curves).

The single term separable potential of Tabakin gives matrix elements which behave more like those from a local potential. The repulsive hump for the 60 MeV curve has a huge maximum of 1.44 fm at $p \sim 4$ fm^{-1}. At the lower initial state energies, the local and separable force curves have nearly the same slope at the on-shell point where they cross; causing a broad region of agreement in the predictions. As k^2 increases the region of agreement narrows and is virtually non-existent above 350 MeV. This seems to indicate that bremsstrahlung at 50 MeV will not distinguish between local and non-local forces, although at higher energies there is a possibility of a distinction.

Figs. 13, 14 and 15 show the symmetric function $\hat{s}(p,k)$ for our three pairs. Each line refers to a fixed $(p+k)$ and is plotted against $|p-k|$. Thus, one is looking

at cross-sectional cuts of the $\hat{s}(p,k)$-surface from along the line k=p in the k,p plane. The curves become flatter as p+k increases, reflecting in part the k^{-1} factor in the diagonal value

$$\hat{s}(k,k) = - \sin \delta(k)/k \qquad .(V-4.1)$$

In general the function $\hat{s}(p,k)$ is smoother for the separable potentials of cases I and II. These potentials, at least case II, were generated with the intention of making a smooth off-shell extension. In contrast, the case III separable force shows very similar behaviour to the local potential for p+k up to 5 fm^{-1}. A general progression in behaviour is noted as we pass from the weakest core potential, case II, through case I to case III. The separable forces show the trend clearly; in case II the lines have negative slope, in case I they are flatter and in case III the slope is positive.

We now examine the fully off-shell matrix elements $K_\ell(p,q;k^2)$. Those corresponding to case I are shown in Figs. 16(i-iv), for k^2 corresponding to 1, 40, 100 and 140 MeV laboratory energy, and initial state momenta q corresponding to 20, 140 and 360 MeV. The final state momentum p varies from 0 to 8 fm^{-1}. These figures also contain matrix elements, calculated by Noyes' separable approximation, to which we shall refer in a moment. The agreement between the separable and local potentials is rather good for p

and q up to 2 fm^{-1} and for k^2 less than 150 MeV lab. For higher values of p or q (4 to 8 fm^{-1}), the matrix elements from the separable potential change little but those of the local potential show the characteristic repulsive hump. The height of the hump decreases as k^2 (off-shell energy) increases. The region of agreement between separable and local forces is limited to p, q and k^2 lying in the range 0 - 100 MeV laboratory energy. We have also considered matrix elements for negative k^2, which are used in bound state problems (for example, reference spectrum method in nuclear matter). Curves very similar to those in Figs. 16(i-iv) are obtained, giving no new information; so they are omitted here.

Instead, we consider variation with $s=k^2$, (both positive and negative) of diagonal matrix elements $K_\ell(p,p;s)$ for several representative p values in Fig. 17 for case I and Fig. 18 for case II respectively. For positive s the local and separable potentials show rather different trends: those from the local force increase slightly more rapidly, then decrease much faster as a function of s. For $s<0$, however the curves show very similar shape. For p corresponding to 40 MeV in case I and 60 MeV in case II the separable and local potentials lead to almost identical matrix elements for $s<0$. We have no explanation for this. The close general agreement would imply that in a nuclear matter calculation the consequences of self consistency,

which amounts to a choice of s, would be similar for the pair of potentials. The precipitous drop in the matrix element as $s \to 0$ reflects the presence of the antibound state near zero energy. The on-shell element has as its limiting value the scattering length of order -24 fm. See Appendix B for details.

For the potentials of case III we have shown in Fig. 19 the s variation of just one diagonal matrix element to show the pole at $s = 2.89$ fm^{-2} for the separable potential. The device which banished such poles from the half-shell matrix elements fails for the fully off-shell ones[17]. For negative s, however, the zero of the form factor leads to other consequences considered below in Fig. 22.

In the reference spectrum approximation, the binding energy of nuclear matter is given by the diagonal but fully off-shell K-matrix elements $K(p,p;-\gamma^2)$ at negative energy $s=-\gamma^2$ and for momenta $p<k_F$. In Figs. 20, 21 and 22 we compare these matrix elements for a broad range of values of γ^2 and for $0<p<2.5$ fm^{-1}. In cases I and II the differences are very small which result ultimately in only small differences in their nuclear matter predictions (Section V-8). In case III, however, the zero of the form factor at $p = 1.7$ fm^{-1} is seen to have a dominating effect on the structure of the matrix elements. At the most probable momentum in nuclear matter, $p \approx 1$ fm^{-1}, the separable potential has matrix elements much less attractive than the corresponding

local potential.

We now consider Noyes' separable approximation. For case I, the curves in Figs. 16(i-iv) show it to be excellent when $s<.25$ fm^{-2} (20 MeV lab.) for the entire range of p and q. It continues to be accurate to several percent for higher s if p and q are less than 1.5 fm^{-1} (200 MeV). Our conclusion differs from that of Reiner[75] who studied some typical square well and hard core potentials. A possible reason for this is the existence of the $^1S_0$ antibound state which, along with the repulsion setting in at 240 MeV, dominates the structure of the matrix elements at low energy.

For negative values of s which occur in bound state problems, Noyes' approximation does not apply. But the similarity of the matrix element behaviour for positive and negative s, as for example in Figs. 17 and 18, indicates that some separable approximation should work reasonably well. In nuclear matter theory arguments for separability have been advanced, generally based on the assumption of a hard core potential. In the $^1S_0$ state separability seems quite good, but it is less so in the $^3S_1$ state. Dahll, Ostgaard and Brandow[77] and Köhler[78] have considered this. In Fig. 23 we compare the exact $K_\ell(p,q;s)$ for case I with the approximation

$$K_\ell^A(p,q;s) = K_\ell(p,p';s)\ K_\ell(p',q;s)/K_\ell(p',p';s) \qquad .(V\text{-}4.2)$$

In the figure, $s = -1.20569$ fm^{-2}, $p = .491058$ and 1.299218 fm^{-1}, while $0<q<4$ fm^{-1}. We have arbitrarily chosen

$p' = .850538\ fm^{-1}$. The agreement is remarkably good for $q<2\ fm^{-1}$. Naturally the agreement could be improved by taking a sum of separable terms.

V-5. Construction of Equivalent p^2-dependent Potentials

Isometric point transformations provide a simple practical way to generate phase shift preserving unitary transformations. If we start from a given Hamiltonian $H=T+v=p^2+v$ and apply a unitary transformation $U = e^{i\Omega}$ to this Hamiltonain, the transformed Hamiltonian is

$$\tilde{H} = e^{i\Omega}(T+v)\ e^{-i\Omega} = T+\tilde{v} \qquad .(V-5.1)$$

Here Ω is an hermitian operator. If v is a local potential, the new potential

$$\tilde{v} = e^{i\Omega}v\ e^{-i\Omega} + e^{i\Omega}[T,e^{-i\Omega}] \qquad (V-5.2)$$

will in general be a non-local one. The transformed Hamiltonian $\tilde{H}$ has the same spectrum as H, but does not yield in general the same phase shifts. Thus an arbitrary unitary transformation leads to a non-local potential, which is only equivalent in respect to the bound state energies. The usual invariance properties of the Hamiltonian are preserved if Ω commutes with the symmetry operators of rotation and of space and time reflection.

Mittelstaedt and Ristig[34] have shown that the transformation does not change the phase shifts if $\langle \underset{\sim}{r}_1|\Omega|\underset{\sim}{r}_2\rangle$

satisfies the condition

$$\lim_{k_1 \to k_2} (k_1 - k_2) \int d\underset{\sim}{r}_1 \, d\underset{\sim}{r}_2 \, \langle \underset{\sim}{r}_1 | \Omega | \underset{\sim}{r}_2 \rangle \, \Psi_{\underset{\sim}{k}_1}(\underset{\sim}{r}_1) \, \Psi_{\underset{\sim}{k}_2}(\underset{\sim}{r}_2) = 0 \qquad \text{(V-5.3)}$$

Here $\Psi_{\underset{\sim}{k}}(\underset{\sim}{r})$ is the scattered wave function. If $\langle \underset{\sim}{r}_1 | \Omega | \underset{\sim}{r}_2 \rangle$ is sufficiently localized ((U-1) $\Psi_{\underset{\sim}{k}}(\underset{\sim}{r})$ is arbitrarily small outside some fixed radius), the integral

$$\int d\underset{\sim}{r}_1 \, d\underset{\sim}{r}_2 \, \langle \underset{\sim}{r}_1 | \Omega | \underset{\sim}{r}_2 \rangle \, \Psi_{\underset{\sim}{k}_1}(\underset{\sim}{r}_1) \, \Psi_{\underset{\sim}{k}_2}(\underset{\sim}{r}_2)$$

will always exist and the condition (V-5.3) will be satisfied for any wave function $\Psi_{\underset{\sim}{k}}(\underset{\sim}{r})$.

If Ω is of the form

$$\Omega = \frac{F(r)}{r} \, \underset{\sim}{r} \cdot \underset{\sim}{p} + \underset{\sim}{p} \cdot \underset{\sim}{r} \, \frac{F(r)}{r} \qquad \text{(V-5.4)}$$

the condition (V-5.3) leads to the requirement

$$\lim_{r \to \infty} F(r) = F'(r) = F''(r) = 0 \qquad \text{(V-5.5)}$$

The primes indicate differentiation with respect to r. The requirement (V-5.5) will naturally be satisfied if F(r) has a finite range. The distortion of the radial scale is given by

$$r \to y(r) = e^{i\Omega r} \, e^{-i\Omega} \equiv r + 2F + \frac{1}{2!} \, 2F(2F)' + \frac{1}{3!} \, 2F(2F(2F)')' + \ldots \qquad \text{(V-5.6)}$$

and the transformed Hamiltonian* by

$$\tilde{H} = B_1(r)p^2\, B_1(r) + B_2(r) + v(y(r)) + \hat{\ell}^2\left(\frac{1}{y^2(r)} - \frac{B_1^2(r)}{r^2}\right) \tag{V-5.7}$$

where

$$B_1(r) = \frac{1}{y'(r)}$$

and

$$B_2(r) = \frac{1}{2}\left(B_1(r)\, B_1''(r) - \frac{1}{2} B_1'^2(r)\right) \quad .$$

In practice the function F(r) need not be considered. Any suitable form of y(r) could be chosen, satisfying the conditions

$$y(r) \xrightarrow{r \to \infty} r + O\left(\frac{1}{r}\right) \;,\; y'(r) > 0 \tag{V-5.8}$$

for the correct asymptotic behaviour and the reversibility of the transformation. The conditions at the origin depend on the original potential and the nature of the transformation desired. For example, if a hard core (radius r_0) is present and is to be removed, $y(0) = r_0$; for a soft core potential $y(0) = 0$.

The analytic expression for our point transformation

---

* $\hat{\ell}$ is the orbital angular momentum operator.

is given by*

$$y(r) = \bar{r} + \lambda \log(1 + (e^{r_0/\lambda} - 1)\, e^{-\bar{r}/\lambda})$$

$$\bar{r} = \frac{r}{\omega(r)}$$

$$\omega(r) = 1 + (\frac{\lambda}{\lambda_0})\ \rho_1 r\ e^{-\rho_0 r} \qquad .(V\text{-}5.9)$$

The meanings of these parameters are: r_0 = hard core radius, λ and ρ_0 determine how rapidly y(r) converges to r. They can be considered as a qualitative measure of the range of the non-local parts in $\tilde{H}$. ρ_1 determines the strength of the factor $e^{-\rho_0 r}$. The quotient λ/λ_0 ensures that for $\lambda \to 0$, the transformation approaches the identity.

We have applied this transformation to our local potential of case I above and the Hamada-Johnston potential. For the case I local potential which has a soft repulsive core, we have set $r_0=0$ and $\lambda_0=\lambda=1$. This choice simplifies the transformation (V-5.9) to

$$y_I(r) = r/(1 + \rho_1\, e^{-\rho_0 r}) \qquad ,(V\text{-}5.10)$$

and does not modify the conditions at the origin. The parameter ρ_0 has been chosen to generate 'short' range momentum dependence. We have considered two sets of ρ_0 and ρ_1,

---

* This form has been used earlier by S. Kistler[39].

their numerical values are given in Table 5.

TABLE 5

PARAMETERS DEFINING THE POTENTIALS I-a AND I-b

Potential	ρ_0 (fm^{-1})	ρ_1 (fm^{-1})
I-a	2.8	2.0
I-b	2.8	3.0

In the case of the Hamada-Johnston potential we have taken r_0 = hard core radius = 0.4855148 fm. This choice completely eliminates the hard core; all the repulsion is simulated by the p^2-dependent terms. We have considered here four sets of values for the parameters. Table 6 gives their numerical values.

TABLE 6

PARAMETERS DEFINING THE POTENTIALS HJ-a, b, c AND d

Potential	λ (fm)	λ_0 (fm)	ρ_0 (fm^{-1})	ρ_1 (fm^{-1})
HJ-a	$\frac{1}{2\mu}$	1.0		0.0
HJ-b	$\frac{1}{2\mu}$	$\frac{1}{2\mu}$	4μ	2.0

TABLE 6 - CONTINUED

HJ-c	$\frac{1}{4\mu}$	1.0		0.0
HJ-d	$\frac{1}{4\mu}$	$\frac{1}{4\mu}$	4μ	2.0

The value μ^{-1} = 1.41549 fm, for the pion Compton wavelength, has been used in the numerical calculations.

The potential HJ-a produces 'intermediate' range, while HJ-c and HJ-d produce 'short' range momentum dependence. The potential HJ-b is of a 'mixed'* character. The choice of ρ_1 equal to 2.0 and 3.0 for the case I potential and equal to 0.0 and 2.0 for the Hamada-Johnston potential is arbitrary. Our aim is only to study the changes in the off-shell properties as the strength and the range of the p^2-dependent terms in the potential are varied.

V-6. Discussion of the Off-shell Behaviour of Equivalent Local and p^2-dependent Potentials

We first discuss the behaviour of the half-shell reaction matrix elements $K_\ell(p,k;k^2)$. Initial state energies k^2 corresponding to 20, 140 and 360 MeV in the laboratory frame were chosen. The final state momentum p runs, as

* The factor $e^{-r/\lambda}$ in the transformation decays with the range $(2\mu)^{-1}$ while the factor $e^{-\rho_0 r}$ decays with the range $(4\mu)^{-1}$.

before, from 0 to 10 fm^{-1}. Figs. 24(i-iii) contain these matrix elements for the local potential of case I and its equivalent p^2-dependent potentials I-a and I-b. We find that, qualitatively, their behaviour is similar. The height of the repulsive hump at $p \sim 3$ fm^{-1} is considerably increased, being 1.1 fm in the local case, 1.7 fm in I-a and 1.95 fm in I-b (referring to the k^2=20 MeV curves). It is an indication of the overall increase in the effective repulsion. At the lower initial state energies, as was the case with the local and equivalent separable forces, the curves for the local and the equivalent p^2-dependent potentials have nearly the same slope at the on-shell point where they cross, causing a broad region of agreement in the predictions. As k^2 increases, the region of agreement narrows and is virtually non-existent above 350 MeV. Figs. 25(i-iii) show the half-shell matrix elements for the Hamada-Johnston and its four equivalent potentials HJ-a, b, c and d, for the initial state energies of 20, 140 and 360 MeV as before. Here we find that the p^2-dependent potentials are much softer than the parent local potential. We should keep in mind that the hard repulsive core present in the Hamada-Johnston potential has been removed by our choice of parameters in the transformation. The potential HJ-a is softest of all. It does not show the usual repulsive hump for lower initial state energies. For k^2=360 MeV, the height of the hump in its case is only 0.12 fm, while for the Hamada-Johnston potential

it is 0.39 fm. The position of the repulsive hump in all the four cases has moved to smaller values of p indicating a broadening of the effective repulsive region in the potentials. The region of agreement near the on-shell point is much narrower here.

We now examine the variation with s (both positive and negative) of the diagonal matrix element $K_\ell(k,k;s)$ for k^2=60 MeV in laboratory frame, in Fig. 26 for the first set (case I (local), I-a and I-b) and Fig. 27 for the second set (Hamada-Johnston, HJ-a, b, c and d) respectively. Qualitatively, the local and the equivalent p^2-dependent potentials show similar behaviour. For positive s, the matrix elements from the potentials I-a and I-b decrease much faster (after the initial increase) with s indicating the presence of stronger repulsion. In the Hamada-Johnston family, all the p^2-dependent potentials have weaker repulsion; their matrix elements decrease less rapidly. Actually the behaviour of HJ-a seems to be more like that of a separable potential (Section V-4). For negative s, all the potentials show a smooth variation. It should be noted that as we move away from s=0, the presence of a strong repulsion in the potential makes the matrix elements decrease faster (after the initial increase) for s>0 and increase faster for s<0.

We have also considered the variation with k of the diagonal matrix elements $K_\ell(k,k;s)$ for several negative values of s. Curves very similar to those in Figs. 20 and

21 are obtained, giving no new information, so they are omitted here.

V-7. Nuclear Matter Calculations

Nuclear matter calculations have been carried out by the reference spectrum method[79]. For the separable forces the reaction matrix elements $K_\ell(p,q;k^2)$ for $k^2=-\gamma^2$ give the reference spectrum G^R-matrix. For the local potentials, the method of Bhargava and Sprung[22] was used, with the difference that the potential energies of intermediate states were set equal to zero[80]. Because we have only $^1S_0$ potentials, the interaction in other states was taken to be the Reid Soft Core potential[9]. The potential energies of occupied states were taken from a recent self consistent calculation[81] with Reid's potential in all states; they can be satisfactorily represented by a quadratic function of momentum. Hence the energy denominator can be expressed as

$$e_N(k') = k'^2+\gamma^2=k'^2-k_0^2+2\Delta k_F^2+\left(\frac{1}{m^*}-1\right)\ (0.6k_F^2-P^2-k_0^2) \qquad \text{(V-7.1)}$$

where $-\frac{\hbar^2}{m}\Delta k_F^2$ is the potential energy of an average particle in the Fermi sea, m* is the 'effective mass' for hole states, k_0 is the relative and P the average momentum of the pair of particles in the initial state. We replace P by its average value for a given k_0. Table 7 gives the numerical values of Δ and m* for different values of the

Fermi momentum.

TABLE 7

OCCUPIED STATE ENERGY SPECTRUM PARAMETERS[+] Δ AND m*

$k_F(fm^{-1})$	Δ	m*
1.0	.945	.775
1.1	.938	.735
1.2	.928	.704
1.3	.908	.67
1.36	.89	.65
1.4	.879	.638
1.5	.841	.609
1.6	.789	.58

[+]These values were obtained by Dr. P. K. Banerjee from a self consistent calculation using Reid Soft Core potential in all states.

The nuclear G-matrix is a solution of

$$G^N = G^R + G^{R^\dagger}\left(\frac{1-Q}{e_N}\right)G^N$$

$$\simeq G^R + G^{R^\dagger}\left(\frac{1-Q}{e_N}\right)G^R + \ldots . \qquad \text{(V-7.2)}$$

The higher order corrections were estimated by the geometric series approximation which is known to be accurate to better than 1% in the $^1S_0$ state[77].

For the binding energy of nuclear matter we require the diagonal G^N-matrix element averaged over sixteen spin and isospin states; this gives a statistical weight of $\frac{3}{8}$ to the $^1S_0$ state. Denoting the partial wave G^R-matrix element by

$$G_0^R(k,k) = K_0(k,k;-\gamma^2) \tag{V-7.3}$$

we have

$$\begin{aligned} \mathcal{G}_0^{av}(k) &= 4\pi \frac{\hbar^2}{m} \frac{3}{8} G_0^N(k,k) \\ &= 4\pi \frac{\hbar^2}{m} \frac{3}{8} \left[G_0^R(k,k) + \frac{2}{\pi} \int_0^\infty \left(\frac{1-Q(k',P)}{k'^2+\gamma^2}\right) \right. \\ &\quad \left. \times |G_0^R(k,k')|^2 k'^2 dk' + \text{higher order terms}\right] \end{aligned} \tag{V-7.4}$$

for the averaged nuclear G-matrix element; the suffix '0' means $\ell=S=j=0$. In the above we have used the angle averaged Pauli operator which is exact for the s-state[20]. Since $\mathcal{G}_0^{av}(k)$ now depends only on k, the contribution to the average potential energy is[22]

$$\bar{U}_0 = 12\rho \int_0^1 x^2(x-1)^2 (x+2) \mathcal{G}_0^{av}(xk_F) dx \tag{V-7.5}$$

with the density $\rho = 2k_F^3/3\pi^2$.

No attempt has been made to make the calculation self consistent because this would have only confused the issue, reflecting more the properties of the Reid potential in other states. Rather for each potential we assume the same occupied spectrum. The differences directly reflect the differences in binding due to the different off-shell continuations. The adjustments for self consistency in general would reduce these differences but would be in large measure due to the $^3S_1$ Reid interaction which is irrelevant for our study.

V-8. Nuclear Matter Results and Their Discussion

The $^1S_0$ state contribution to the binding energy per particle is shown in Figs. 28, 29 and 30 as a function of the Fermi momentum, for the various cases.

We first consider the equivalent separable and local potentials (Fig. 28). In case I, where the local potential is quite hard, the separable and local potentials give practically the same contribution. For case II, the separable potential is almost uniformly $\sim$ 0.5 MeV less attractive than the local potential. The situation is very different in case III. At normal density (k_F = 1.36 fm^{-1}), the separable force gives only -9.5 MeV while the local potential gives -14.6 MeV. The difference increases with density. It is due to a zero in the form factor g(k) employed by

Tabakin, resulting in a zero of the (off-shell) G-matrix element (eq. (V-7.3), Fig. 22). This generally reduces the size of the G-matrix elements significantly. It is also striking that potentials I and II give results very similar to that of the Reid potential also included in Fig. 28. The principal qualitative difference is that $\bar{U}(k_F)/2A$ for Reid is increasing slightly less rapidly with increasing density. One would like to ascribe this tendency to a greater repulsion, but the local potential of case I is of comparable strength. Potentials I and II would saturate at a slightly higher density (by 0.05 fm^{-1}) than Reid, potentials III at a lower density (1.2, 1.4 fm^{-1}).

The p^2-dependent potentials I-a and I-b produce (Fig. 29) a slower variation of $\bar{U}(k_F)/2A$ with density indicating a greater role played by p^2-simulated repulsion. At k_F = 1.0 fm^{-1}, they give same contribution (-8.5 MeV) as the equivalent case I local potential, but at k_F = 1.6 fm^{-1}, their contributions are -19.7 and -18.2 MeV respectively while the local potential contributes -21.9 MeV. The situation is opposite in the case of Hamada-Johnston and its equivalent potentials HJ-a, b, c and d (Fig. 30). At k_F = 1.36 fm^{-1}, Hamada-Johnston gives a contribution of -13.9 MeV while its equivalent ones give -15.9, -16.5, -16.5 and -16.1 MeV respectively. HJ-b and HJ-c give practically the same contribution at all densities (k_F = 1.0 to 1.6 fm^{-1}). HJ-a is uniformly about 0.5 MeV more attractive than HJ-b and HJ-c.

HJ-d shows a slightly different variation of $\bar{U}(k_F)$. It is more attractive than HJ-a at lower k_F, and less at higher.

Coester et. al.[33] have given a very interesting argument relating the saturation properties of a family of phase equivalent central potentials to the wound integral of the nuclear matter wave function. However, this argument ignores the decisive saturating effect of the tensor force, which would come into play when we combine our $^1S_0$ potentials with the remainder of Reid potential. Since potentials I, II and Reid span a great range in the height of the repulsive core, it seems clear that this by itself is not a great factor in increasing or decreasing the binding energy of nuclear matter. The reason for this apparent insensitivity to greater core repulsion is that, once we have decided to use zero potential energy in intermediate states, there is no way for very high relative energy collisions to influence the calculation. However in all cases it will be necessary to add on the contribution from three body clusters. Here high energy collisions do occur. The results of Dahlblom[82] and Day[83] suggest that greater repulsion can cause a reduction of perhaps 1 to 2 MeV per particle, a third of which could be ascribed to $^1S_0$ interaction.

V-9. Conclusion

A practical method has been presented, for the $^1S_0$ state, for the calculation of a local potential phase

equivalent to a given separable potential. The explicit solution given here covers the case where the S-matrix is of rational form, which includes the majority of separable models proposed to date. The method was applied to the separable potentials of Mongan* and Tabakin. An extensive comparison of the half-shell reaction matrix elements indicated that at low initial momenta and for elements not too far off the energy shell, there is little difference between the predictions of phase equivalent local and separable potentials. For initial or final state momenta greater than $\sim$ 1.7 fm^{-1} (250 MeV) very different results can be obtained, but comparable differences are observed between strong core and soft core local potentials. A study of the off-shell matrix elements leads to similar conclusions.

The potentials considered cover a range from very strong repulsive cores to very weak ones. This feature is

---

* A better fit to the scattering data has, recently, been obtained with this potential model by Hammann and Ho-kim[21]. The equivalent local potential obtained from it using new values of the parameters (ρ_1=18.275 $fm^{-3/2}$, a_1=1.5 fm^{-1}, ρ_2=56.262 $fm^{-3/2}$, a_2=3.5 fm^{-1}; see eq. V-2.2) was found to be intermediate between those of case I and case II. It has a narrow attractive pocket ($\sim$2 BeV, width $\sim$0.1 fm) followed by a repulsion of height $\sim$400 MeV at 0.25 fm; the attraction reaches a maximum of 41 MeV at 1.1 fm.

reflected in the behaviour of the half-shell matrix elements, principally in Figs. 10, 11 and 12. The localization of repulsion inside 0.5 fm for a local potential is reflected by the peak in the off-shell matrix elements at $p \sim 3$ fm^{-1}. Conversely the separable potentials usually (not case III) give a more smooth behaviour in this region.

Calculations of the symmetric half-shell function $\hat{s}(p,k)$ of Baranger et. al. were carried out. They give an idea of the behaviour of this function for realistic force models of the types generally considered. This function provides an alternative way of looking at the half-shell matrix elements. Some characteristic differences between strong core and weak core potentials may hold; Figs. 13, 14 and 15 illustrate them. The separable forces do tend to give a more constant value for $\hat{s}(p,k)$ as one goes off-shell. This function seems to magnify the differences between different forces. How is it that we find such close agreement between the half-shell matrix elements of many potentials when Baranger et. al. have shown that the behaviour of $\hat{s}(p,k)$ is arbitrary for $p \neq k$? Apparently there is a built in compensation between the symmetric and antisymmetric functions $\hat{s}$ and $\hat{a}$. Since $\hat{s}^2 - \hat{a}^2 = 1$, this is likely to occur, especially near the on-shell point.

The separable approximation of Noyes was found to be valid over a considerable range in p, q, or s for the reaction matrix. A similar separable approximation for

negative s matrix elements has been proposed by C. W. Wong[84] and B. H. Brandow[77] from their experience in nuclear matter calculations; we agree that this is remarkably good for uncoupled states. If it were really believed (which it is not) that the underlying potential were local, it would be much more accurate to use Noyes' separable approximation to the t_ℓ-matrix than to use a phase equivalent separable potential to generate a separable t_ℓ-matrix. In any case, the error in such an approximation is negligible compared to the basic uncertainty in the correct off-shell extension of the t_ℓ (or K_ℓ) matrix.

Equivalent momentum dependent potentials were obtained from the local potential of case I and the Hamada-Johnston potential. The comparison of the half-shell matrix elements indicated that wide variations in their behaviour could be produced; though, qualitatively, the shape of the curves remains similar to those from a local potential. When the hard core of the local potential was removed, the resulting p^2-dependent potentials were found to be much softer. It also had the effect of narrowing the small region of agreement around the on-shell point.

Nuclear matter calculations were carried out using all the sets of equivalent potentials in the $^1S_0$ state, and Reid Soft Core potential in the others. Small differences ($\lesssim$0.5 MeV) in the energy per particle, were found for the local and separable pairs of case I and case II. In

case III, the separable potential gave ∿5 MeV less binding (at k_F = 1.36 fm^{-1}) than the equivalent local potential. Larger differences (∿2 MeV at k_F = 1.36 fm^{-1}) were found amongst the sets of equivalent local and p^2-dependent potentials. However, in all cases, the differences are smaller than what one would expect from the behaviour of off-shell matrix elements at very high momenta. The reason is that after the potential energies of unoccupied states are set equal to zero, there is no way for far off-shell matrix elements to play a great role.

CHAPTER VI

SUMMARY AND COMMENTS

The off-shell behaviour of the nuclear reaction matrix has been investigated by developing (1) 'super' soft core local potentials SSC and SSC-NP-2 and several sets of phase shift equivalent separable, local and p^2-dependent potentials. The potentials SSC and SSC-NP-2 were developed (Sections IV-1 and 2) by assuming a very different high energy phase shift extrapolation (see eq. IV-2.1 and Fig. 4). The off-shell behaviour of these potentials was compared with that of the well known potentials of Reid and Hamada and Johnston in an attempt to see how the differences in the high energy on-shell behaviour (where the experimental data do not exist) affect the off-shell behaviour. Phase shift equivalent potentials (Sections V-2, 3 and 5) were employed to study the effects of different forms of non-locality on the off-shell behaviour. We have discussed our results at length in Sections IV-3, IV-4, V-4, V-6 and V-8, and gave our conclusions in Sections IV-5 and V-9. Here we summarize the main features and make some general comments.

Our study with local potentials indicated that the reaction matrix elements $K_0(p,q;s)$, when plotted against p for fixed values of q and s, show a repulsive hump*

---

* This feature was discussed by Bethe, Brandow and Petschek[79] for the nuclear matter G-matrix.

at $p \sim 3.5$ fm^{-1} indicating the localization of the repulsion at about 0.5 fm. The height of this hump decreases as the potential becomes softer. Greater differences in the behaviour are observed for higher q and s than for lower values indicating the greater role played by the repulsion as the energy increases. Momentum dependent potentials also give rise to similar behaviour, though the height of the hump and, to some extent, its position can be varied by choosing different expressions for the function y(r) (Section V-5). In contrast to this, the matrix elements from the separable potentials (with the exception of Tabakin's one term separable potential) show a smoother variation and are more repulsive for $p,q \gtrsim 3.5$ fm^{-1}. On the other hand diagonal matrix elements K(p,p;s) in all the cases show rather similar behaviour when plotted against p or s.

At the on-shell point the curves for the equivalent potentials were found to have almost the same slope with the result that in a region of about 100 MeV around the on-shell point, their behaviours are very similar. As s increases this region shrinks and does not exist for $s \gtrsim 4.5$ fm^{-2}. This shows why the experiments at low energy which do not go far off-shell are not suitable to study these differences.

The effective range formula for the low energy behaviour of the on-shell reaction matrix elements was generalized to the off-shell case (Appendix B). It was found

that the expansion

$$[K_0(p,q;k^2)]^{-1} = \frac{1}{a_0} - \frac{1}{2} r_0 k^2 - \frac{w_0}{a_0^2} (p^2+q^2-2k^2) + \ldots$$

involving a parameter w_0 besidesthe scattering length a_0 and the effective range r_0, gives a very good empirical fit to our off-shell matrix elements for p^2, q^2, $k^2 \lesssim 10$ MeV. This parameter (w_0) can be interpreted as the wound integral of the zero energy wave function (eq. (B.9)).

In nuclear matter calculations the two term separable potentials of Mongan and Tabakin and their equivalent local potentials give almost the same contribution to the energy per particle, although intermediate states up to about 3.5 fm^{-1} are involved in the second order correction term. The reason is that (i) the factor $\frac{1-Q(P,k')}{k'^2+\gamma^2}$ appearing in the correction term (eq. (V-7.4)) severely damps the possible differences and (ii) the contributions from three and four body clusters etc. have been ignored. It appears, contrary to what we believed earlier, that even nuclear matter calculations are not a very sensitive means of distinguishing the off-shell behaviour so far as equivalent separable and local potentials are concerned. Equivalent p^2-dependent potentials show relatively larger differences in the binding energy per particle. The potentials HJ-a, b, c and d give about 2.5 MeV more binding than the Hamada-Johnston potential at k_F=1.36 fm^{-1}, indicating that additional

binding can be obtained by removing the hard core. This would, ordinarily, move the nuclear matter saturation point to higher values of the Fermi momentum k_F. Our feeling is that its position can be maintained at any fixed value by applying similar isometric point transformations to other partial waves (in particular the $^3S_1$ state) and adjusting the parameters.

Tabakin's one term separable potential has a very different behaviour* because of the zero of the Jost function on the real k-axis. Its half-shell reaction matrix elements (where this zero does not matter) behave more like those from a local potential. Fully off-shell matrix elements $K_0(p,q;s)$ naturally have a pole at $s=k_c^2$ and vanish for $s<0$ whenever p or q is equal to k_c. In nuclear matter this potential gave a contribution of -9.5 MeV to the energy per particle at $k_F=1.36$ fm^{-1} while its equivalent local potential gave a contribution of -14.6 MeV.

It appears that proton-proton bremsstrahlung experiments at an energy of about 200 MeV or more with protons scattered at angles less than $\sim 25^\circ$ will be more sensitive to the differences in the off-shell behaviour. These calculations use half-shell matrix elements where the differences are more predominant (rather than fully off-shell

---

* Some other unfamiliar features of this potential have recently been discussed by Leung and Park[85].

diagonal matrix elements which play the main role in nuclear matter calculations) and are free from uncertainties regarding the contributions from three and four body clusters etc. At lower energies proton-proton bremsstrahlung will naturally be much less sensitive than the nuclear matter calculations.

Our method (Section V-1) of constructing a local potential from a separable potential gives only a pair of equivalent potentials rather than a whole family and is, therefore, not well suited to explore the off-shell behaviour over a wider range. We have no available free parameters to vary. In this respect phase shift equivalent p^2-dependent potentials have more room for manoeuvrability. One can start with a local potential having OPEP behaviour at large distances and introduce p^2-dependent terms at small and intermediate distances[86]. Another advantage is that the method can also be used for higher partial waves and can easily include Coulomb, spin-orbit and tensor forces.

If one is interested in reproducing a particular off-shell behaviour, it may be advantageous* to start from the symmetric function $\hat{s}_\ell(p,k)$ of Baranger et. al. The off-shell and on-shell behaviours may be separated by writing

---

* A similar suggestion, using Noyes-Kowalski half-shell functions $f_\ell(p,k)$ instead of $\hat{s}'_\ell(p,k)$ was made by Mongan[30,87].

it as

$$\hat{s}_\ell(p,k) = \hat{s}'_\ell(p,k)\ \hat{t}_\ell(k) \quad .$$

Here the on-shell t_ℓ-matrix $\hat{t}_\ell(k)$ ($\equiv \hat{s}_\ell(k,k) \equiv -\sin\delta_\ell(k)/k$) takes care of the on-shell data. The function $\hat{s}'_\ell(p,k)$ can be varied arbitrarily with the condition $\hat{s}'_\ell(k,k)=1$. Figs. 13, 14 and 15 suggest that

$$\hat{s}'_\ell(p,k) = 1 + \frac{\eta_1(p-k)^2}{1+\eta_2(p-k)^2}$$

may be a good form to use. η_1 and η_2 are the available parameters. Such a representation will be very useful in determining isospin T=1 matrix elements via the high energy proton-proton bremsstrahlung experiments. However, there is one disadvantage in this[33]: the difficulty in translating requirements on the tail of the potential (which is known to be OPEP) into restrictions on the t_ℓ-matrix.

The separable approximation* of Noyes was found to be quite accurate for energies less than about 200 MeV in the laboratory frame. We feel that, if the potential were really local, this approximation would be much more accurate than using a phase shift equivalent separable potential to generate a separable t_ℓ-matrix.

* This approximation has recently been improved[88] by adding additional separable terms. The non-physical poles in the Kowalski-Noyes approximation due to the zeroes of the on-shell t_ℓ-matrix are cancelled by these terms.

APPENDIX A

MODIFICATIONS IN THE METHOD OF CHAPTER III FOR THE CASE OF SECOND ORDER POLES

Here we present the modifications required in the procedure given in Chapter III for calculating the kernel $A(t,x)$ when the S-matrix has second order poles in the upper half k-plane. The method, in principle, consists of breaking these poles into neighbouring simple poles and then allowing them to coalesce. We first illustrate the the method by considering a simple S-matrix

$$S(k) = \left[\frac{(k-i\alpha)(k+i\beta)}{(k+i\alpha)(k-i\beta)}\right]^2 \qquad (A.1)$$

We replace the double pole at $k=i\beta$ by simple poles at $i\beta$ and $i\beta' = i(\beta+\varepsilon)$. The kernels $F(x+y)$ and $A(t,x)$ for the modified S-matrix can be easily obtained using eqs. (III-2.7) and (III-2.8)

$$F(x+y) = -\frac{1}{\varepsilon}\left(c'e^{-\beta'(x+y)} - ce^{-\beta(x+y)}\right) \qquad (A.2)$$

$$A(t,x) = \frac{1}{\varepsilon\Delta(t)}\left[c'e^{-\beta'(t+x)} - ce^{-\beta(t+x)} + \frac{cc'e^{-(\beta'+\beta)t}}{2\beta\beta'(\beta'+\beta)}\left(\beta'e^{-(\beta t+\beta' x)} - \beta e^{-(\beta' t+\beta x)}\right)\right] \qquad (A.3)$$

where

$$c' = 2\beta'(\sigma_2 + \sigma_1 \beta'^2)/(\beta' + \alpha)^2$$

$$c = 2\beta\ (\sigma_2 + \sigma_1 \beta^2)/(\beta + \alpha)^2 \qquad (A.4)$$

$$\sigma_1 = 2\alpha - \beta - \beta'$$

$$\sigma_2 = 2\alpha\beta\beta' - \alpha^2(\beta + \beta').$$

The terms containing β' in eq. (A.2) can be expanded in a Taylor series

$$c'e^{-\beta'(t+x)} - ce^{-\beta(t+x)} = (c_0 + \varepsilon\ \dot{c}_0' + \ldots.)e^{-\beta(t+x)}(1-\varepsilon(t+x)+\ldots.)$$

$$-(c_0 + \varepsilon\ \dot{c}_0 + \ldots..)e^{-\beta(t+x)}$$

$$= \varepsilon\{-c_0(t+x) + (\dot{c}_0' - \dot{c}_0)\}e^{-\beta(t+x)} + \ldots.. \qquad (A.5)$$

Here $c_0 = c(\beta'=\beta) = c'(\beta'=\beta)$, $\dot{c}_0' = \left(\frac{dc'}{d\beta'}\right)_{\beta'=\beta}$ and $\dot{c}_0 = \left(\frac{dc}{d\beta'}\right)_{\beta'=\beta}$.

Similarly

$$e^{-(\beta'+\beta)t}(\beta'\ e^{-(\beta t+\beta' x)} - \beta\ e^{-(\beta' t+\beta x)})$$

$$= \{(\beta+\varepsilon)(1 - \varepsilon(t+x) + \ldots..)$$

$$-\beta(1 - 2\varepsilon t + \ldots.)\}e^{-3\beta t-\beta x}$$

$$= \varepsilon\ \{\beta(t-x) + 1\}e^{-3\beta t-\beta x} + \ldots. \qquad (A.6)$$

The limit $\varepsilon \to 0$ can now be taken. We find

$$A(t,x) = \frac{1}{\Delta(t)}\ [\{-c_0(t+x) + (\dot{c}_0' - \dot{c}_0)\}$$

$$+ \frac{c_0^2 e^{-2\beta t}}{4\beta^3}\ \{\beta(t-x)+1\}]e^{-\beta(t+x)} \qquad (A.7)$$

The function $\Delta(t)$ appearing in eq. (A.7) can be similarly treated. We get

$$\Delta(t) = 1 + \left(\frac{c_0 t}{\beta} + \frac{c_0}{2\beta^2} - \frac{\dot{c}_0' - \dot{c}_0}{2\beta}\right) e^{-2\beta t} - \frac{c_0^2}{16\beta^4} e^{-4\beta t} \qquad (A.8)$$

It is to be noted that the relation

$$A(x,x) = \frac{d}{dx}\{\log \Delta(x)\}$$

is preserved.

In the case when there are more than one double pole the forms of eqs. (A.7) and (A.8) become a bit complicated. We have used the following procedure to evaluate them.

We break each double pole into two simple poles (two members) β_1, $\beta_1' = \beta_1 + \varepsilon_1$, β_2, $\beta_2' = \beta_2 + \varepsilon_2$, etc. and treat the terms not involving any member of the double poles in the usual way (the limit $\varepsilon \to 0$ can be taken straight away). The terms containing both members of the double poles are treated in a similar way. The factors $(\beta_1'-\beta_1)^2$, $(\beta_2'-\beta_2)^2$, etc. occurring in the denominator cancel exactly with those in the numerator. The terms involving members belonging to different double poles are grouped together according to the number of the members. The number of terms in a group is 2^{n_d} where n_d is the number of double poles. In the terms containing both members of some of the double poles, we take the limit $\varepsilon \to 0$ corresponding to these double poles directly. Then such terms are grouped together and evaluated

as indicated above.

This method can be generalized for higher order poles.

APPENDIX B

LOW ENERGY BEHAVIOUR OF OFF-SHELL REACTION MATRIX ELEMENTS $K_o(p,k;\tau^2)$

The on-shell K-matrix elements obey the effective range formula at laboratory energies up to about 10 MeV corresponding to $\tau^2 \approx 0.25$ fm^{-2}. This is simply a power series expansion of the inverse of the on-shell K-matrix element, the linear term in powers of momentum being absent. The inverse has to be used because of the nearby antibound state pole, which would otherwise limit the radius of convergence to $\tau^2 \lesssim 0.0016$ fm^{-2}. We now show that to describe the off-shell behaviour, a further parameter is required which can be interpreted as the wound integral of the zero energy wavefunction.

Considering an uncoupled $\ell=0$ state, the off-shell K_o-matrix element is determined by the solution of

$$(\frac{d^2}{dr^2}+s)\psi(k,s,r) = v(r)\psi(k,s,r)+(s-k^2)\sin(kr), \quad s=\tau^2 \qquad (B.1)$$

Introducing the wave defect

$$\chi(k,s,r) = \phi(k,r) - \psi(k,s,r)$$

where $\phi(k,r) = \sin(kr)$, we find

$$(\frac{d^2}{dr^2}+s)\ \chi(k,s,r) = -v(r)\ \psi(k,s,r)$$

with

$$\chi(k,s,r=0) = 0$$

or $\chi(k,s,r=c) = \sin(kc)$ for hard core potential of radius c

and

$$\chi(k,s,r\to\infty) \to A(k,\tau)\cos(\tau r),\ s=\tau^2>0$$
$$\to A(k,\tau)e^{-\gamma r},\ s=-\gamma^2=\tau^2<0 \qquad (B.2)$$

provided the potential can be neglected at large r. At large distances the asymptotic limit of χ, $\bar{\chi}$, satisfies

$$\left(\frac{d^2}{dr^2}+s\right)\bar{\chi}(k,s,r) = 0 \qquad (B.3)$$

We require $\bar{\chi}$ at all r, just as in the usual derivation of the effective range theory. Combining eqs. (B.1) and (B.3) with the free wave equation

$$\left(\frac{d^2}{dr^2}+p^2\right)\phi(p,r) = 0 \qquad (B.4)$$

we get

$$\{\phi(p,r)\chi'(k,s,r)-\chi(k,s,r)\phi'(p,r)\}\Big|_a^R + (\tau^2-p^2)\int_a^R \phi(p,r)\chi(k,s,r)dr$$
$$= -\int_a^R \phi(p,r)v(r)\psi(k,s,r)dr$$

$$\{\phi(p,r)\bar{\chi}'(k,s,r)-\bar{\chi}(k,s,r)\phi'(p,r)\}\Big|_a^R+(\tau^2-p^2)\int_a^R \phi(p,r)\bar{\chi}(k,s,r)dr=0$$

Letting the distances $R\to\infty$, $a\to 0$ only the value of $\bar{\chi}$ at r=0

contributes from the boundary terms. This gives

$$\frac{A(k,\tau)}{k} - \frac{(\tau^2-p^2)}{pk}\int_0^\infty \phi(p,r)\{\chi(k,s,r)-\bar{\chi}(k,s,r)\}dr$$

$$= \frac{1}{pk}\int_0^\infty \phi(p,r)v(r)\psi(k,s,r)dr$$

$$= K_o(p,k;\tau^2) \ . \qquad (B.5)$$

Considering the half-shell element $\tau^2=p^2$ (possible only when $\tau^2>0$) we identify

$$A(k,\tau) = kK_o(\tau,k;\tau^2) \equiv kK_o(k,\tau;\tau^2)$$

This gives

$$K_o(p,k;\tau^2) = K_o(k,\tau;\tau^2) + \frac{(p^2-\tau^2)}{pk}\int_0^\infty \phi(p,r)\{\bar{\psi}(k,s,r)-\psi(k,s,r)\}dr. \qquad (B.6)$$

Here $\bar{\psi}$ represents the asymptotic limit of ψ in analogy to eq. (B.3). A well known special case of this result is an expression for the half-shell element[89]

$$K_o(p,k;k^2) = -\frac{\tan\delta_o(k)}{k} + \frac{(p^2-k^2)}{pk}\int_0^\infty \phi(p,r)\{\bar{\psi}(k,r) - \psi(k,r)\}dr, \qquad (B.7)$$

where $\psi(k,r) \equiv \psi(k,k^2,r)$. Obviously the half-shell element in eq. (B.6) can be replaced by eq. (B.7).

At low energies

$$\frac{1}{p}\ \phi(p,r) = \frac{\mathrm{Sin}(pr)}{p} \approx r - 0(\frac{p^2r^3}{6})$$

while

$$\{\frac{\bar{\psi}(k,s,r) - \psi(k,s,r)}{k}\} \approx \lim_{k,s\to 0} \{\frac{\bar{\psi}(k,s,r) - \psi(k,s,r)}{k} + O(k,\tau).$$

Thus if we are interested only in corrections of order p^2, k^2, $\tau^2(=s)$ we can write

$$K_o(p,k;\tau^2) \approx K_o(k,\tau;\tau^2) + w_o(p^2-\tau^2) \tag{B.8}$$

where

$$w_o = \lim_{k,s\to 0} \int_0^\infty r\{\frac{\bar{\psi}(k,s,r) - \psi(k,s,r)}{k}\}dr. \tag{B.9}$$

This is a wound integral in the same sense as in the Brueckner theory[77]. However we should note that this zero energy wound integral has a value much larger than the usual Brueckner wound integral which is evaluated far off-shell.

Using relation (B.8) in a half-shell case we deduce

$$K_o(p,k;\tau^2) \approx K_o(\tau,\tau;\tau^2) + w_o(p^2+k^2-2\tau^2)$$

$$\approx \frac{a_o}{1 - \frac{1}{2} a_o r_o \tau^2} + w_o(p^2+k^2-2\tau^2)$$

or

$$[K_o(p,k;\tau^2)]^{-1} \approx \frac{1}{a_o} - \frac{1}{2} r_o \tau^2 - \frac{w_o}{a_o^2}(p^2+k^2-2\tau^2) \tag{B.10}$$

where we have used the effective range form of the on-shell K-matrix elements with the same accuracy as before. The

symbols a_o and r_o are the scattering length and the effective range. Thus the result is that three parameters, a_o, r_o and w_o suffice to describe the low energy off-shell behaviour.

In Figs. 31, 32 and 33 we have tested this formula against our results for the case I local potential. The scattering length and the effective range for this case are -23.99 fm and 2.37 fm respectively, while the parameter w_o, obtained from the limiting value of the slope of $[K_o(k,k;s)]^{-1}$ vs k^2 curves for a fixed small value of s, is 16 fm^3. The inverse of reaction matrix element has been plotted against p^2, k^2 or $s(=\tau^2)$ for ease in comparison. Fig. 31 shows diagonal matrix elements $K_o(k,k;s)$ plotted against k^2 for fixed values of s, while in Fig. 32 they are plotted against s for fixed k^2. Fig. 33 shows half-shell matrix elements $K_o(p,k;k^2)$ plotted against p^2. In all cases we find that the agreement is very good up to p^2, k^2, $s(=\tau^2)$ of order 0.1 fm^{-2}. The curves are almost parallel straight lines; their curvature gradually begins to change as the energy increases. It is observed that the slope of the half-shell curves in Fig. 33 is just half that of the fully off-shell ones of Fig. 31, in agreement with the prediction of the formula (B.10) for the low energy behaviour.

The on-shell effective range formula is often used for negative τ^2, to relate the deuteron binding energy to the $^3S_1$ state a_o and r_o. The present off-shell formula (B.10) should be equally applicable to negative τ^2. However,

we should keep in mind that $K_o^{-1}(p,k;\tau^2)$ is not analytic at s=0 in $s(=\tau^2)$ plane. The step function in eqs. (II-3.8-10) indicates just this. If $K_o'^{-1}$ defines the analytic continuation of K_o^{-1} from $\tau^2>0$ to $\tau^2<0$, eqs. (II-3.9) and (II-3.11) give

$$K_o^{-1} = t_o = K_o'^{-1} - \gamma \tag{B.11}$$

for $\tau^2 = -\gamma^2<0$. The expression (B.10) gives this K' instead of K. The generalization

$$[K_o(p,k;\tau^2)]^{-1} \approx \frac{1}{a_o} - \frac{1}{2}r_o\tau^2 - \frac{w_o}{a_o^2}(p^2+k^2-2\tau^2) - |\tau|\,\theta(-\tau^2) \tag{B.12}$$

obtained by using (B.11) in (B.10) is applicable both for positive and negative τ^2.

REFERENCES

(1) R. A. Bryan and B. L. Scott, Phys. Rev. 135B (1964) 434

(2) A. Scotti and D. Y. Wong, Phys. Rev. 138B (1965) 145

(3) E. L. Lomon and H. Feshbach, Rev. Mod. Phys. 39 (1967) 611

(4) D. Kiang, M. A. Preston and P. C. Yip, Phys. Rev. 170 (1968) 907

(5) H. Sugawara and F. Von Hippel, Phys. Rev. 172 (1969) 1764

(6) J. L. Gammel and R. M. Thaler, Phys. Rev. 107 (1957) 291, 1337

(7) T. Hamada and I. D. Johnston, Nucl. Phys. 34 (1962) 382

(8) K. E. Lassila, M. H. Hull, H. M. Ruppel, F. A. MacDonald and G. Breit, Phys. Rev. 126 (1962) 881

(9) R. V. Reid, Jr., Ann. Phys. (N.Y.) 50 (1968) 411

(10) C. N. Bressel, A. K. Kerman and B. Rouben, Nucl. Phys. A124 (1968) 624

(11) A. M. Green, Phys. Lett. 1 (1962) 136
A. M. Green, Nucl. Phys. 33 (1962) 218

(12) F. Tabakin and K. T. R. Davies, Phys. Rev. 150 (1966) 79

(13) J. H. Naqvi, Nucl. Phys. 58 (1964) 289

(14) F. Tabakin, Ann. Phys. (N.Y.) 30 (1964) 51

(15) T. R. Mongan, Phys. Rev. 175 (1968) 1260

(16) T. R. Mongan, Phys. Rev. 178 (1969) 1597

(17) F. Tabakin, Phys. Rev. 174 (1968) 1208

(18) G. L. Strobel, Nucl. Phys. A116 (1968) 465

(19) H. C. Lee, Thesis, McGill University (1969), unpublished

(20) R. J. W. Hodgson, Can. J. Phys. 47 (1969) 499

(21) T. F. Hammann and Q. Ho-kim, Nuovo Cimento 64B (1969) 356

(22) P. C. Bhargava and D. W. L. Sprung, Ann. Phys. (N.Y.) 42 (1967) 222

(23) P. K. Banerjee and D. W. L. Sprung, private communication

(24) V. Brown, Phys. Rev. 177 (1969) 1498

(25) D. Marker and P. Signell, Phys. Rev. 185 (1969) 1286

(26) R. P. Lynch and T. T. S. Kuo, Nucl. Phys. A95 (1967) 561

(27) R. Laughlin and B. L. Scott, Phys. Rev. 171 (1968) 1196

(28) K. L. Kowalski, Phys. Rev. Lett. 15 (1965) 798

(29) H. P. Noyes, Phys. Rev. Lett. 15 (1965) 538

(30) T. R. Mongan, Phys. Rev. 180 (1969) 1514

(31) H. Ekstein, Phys. Rev. 117 (1960) 1590

(32) H. Fiedeldey, Nucl. Phys. A135 (1969) 353

(33) F. Coester, S. Cohen, B. Day and C. M. Vincent, preprint

(34) P. Mittlstaedt and M. Ristig, Z. Physik 193 (1966) 349

(35) M. Ristig, Z. Physik 199 (1967) 325

(36) G. A. Baker, Jr., Phys. Rev. 128 (1962) 1485

(37) M. Ristig and S. Kistler, Z. Physik 215 (1968) 419

(38) M. D. Miller, M. S. Sher, P. Signell, N. R. Yoder and D. Marker, Phys. Lett. 30B (1969) 157

(39) S. Kistler, Z. Physik 223 (1969) 447

(40) M. L. Goldberger and K. M. Watson, Collision Theory (Wiley, New York, 1964)

(41) R. Jost and A. Pais, Phys. Rev. 82 (1951) 840

(42) R. G. Newton, J. Math. Phys. 1 (1960) 319

(43) J. E. Beam, Phys. Lett. 30B (1969) 67

(44) D. Gutkowski and A. Scalia, J. Math. Phys. 9 (1968) 588

(45) K. M. Watson and J. Nuttal, Topics in Several Particle Dynamics (Holden-Day, California, 1967)

(46) K. L. Kowalski and D. Feldman, J. Math. Phys. 2 (1961) 499; 4 (1963) 507

(47) J. Y. Guennégues, Nuovo Cimento 42A (1966) 549

(48) D. Y. Wong and G. Zambotti, Phys. Rev. 154 (1967) 1540

(49) J. S. Ball and D. Y. Wong, Phys. Rev. 169 (1968) 1362

(50) M. G. Fuda, Phys. Rev. 174 (1968) 1134

(51) D. R. Hartree, Numerical Analysis (Oxford, 1958)

(52) E. C. Ridley, Proc. Cambridge Phil. Soc. 53 (1957) 442

(53) S. A. Moszkowski and B. L. Scott, Ann. Phys. (N.Y.) 11 (1960) 65

(54) I. M. Gel'fand and B. M. Levitan, Izvestia Akad. Nauk S.S.S.R. Ser. Math. 15 (1951) 309

(55) V. A. Marchenko, Dokl. Akad. Nauk S.S.S.R. 72 (1950) 47. See also V. deAlfaro and T. Regge, Potential Scattering (North-Holland Publishing Co., Amsterdam, 1965), p. 150

(56) R. Omnes, Nuovo Cimento 21 (1961) 524

(57) M. Bolsterli and J. Mackenzie, Physics (U.S.A.) 2 (1965) 141

(58) F. Tabakin, Phys. Rev. 177 (1969) 1443

(59) A. Martin, Nuovo Cimento 19 (1961) 1257

(60) R. Jost and W. Kohn, Kgl. Danska Videnskab. Selskab Mat. Fys. Medd 27, No. 9 (1953)

(61) R. G. Newton and R. Jost, Nuovo Cimento 1 (1955) 590

(62) R. G. Newton, Phys. Rev. 100 (1955) 412

(63) R. G. Newton and T. Fulton, Phys. Rev. 107 (1957) 1103

(64) J. Benn and G. Scharf, Nucl. Phys. A134 (1969) 481

(65) V. Bargmann, Rev. Mod. Phys. 21 (1949) 488

(66) M. H. MacGregor, R. A. Arndt and R. M. Wright, Phys. Rev. 182 (1969) 1714

(67) M. J. D. Powell, J. Computer 7 (1964) 155

(68) M. Razavy, Nucl. Phys. 50 (1964) 465

(69) A. Kallio and B. D. Day, Nucl. Phys. A124 (1969) 177

(70) J. P. Elliott, A. D. Jackson, H. A. Mavromatis, E. A. Sanderson and B. Singh, Nucl. Phys. A121 (1968) 241

(71) D. W. L. Sprung and M. K. Srivastava, Nucl. Phys. A139 (1969) 605

(72) M. K. Srivastava, Nucl. Phys. A144 (1970) 236

(73) A. N. Mitra and V. L. Narasimham, Nucl. Phys. 14 (1960) 407

(74) Y. Yamaguchi, Phys. Rev. 95 (1954) 1628

(75) A. S. Reiner, Nuovo Cimento 51A (1967) 1

(76) M. Baranger, B. Giraud, S. K. Mukhopadhyay and P. U. Sauer, Nuc. Phys. A138 (1969) 1

(77) G. Dahll, E. Ostgaard and B. H. Brandow, Nuc. Phys. A124 (1969) 481

(78) H. S. Köhler, Nuc. Phys. A128 (1969) 273

(79) H. A. Bethe, B. H. Brandow and A. G. Petschek, Phys. Rev. 129 (1963) 225

(80) R. Rajaraman and H. A. Bethe, Rev. Mod. Phys. 39 (1968) 745

(81) P. K. Banerjee and D. W. L. Sprung, to be published

(82) T. K. Dahlblom, Thesis, Acta. Acad. Aboensis Ser B, Vol. 29, (1969), No. 6

(83) B. Day, "Four Body Clusters in Nuclear Matter", ANL preprint

(84) C. W. Wong, private communication to Dr. D. W. L. Sprung

(85) C. C. H. Leung and S. C. Park, Phys. Rev. 186 (1969) 1297

(86) P. Signell, "The Nuclear Potential" in Advances in Nuclear Physics, Vol. II, Eds. M. Baranger and E. Vogt (Plenum Press, N.Y., 1969)

(87) T. R. Morgan, Phys. Rev. 184 (1969) 1888

(88) T. A. Osborn, Nuc. Phys. A138 (1969) 305

(89) T. Fulton and P. Schwed, Phys. Rev. 115 (1959) 973

FIGURE CAPTIONS

Figure 1 Complex k-plane, showing the redundant poles (marked x, at $k=i\beta$) and resonance poles (marked 0, at $k=-i\alpha$) of the S-matrix, eq. (IV-2.1), fitted to observed phase shifts.

Figure 2 N-P $^1S_0$ phase shifts of MacGregor, Arndt and Wright (a) compared to potential models SSC (b), SSC-NP-2 (c), and Reid Soft Core (d). Phases are in degrees.

Figure 3 Potentials SSC (solid line), SSC-NP-2 (dash line), and Reid Soft Core (dot line), in MeV, plotted as functions of r (fm).

Figure 4 High energy phase shift for several potentials: (a) SSC-NP-2, (b) SSC, (c) Reid Soft Core, (d) Hamada-Johnston, (e) a pure hard core of radius 0.3 fm. Small circles are points on the energy dependent phase shift analysis (Ref. 66) while the error bars indicate three of their single energy analyses at 630 MeV.

Figure 5(i) Radial wave functions compared to the unperturbed (sin kr) plotted for the potential SSC-NP-2 at E=20 MeV laboratory energy.

Figure 5(ii) Same as Fig. 5(i), but for E=60 MeV.

Figure 5(iii) Same as Fig. 5(i) but for E=140 MeV.

Figure 5(iv) Same as Fig. 5(i) but for E=240 Mev.

Figure 5(v) Same as Fig. 5(i) but for E=360 MeV.

Figure 6(i) Ratio of half-off-energy-shell to on-energy-shell matrix elements as a function of the final state momentum p. Several potentials are shown as follows: (a) SSC, (b) SSC-NP-2, (c) Reid Soft Core, (d) Hamada-Johnston, (e) the separable potential, case 2 of Mongan[16]. Initial state energy is 20 MeV.

Figure 6(ii) Same as Fig. 6(i) but for initial state energy 60 MeV.

Figure 6(iii) Same as Fig. 6(i) but for initial state energy 140 MeV.

Figure 6(iv) Same as Fig. 6(i) but for initial state energy 360 MeV.

Figure 7 Diagonal relative matrix elements of the $^1S_0$ potential between oscillator states, as function of the oscillator length $b = \sqrt{\frac{\hbar}{m\omega}}$. Curve (a) is for potential SSC-NP-2, (b) for SSC, (c) for the matrix elements of Elliott et. al.[70].

Figure 8 Equivalent local potentials of case I (Mongan, dotted line) and case II (Tabakin two term, dash-dot line) compared to Reid Soft Core potential (solid line).

Figure 9 Equivalent local potential of case III

Figure 9 (cont'd.)

(Tabakin one term, dash-dot line) compared to Hamada-Johnston potential (solid line). The distance, in fm, starts at the Hamada-Johnston hard core radius.

Figure 10 Half-shell reaction matrix elements for case I. Lines a, c and e are for the local potential for initial energies of 60, 200 and 360 MeV respectively. Lines b, d and f are the corresponding curves for the separable potential.

Figure 11 Same as Fig. 10 but for case II.

Figure 12 Same as Fig. 10 but for case III. Small insert at upper left belongs to the lower left corner.

Figure 13 Symmetric half-shell function of Baranger et. al. for case I potentials. Broken lines are for the separable potential and the solid ones for the equivalent local potential. The left of the figure is the on-shell point for each curve. Pairs of lines a to g correspond to the indicated value of (p+k) in fm^{-1}. The abscissa $|p-k|$ measures the off-shell distance in fm^{-1}.

Figure 14 Same as Fig. 13 but for case II. Note again that the pair of corresponding lines join on the left.

Figure 15 Same as Fig. 13 but for case III.

Figure 16 Fully off-shell matrix elements for the potentials of case I. Solid lines are for the separable potential, dashed lines are for the local potential and dotted lines for the separable approximation of Noyes. The curves correspond to the initial momentum q as follows: a: 20 MeV, b: 60 MeV, c: 140 MeV, d: 240 MeV, e: 360 MeV. The four parts correspond to different starting energies as follows: 16(i): k^2=1 MeV, 16(ii): k^2=40 MeV, 16(iii): k^2=100 MeV, 16(iv): k^2=140 MeV. Note that in part (i) dotted lines for the separable approximation of Noyes have not been drawn for q corresponding to 60 and 240 MeV.

Figure 17 Off-shell behaviour of diagonal matrix elements for the case I potentials. Solid lines are for the local potential and dashed lines for the separable. Different pairs of lines correspond to different momenta k as follows: a: 20 MeV, b: 40 MeV, c: 60 MeV, d: 140 MeV, e: 360 MeV.

Figure 18 Same as Fig. 17 but for the case II potentials.

Figure 19 Off-shell behaviour of a typical diagonal matrix element for the case III potentials. The momentum k corresponds to 60 MeV. Notice that the separable potential gives rise to a pole, due to the zero of the Jost function on the real s-axis.

Figure 20 Diagonal off-shell negative energy matrix element for the case I potentials. Solid lines are for local potential and dashed lines are for separable potential. Curves a, b and c correspond to $\gamma^2 = 0.25$, 2.25 and 5.76 fm^{-2} respectively.

Figure 21 Same as Fig. 20 but for the case II potentials.

Figure 22 Same as Fig. 20 but for the case III potentials. Notice the zero of the off-shell matrix element for the separable potential due to the zero of the form factor at k=1.7 fm^{-1}.

Figure 23 Separable approximation to the negative energy off-shell matrix elements of the case I local potential. The abscissa is the momentum q in fm^{-1}. Curves a and b are for momentum p corresponding to 40 MeV and 140 MeV respectively. The solid line is the actual value and dotted line is the separable approximation of eq. (V-4.2).

Figure 24(i) Half-shell reaction matrix elements for the case I local potential and its equivalent p^2-dependent potentials I-a and I-b. Initial state energy is 20 MeV.

Figure 24(ii) Same as Fig. 24(i) but for initial state energy of 140 MeV.

Figure 24(iii) Same as Fig. 24(i) but for initial state energy of 360 MeV.

Figure 25(i) Half-shell reaction matrix elements for Hamada-Johnston (HJ) and its equivalent p^2-dependent potentials HJ-a, HJ-b, HJ-c and HJ-d. Initial state energy is 20 MeV.

Figure 25(ii) Same as Fig. 25(i) but for initial state energy of 140 MeV.

Figure 25(iii) Same as Fig. 25(i) but for initial state energy of 360 MeV.

Figure 26 Off-shell behaviour of a typical diagonal matrix element for the case I local potential and its equivalent p^2-dependent potentials I-a and I-b.

Figure 27 Off-shell behaviour of a typical diagonal matrix element for Hamada-Johnston (HJ) and its equivalent p^2-dependent potentials HJ-a, HJ-b, HJ-c and HJ-d.

Figure 28 Contribution to binding energy per particle in nuclear matter from several $^1S_0$

Figure 28 (cont'd.)

state potentials. Curve RSC is for Reid Soft Core potential. Pairs of curves labelled I, II, III refer to pairs of phase equivalent local (solid lines) and separable (dashed lines) potentials of cases I, II and III respectively.

Figure 29 Same as Fig. 28 but for the case I separable and local potentials and their equivalent p^2-dependent potentials I-a and I-b.

Figure 30 Same as Fig. 28 but for Hamada-Johnston (HJ) and its equivalent p^2-dependent potentials HJ-a, HJ-b, HJ-c and HJ-d.

Figure 31 Inverse of reaction matrix elements $K_0(k,k;s)$ for s=0, 1, 2 and 4 MeV. Solid lines give exact variation for the case I local potential while the dashed ones correspond to the formula (B.10).

Figure 32 Off-shell behaviour of the inverse of diagonal matrix elements $K_0(k,k;s)$ for (a) $k=0.15$ fm^{-1} and (b) $k=0.3$ fm^{-1}. Solid lines give exact variation for the case I local potential while the dashed ones correspond to the formula (B.10).

Figure 33 Inverse of half-shell reaction matrix elements $K_0(p,k;k^2)$ for k=0.05, 0.15, 0.25

Figure 33 (cont'd.)

and 0.35 fm^{-1}. Solid lines give exact variation for the case I local potential while the dashed ones correspond to the formula (B.10).

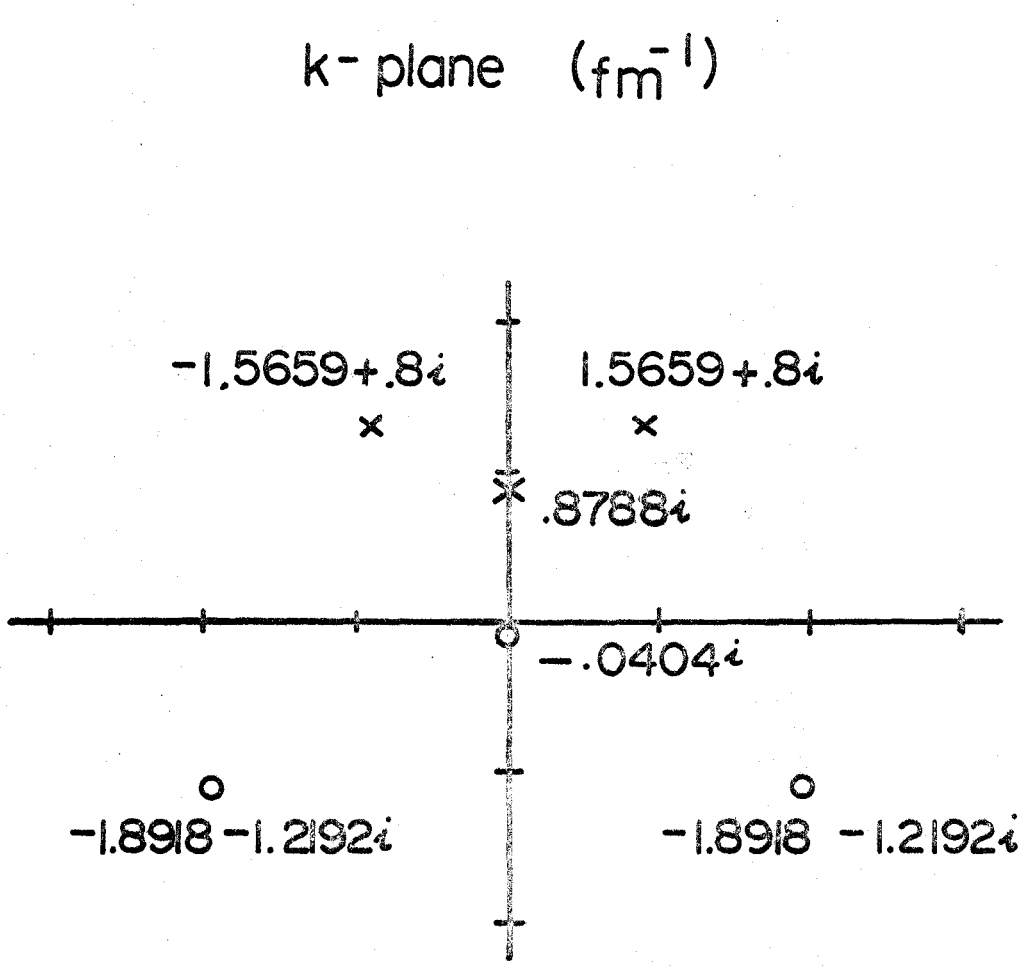
k - plane (fm⁻¹)
-1.5659+.8i
1.5659+.8i
.8788i
-.0404i
-1.8918 -1.2192i
-1.8918 -1.2192i

Figure 1

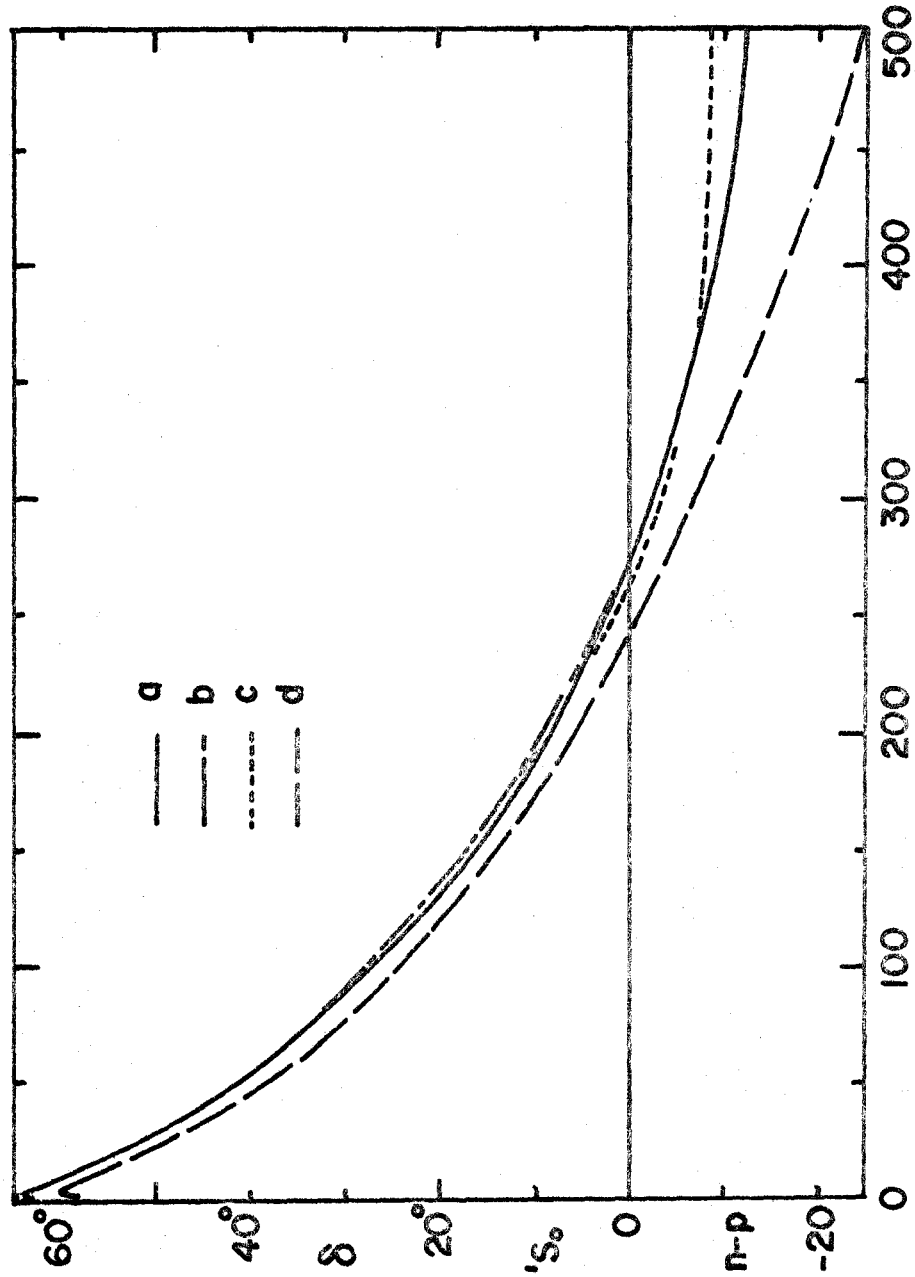

Figure 2

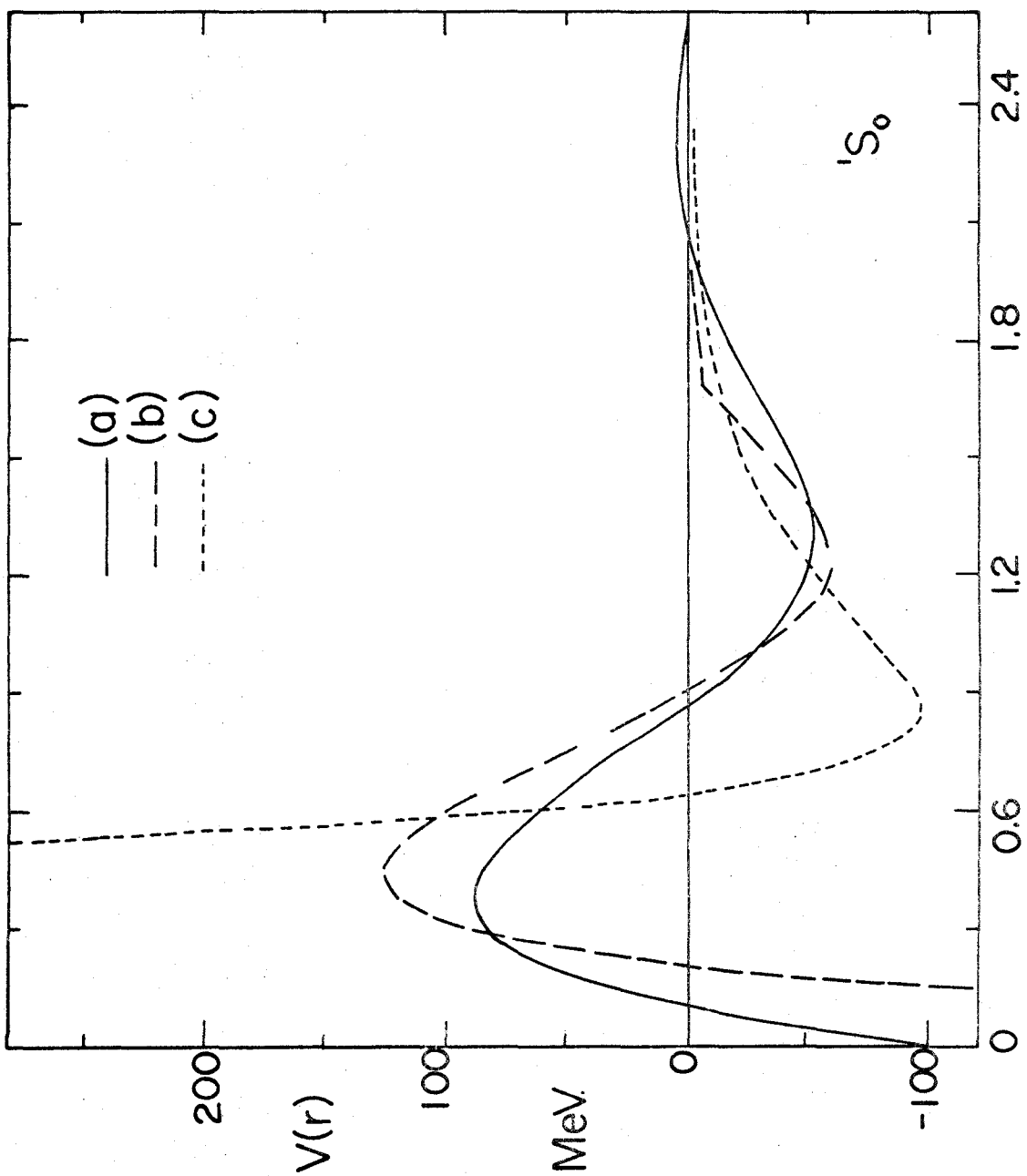

Figure 3

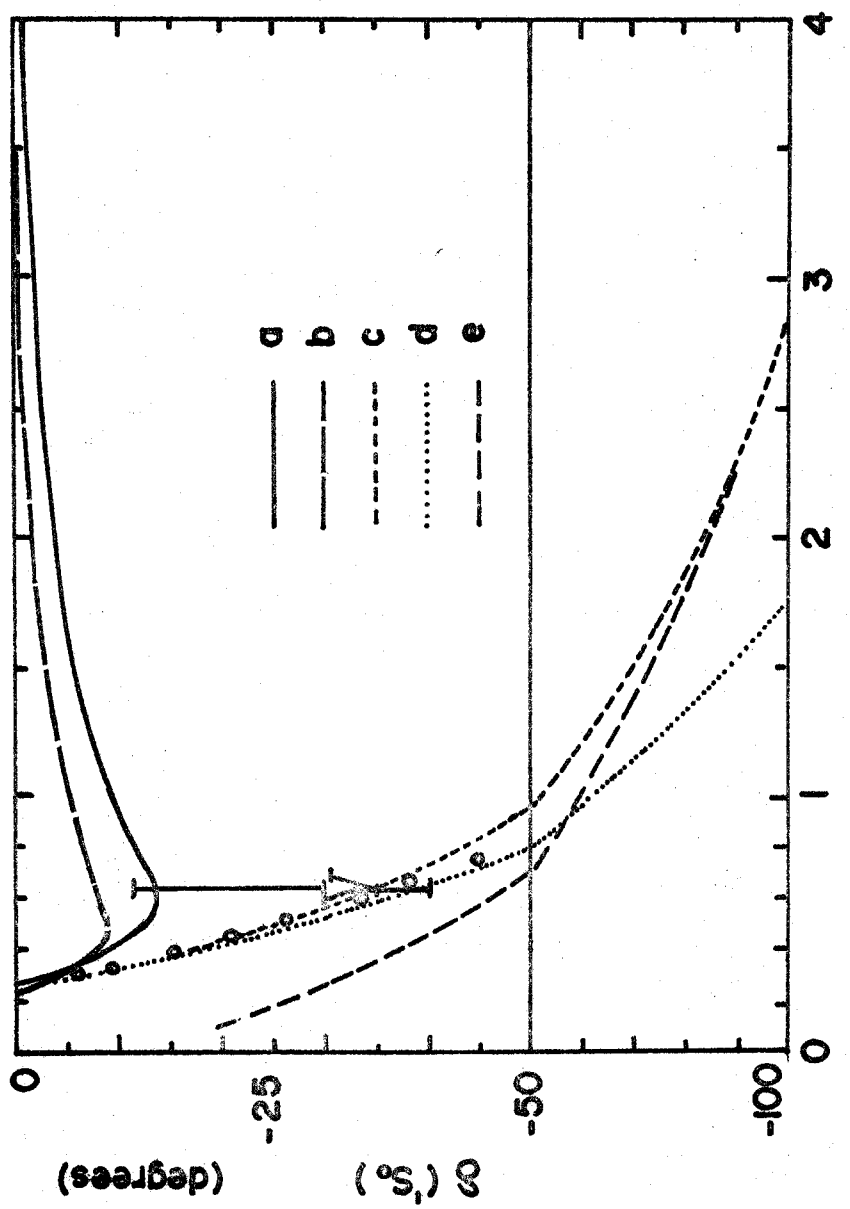

Figure 4

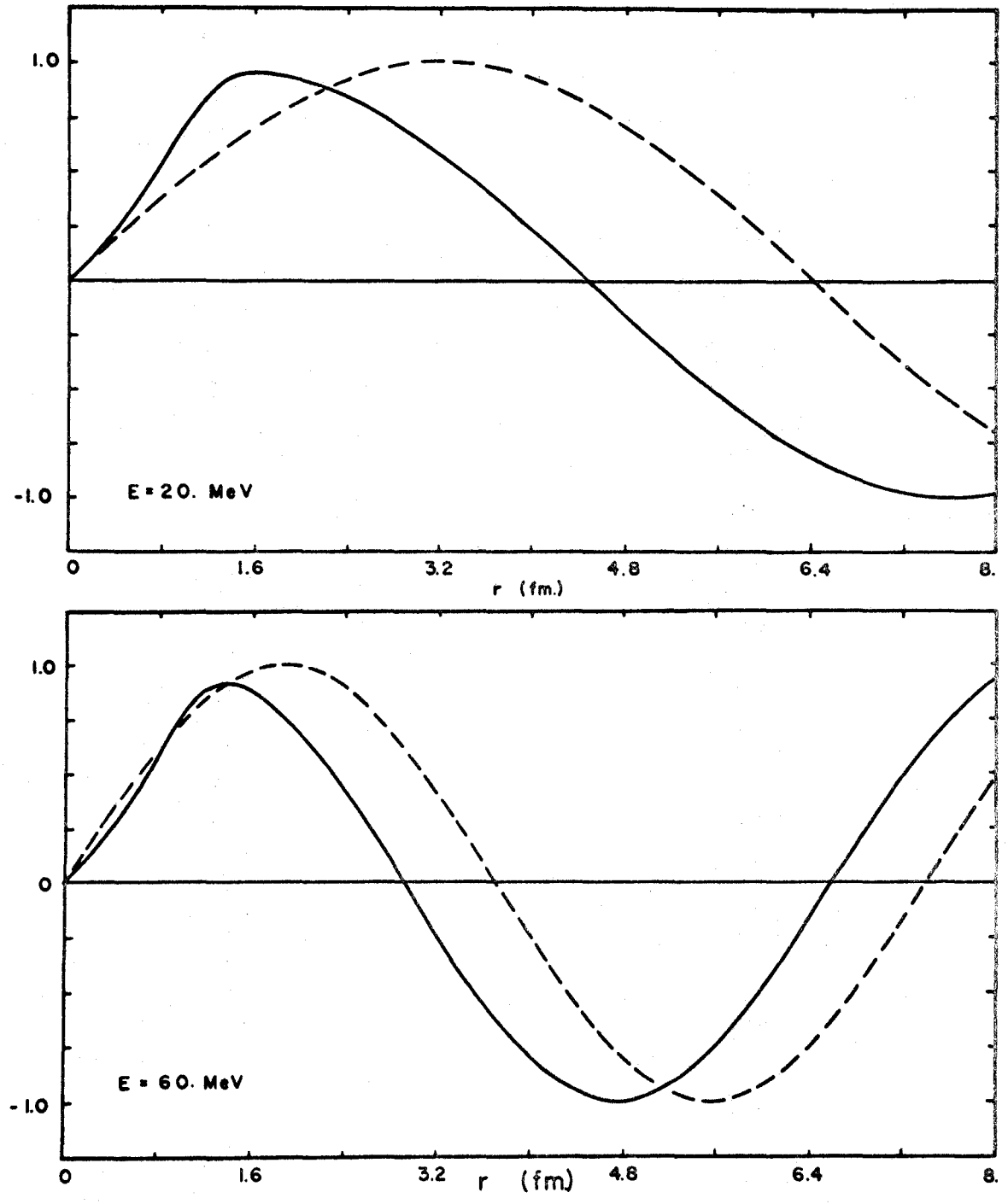

Figures 5(i) and 5(ii)

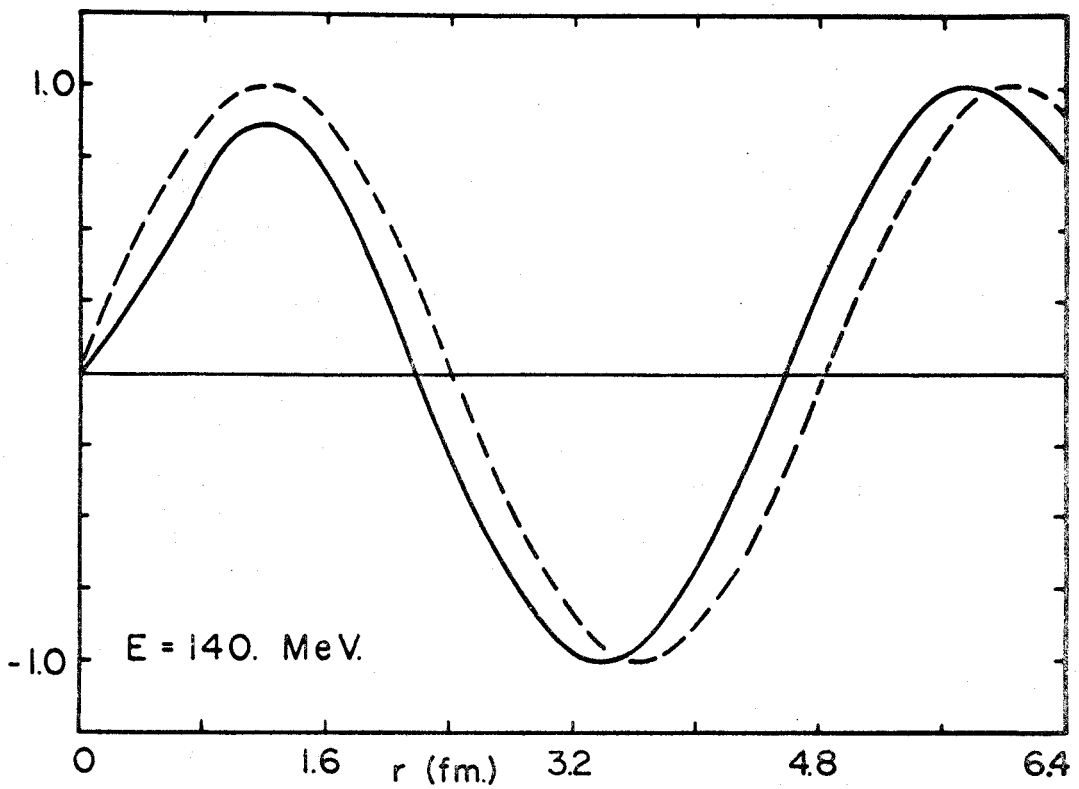

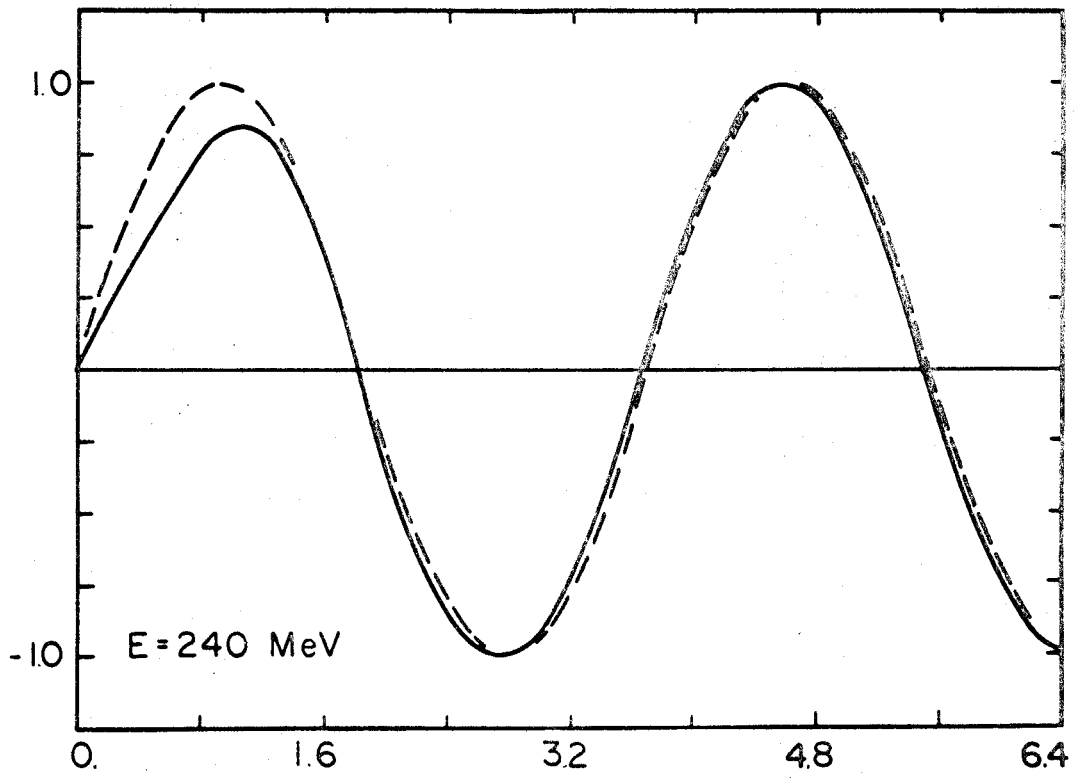

Figures 5(iii) and 5(iv)

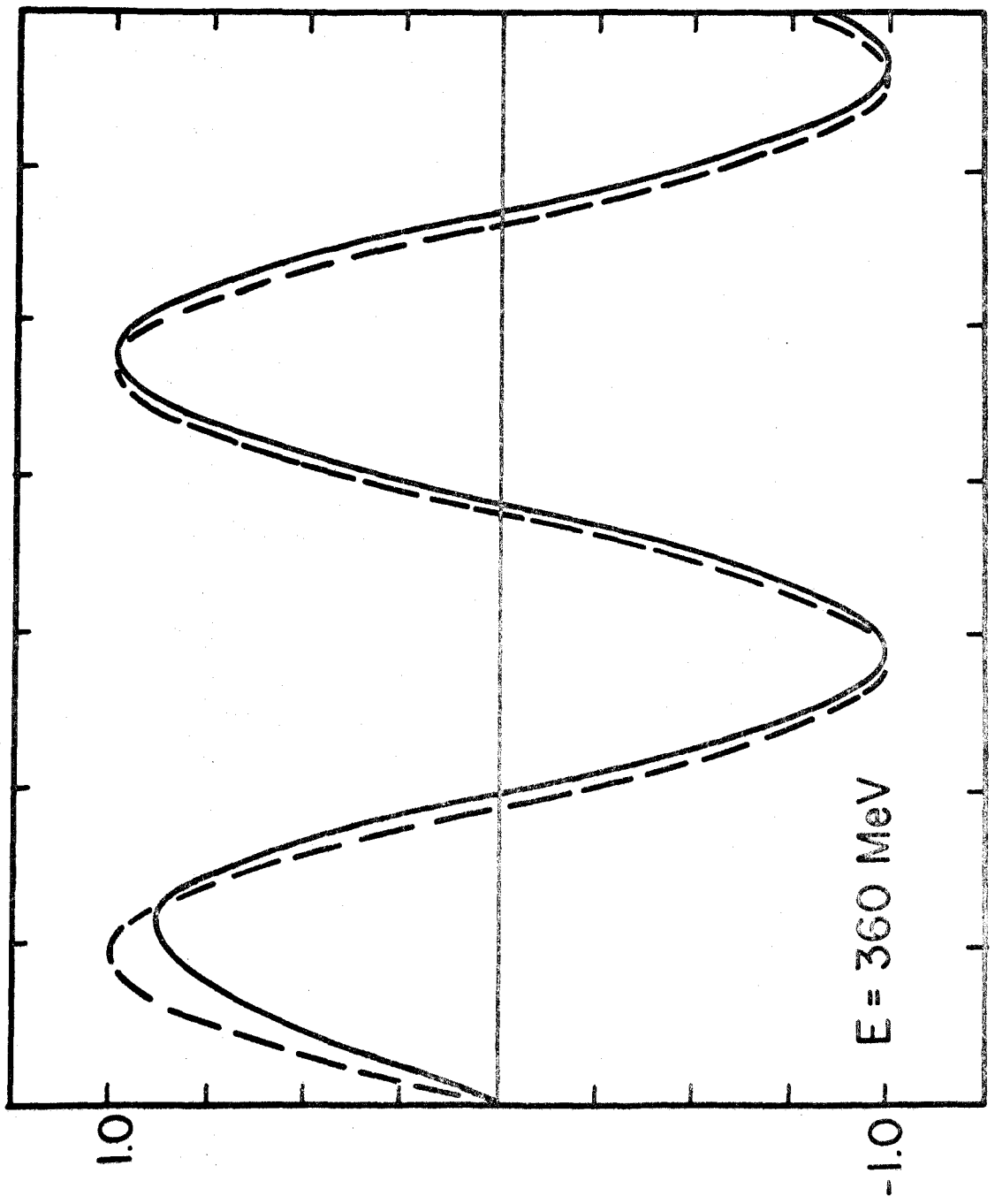

Figure 5(v)

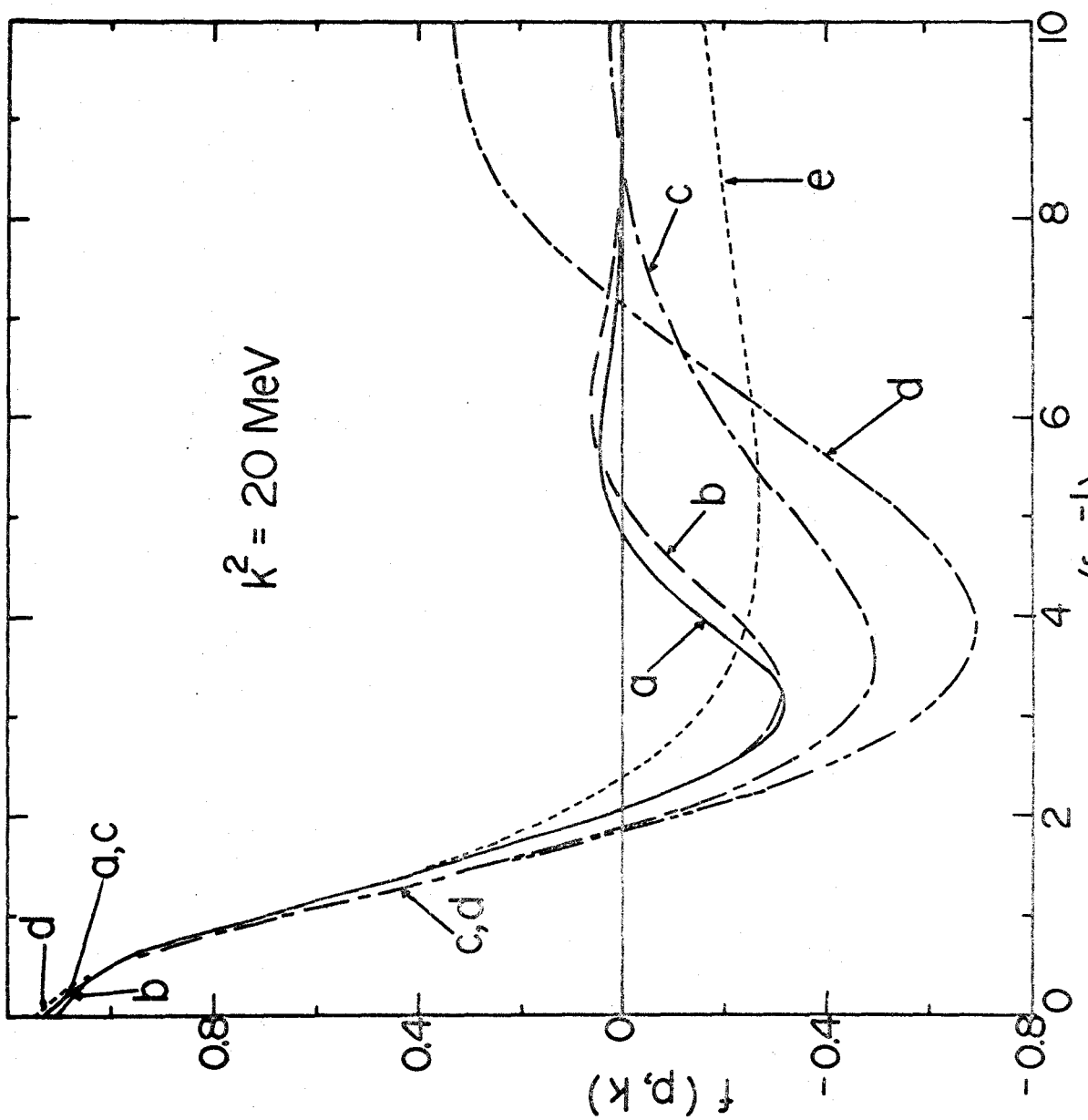

Figure 6(i)

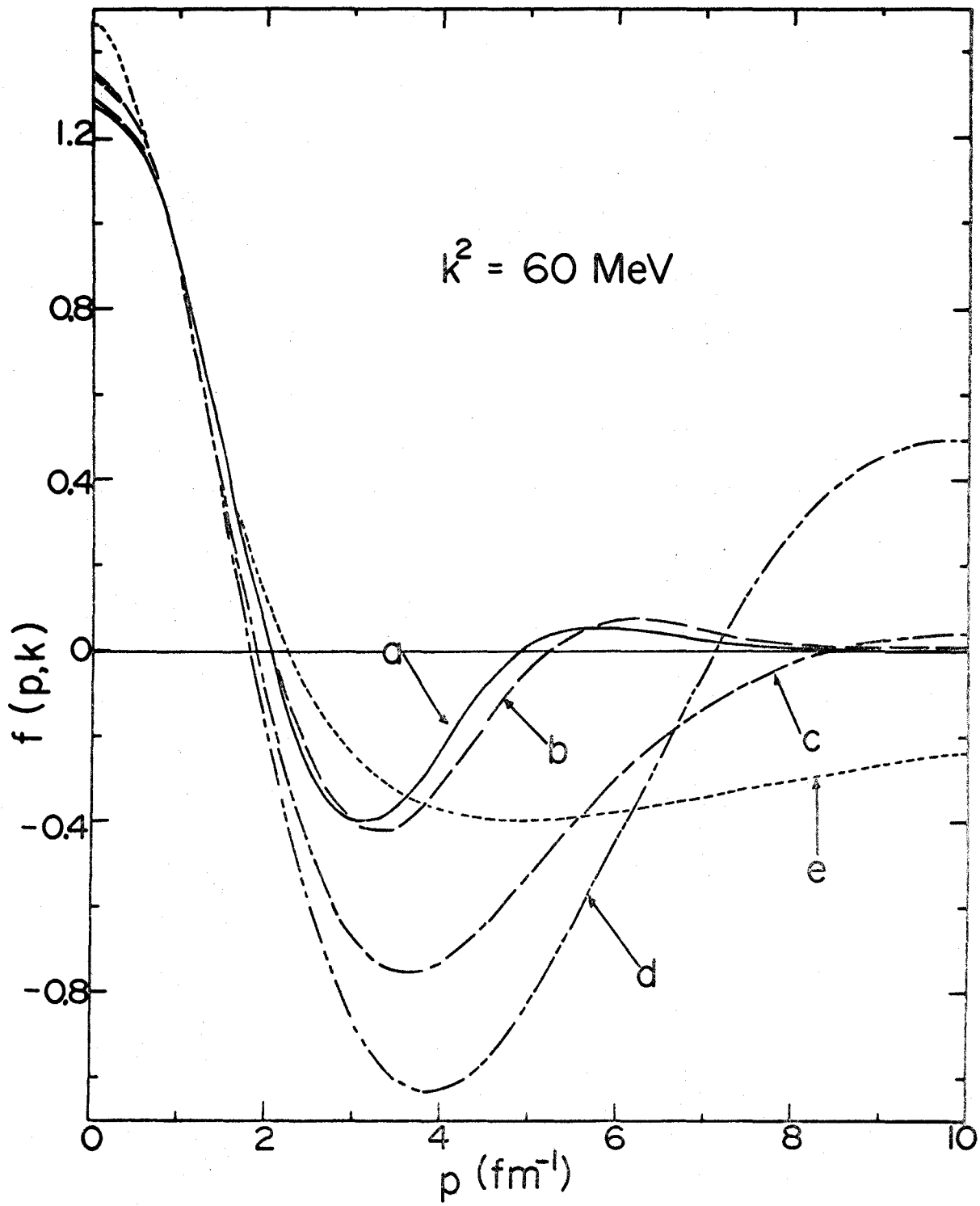

Figure 6(ii)

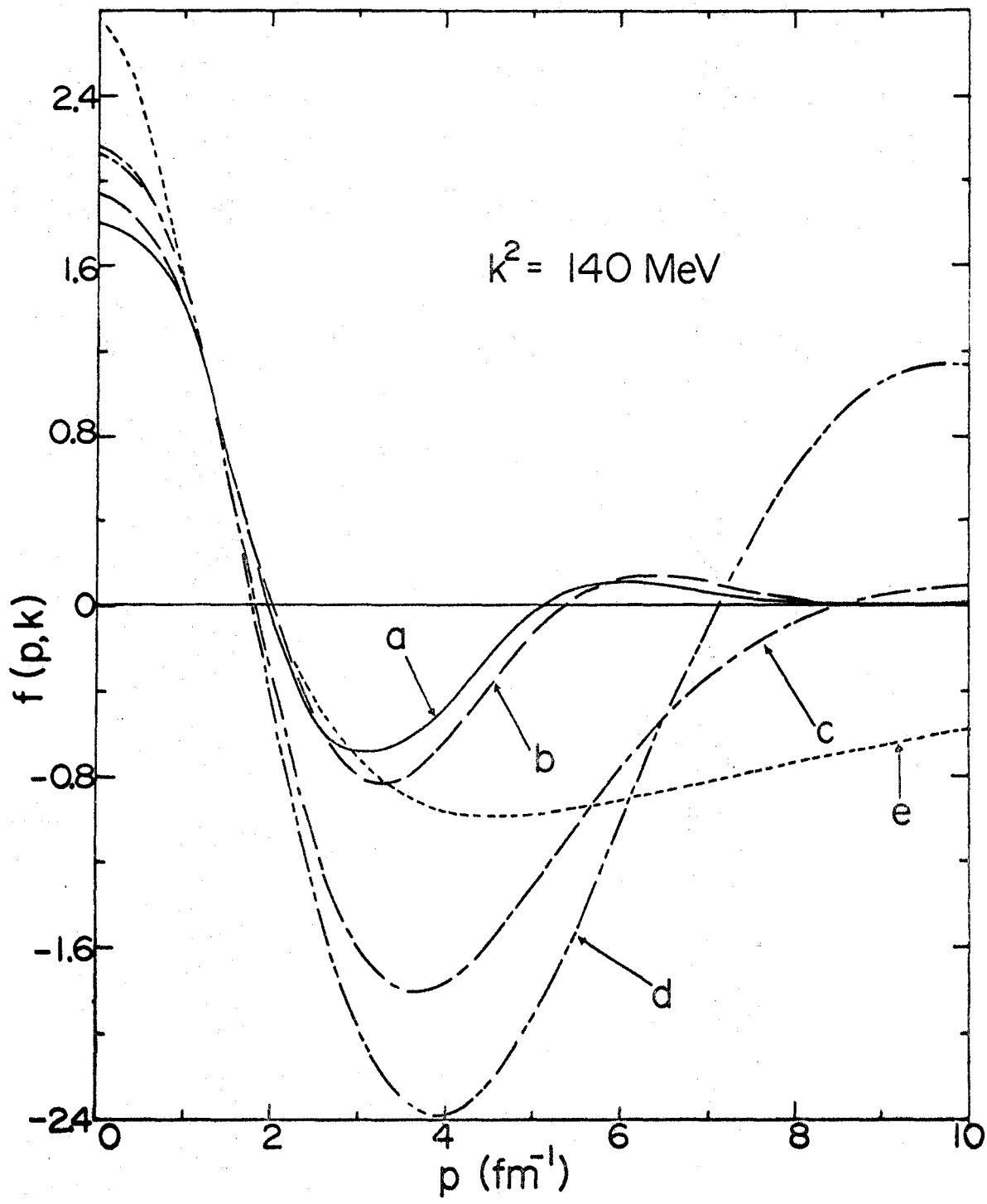

Figure 6(iii)

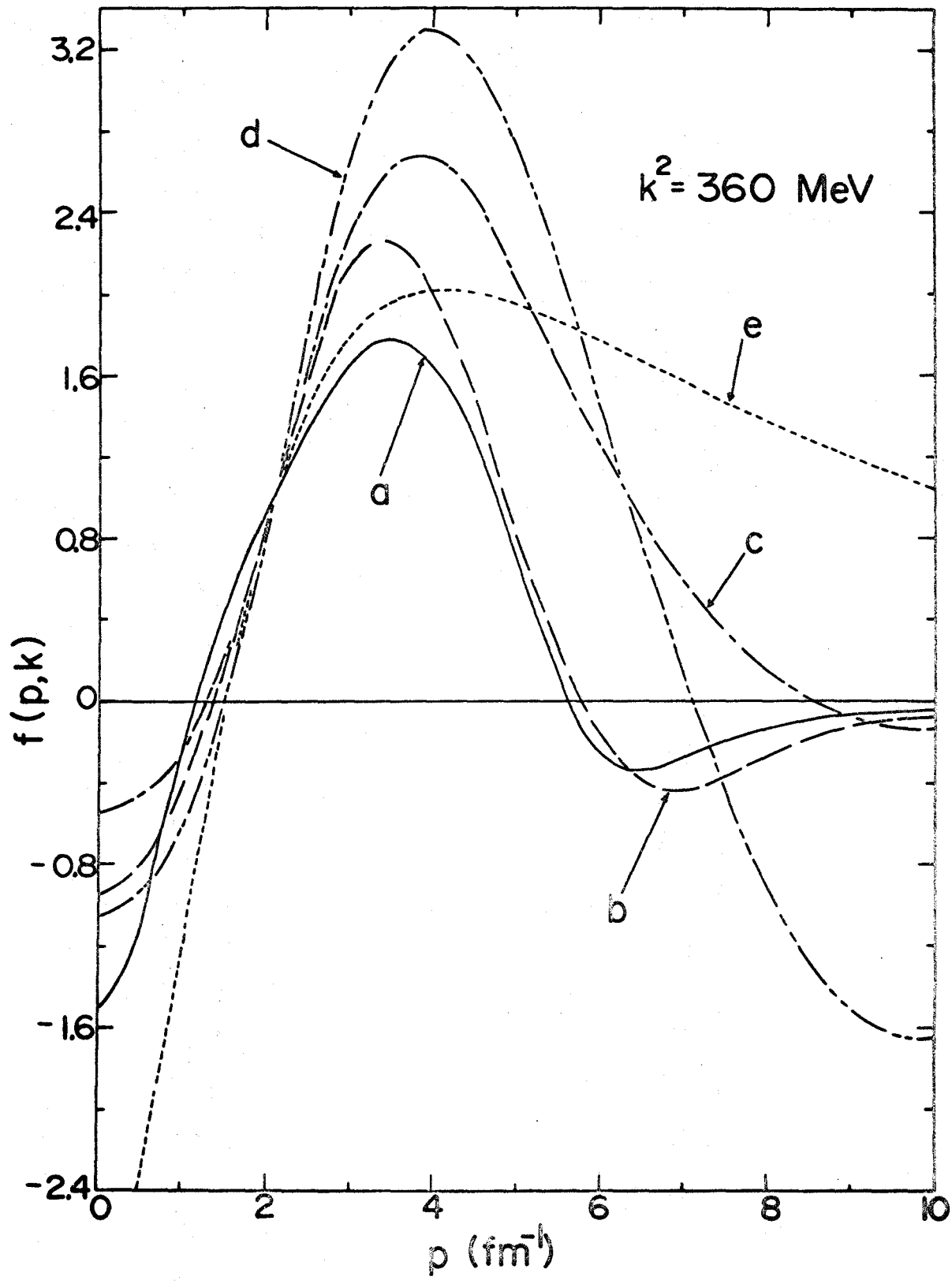

Figure 6(iv)

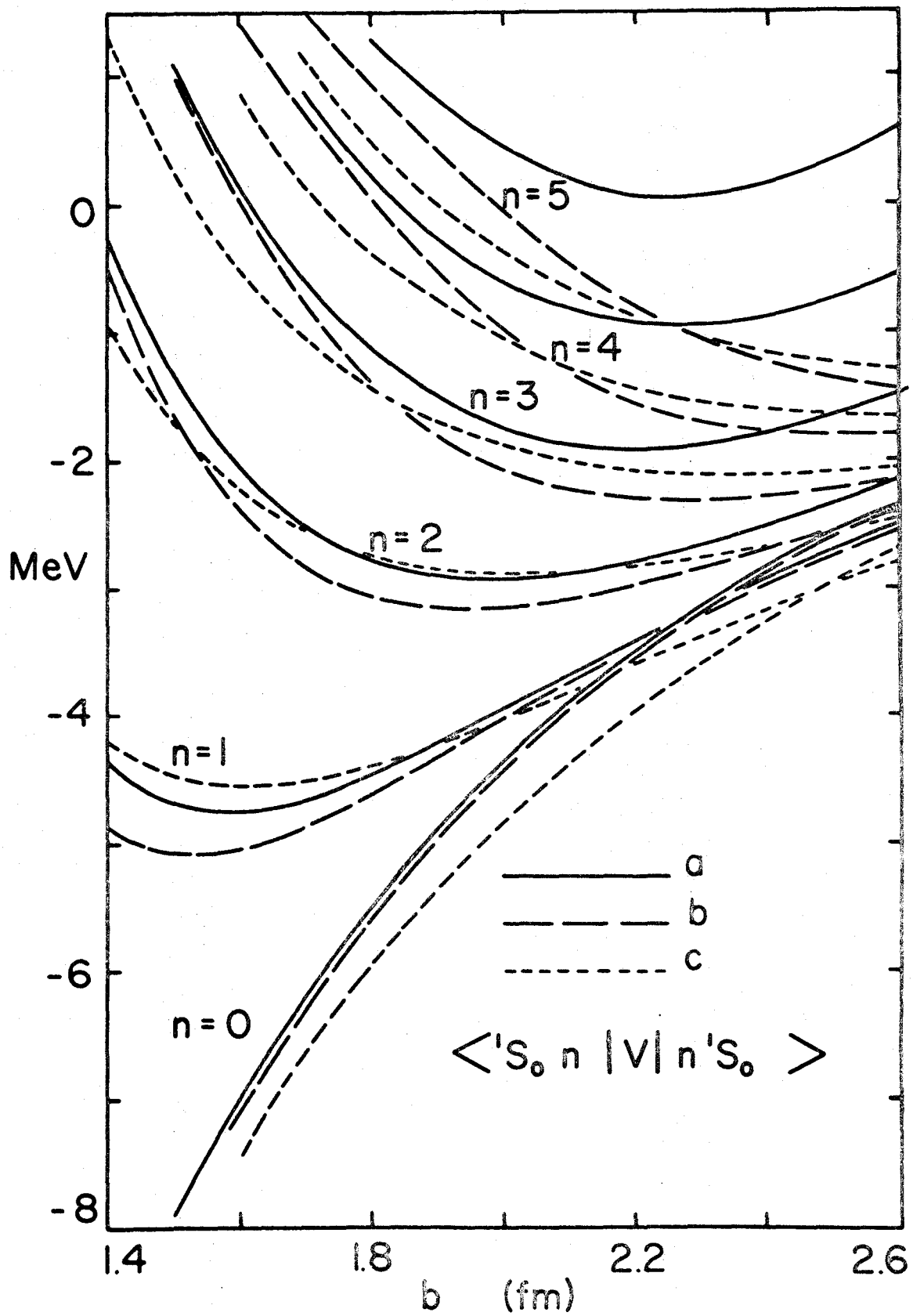

Figure 7

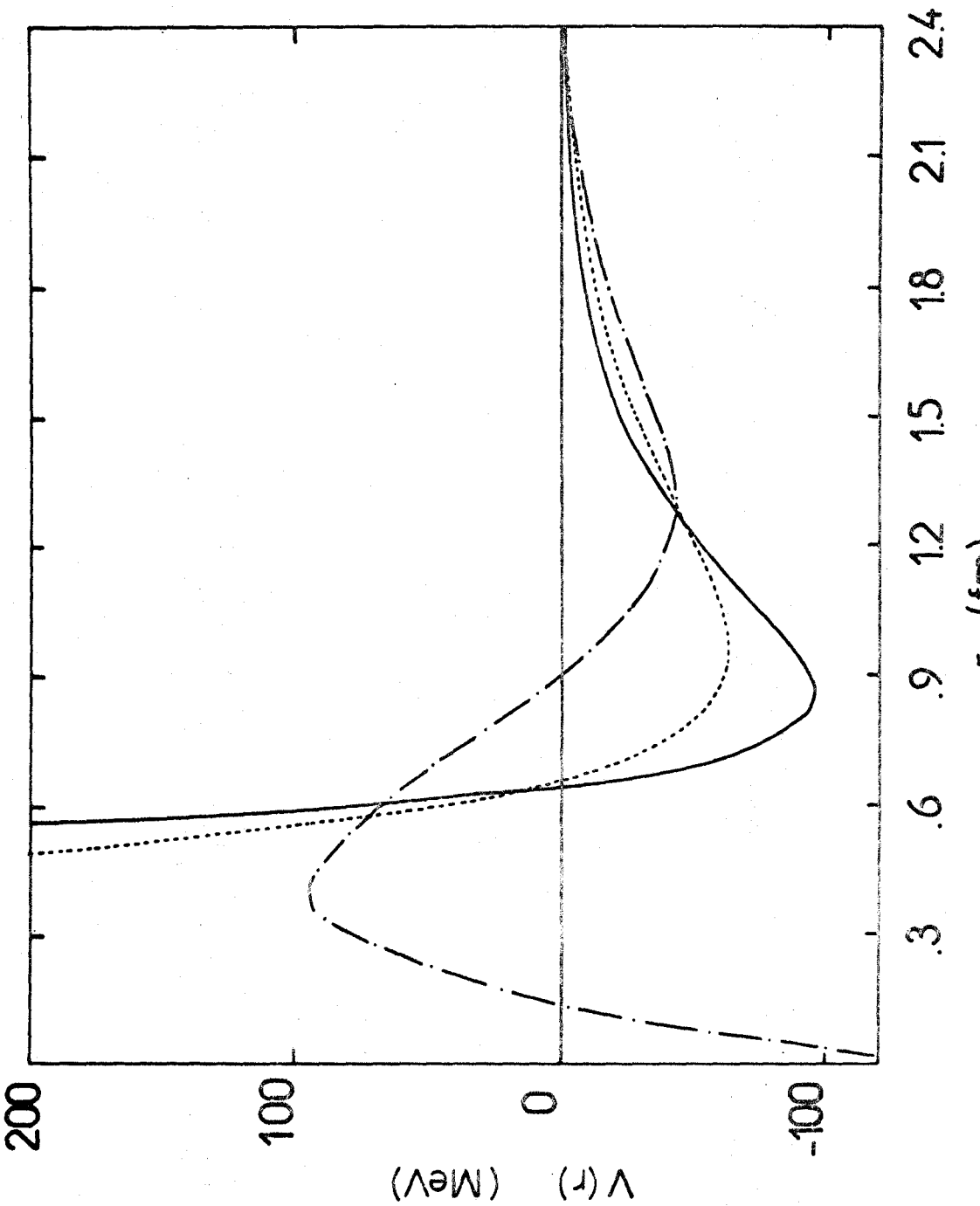

Figure 8

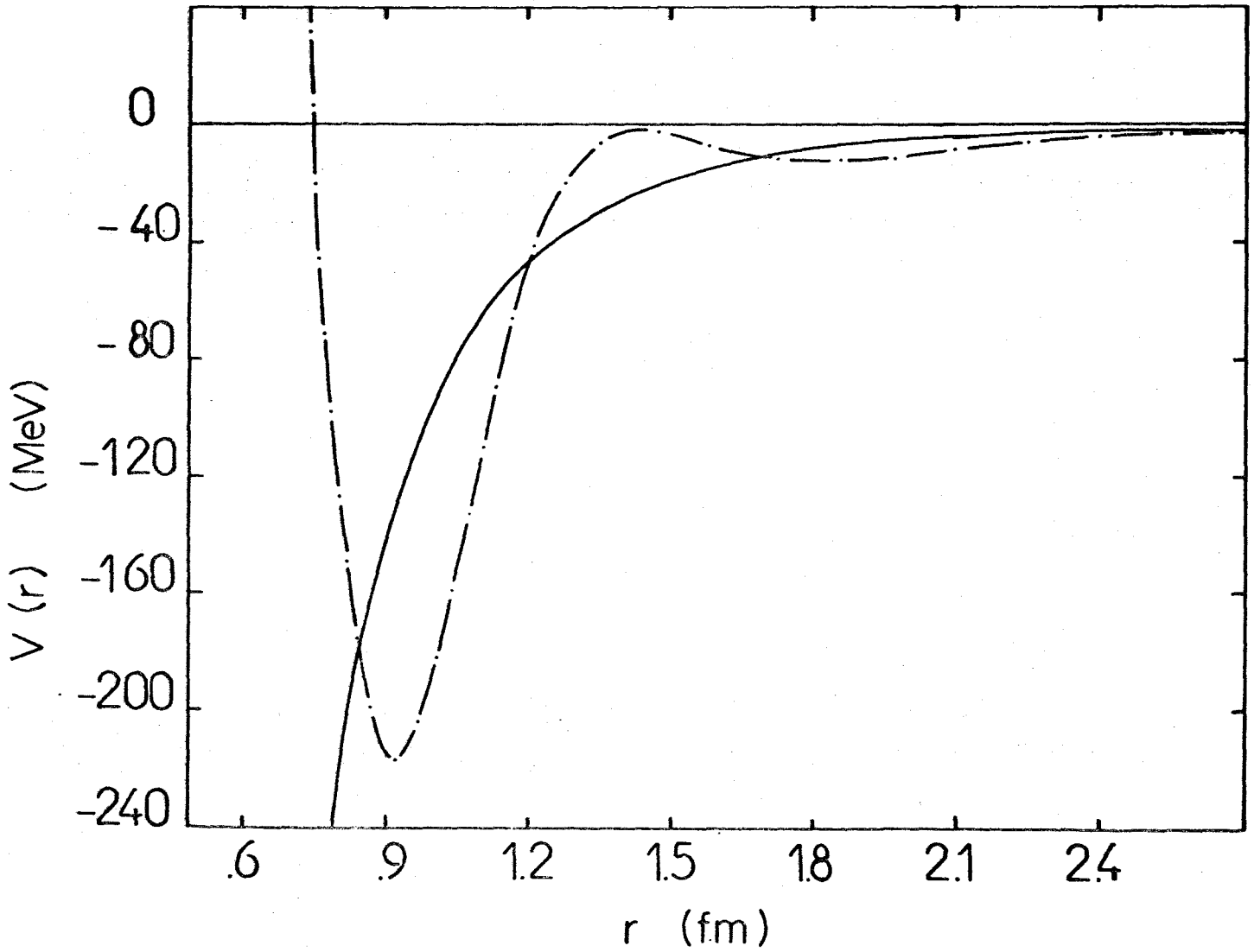

Figure 9

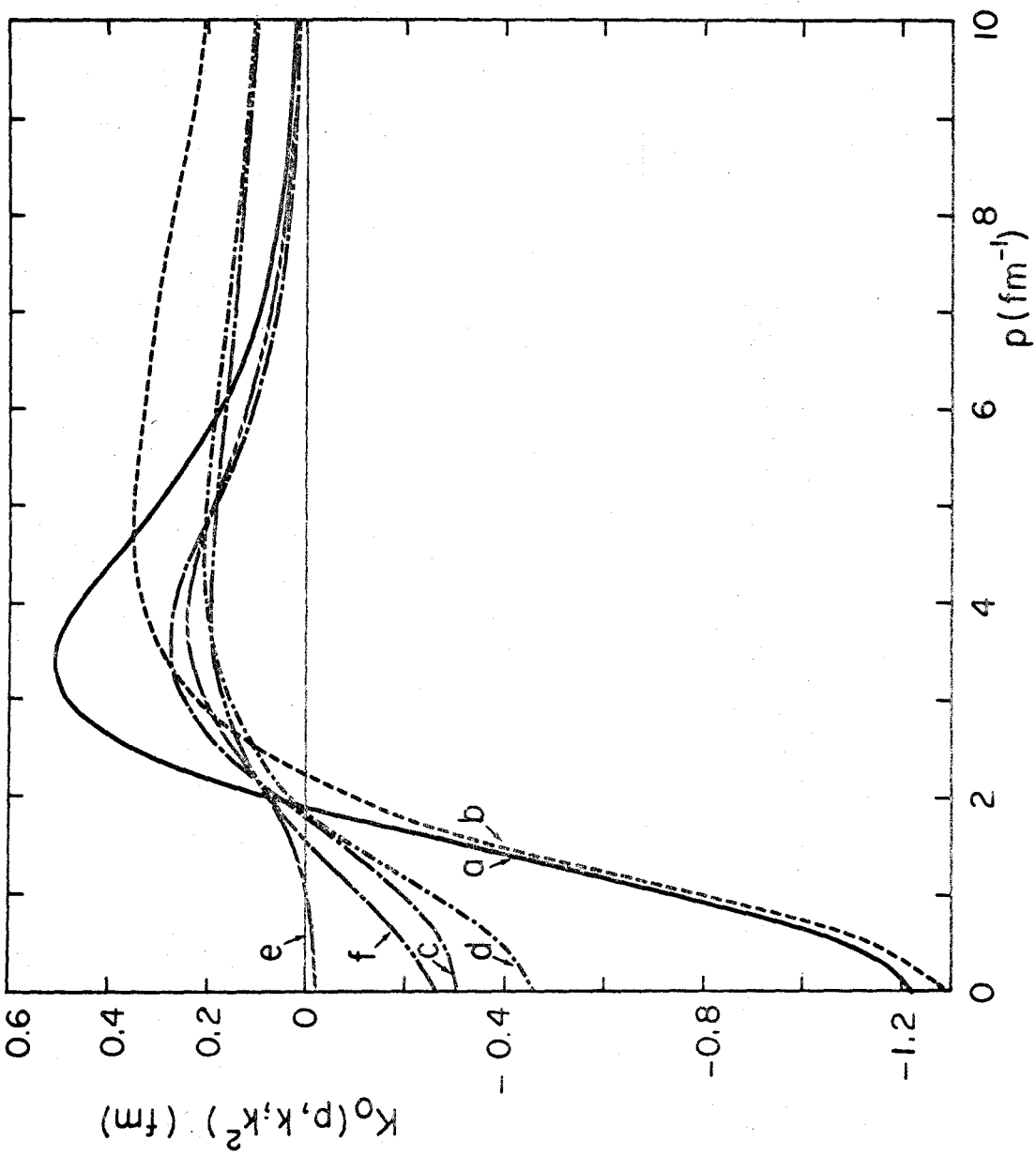

Figure 10

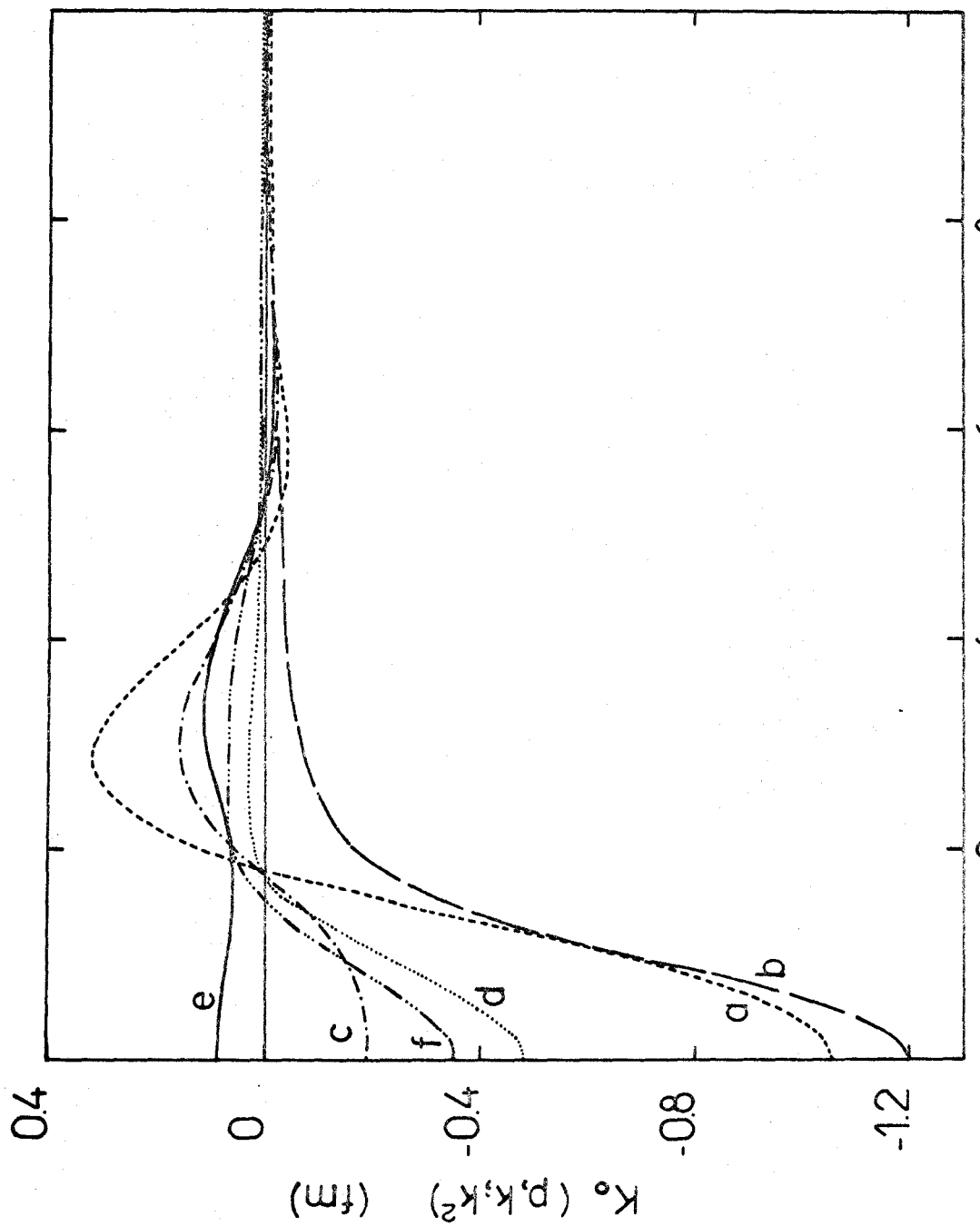

Figure 11

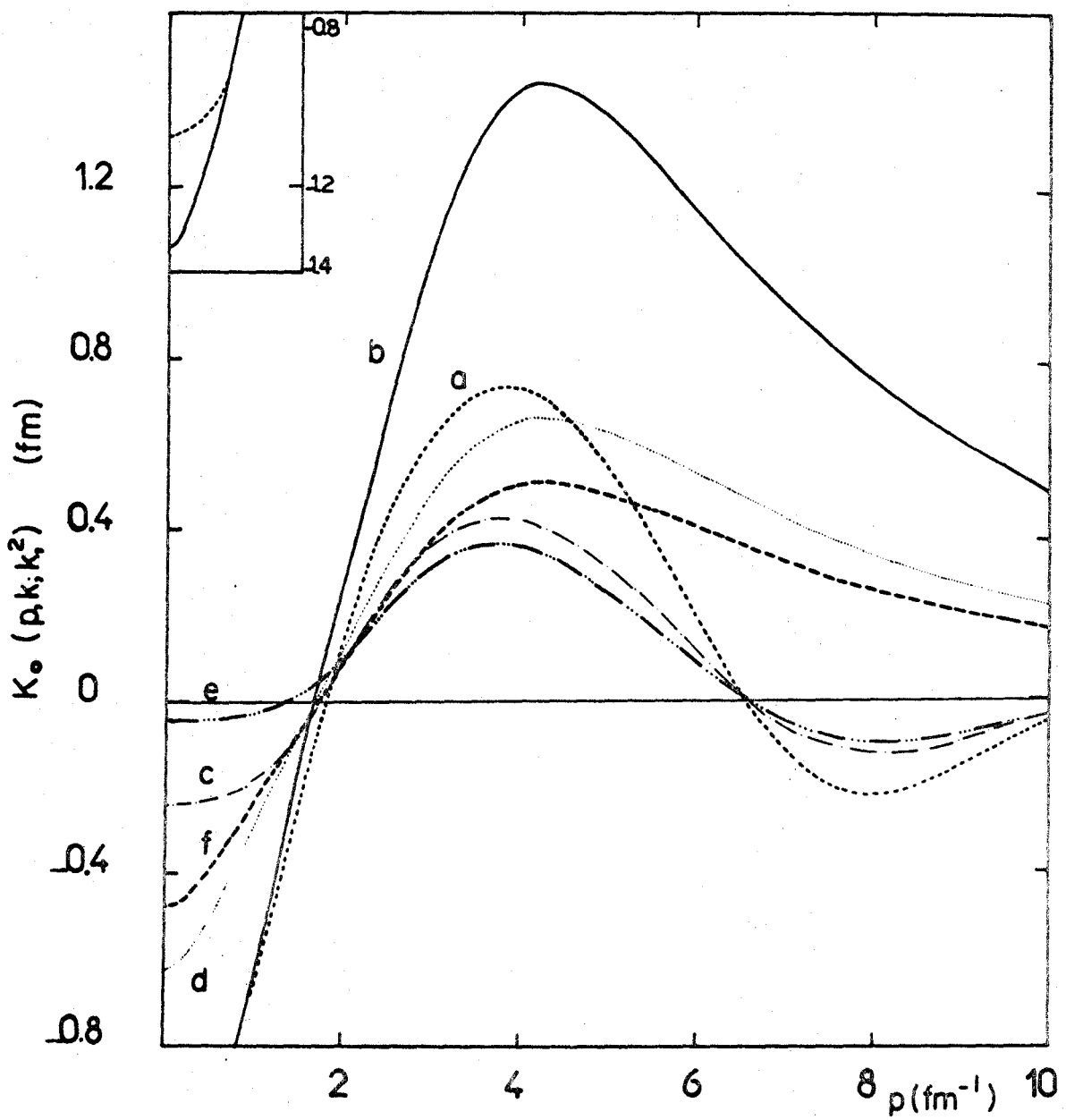

Figure 12

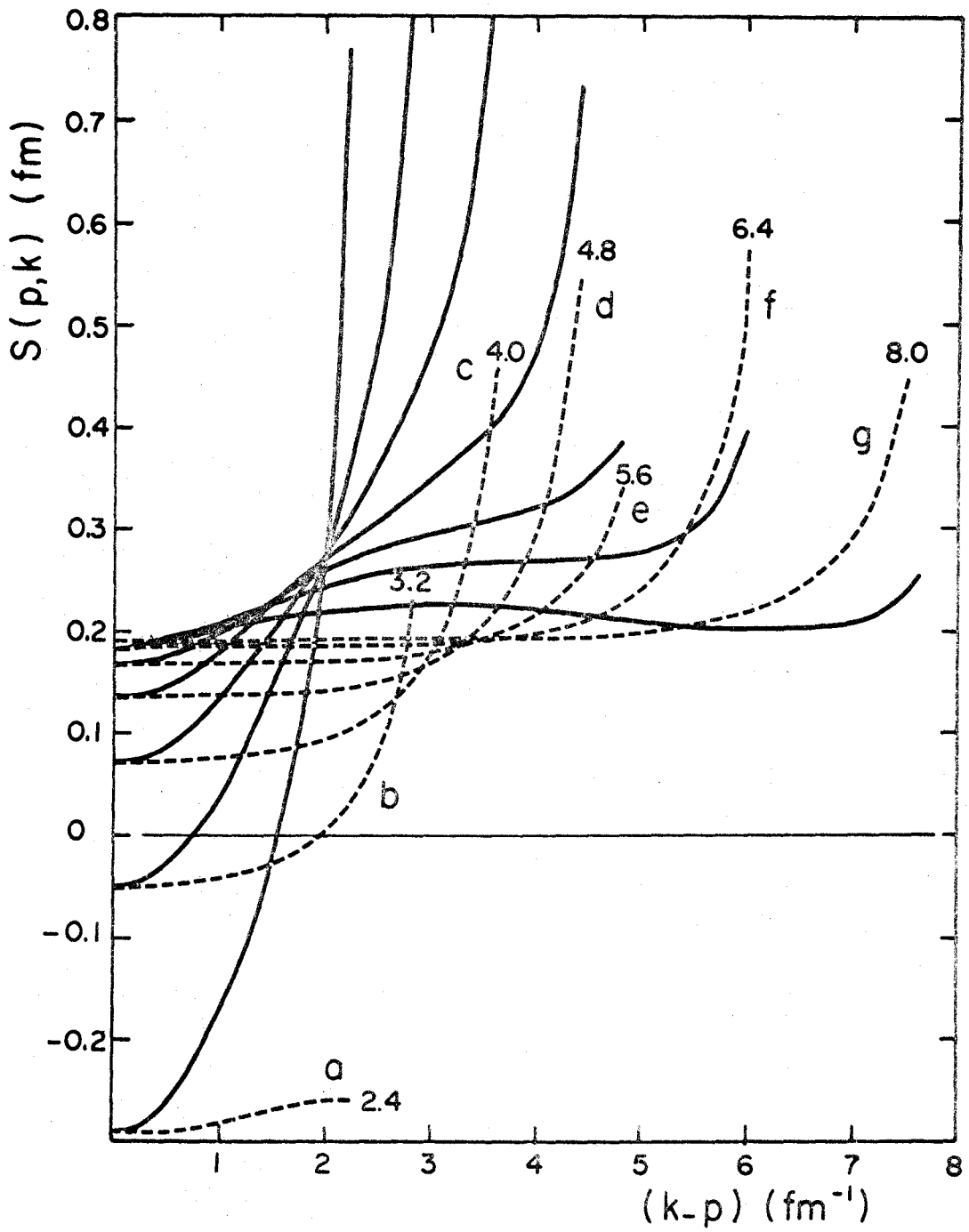
S(p,k) (fm)
0.8
0.7
0.6
0.5
0.4
0.3
0.2
0.1
0
-0.1
-0.2
1
2
3
4
5
6
7
8
(k-p) (fm⁻¹)
a
2.4
b
3.2
c
4.0
d
4.8
e
5.6
f
6.4
g
8.0

Figure 13

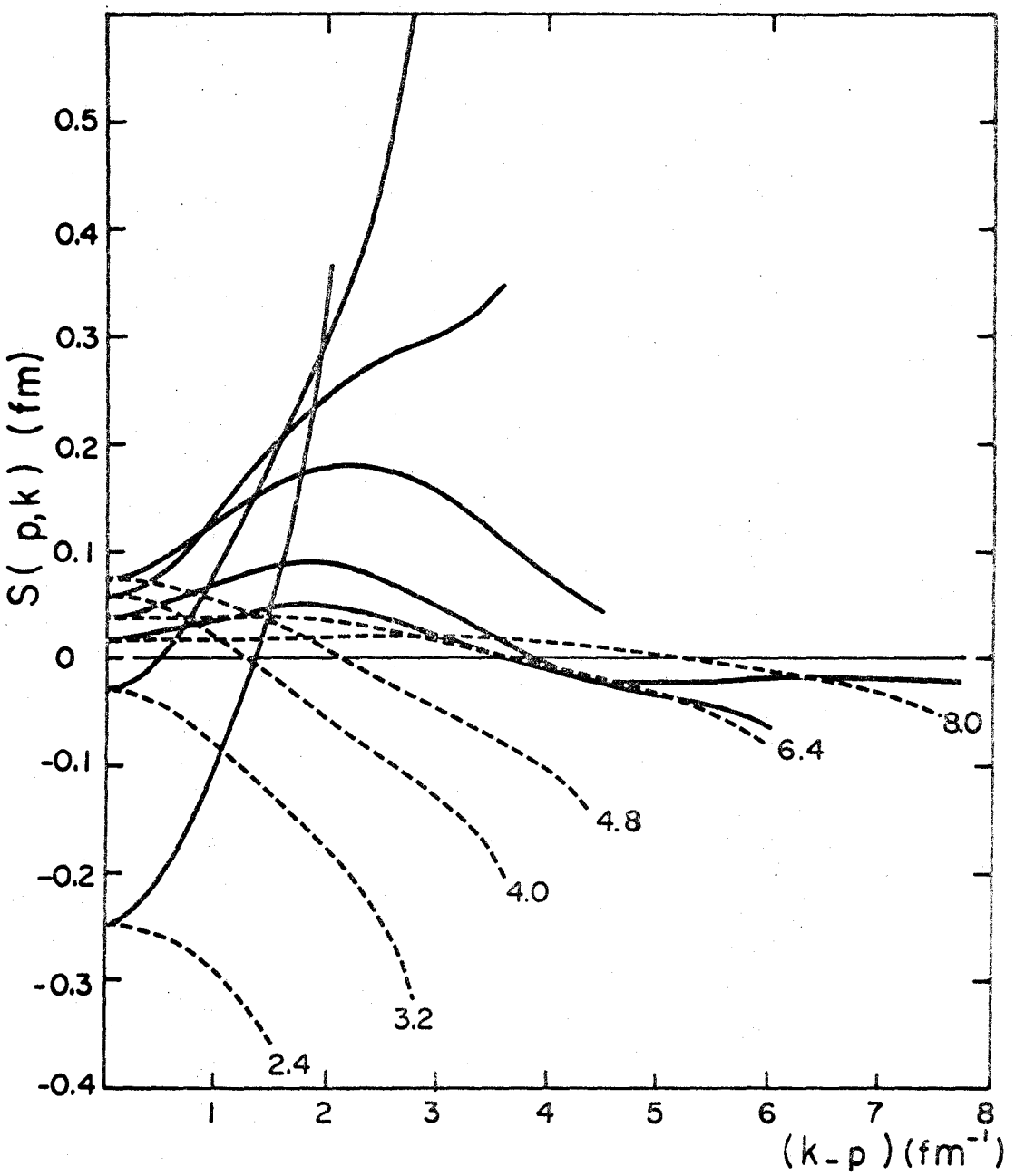

Figure 14

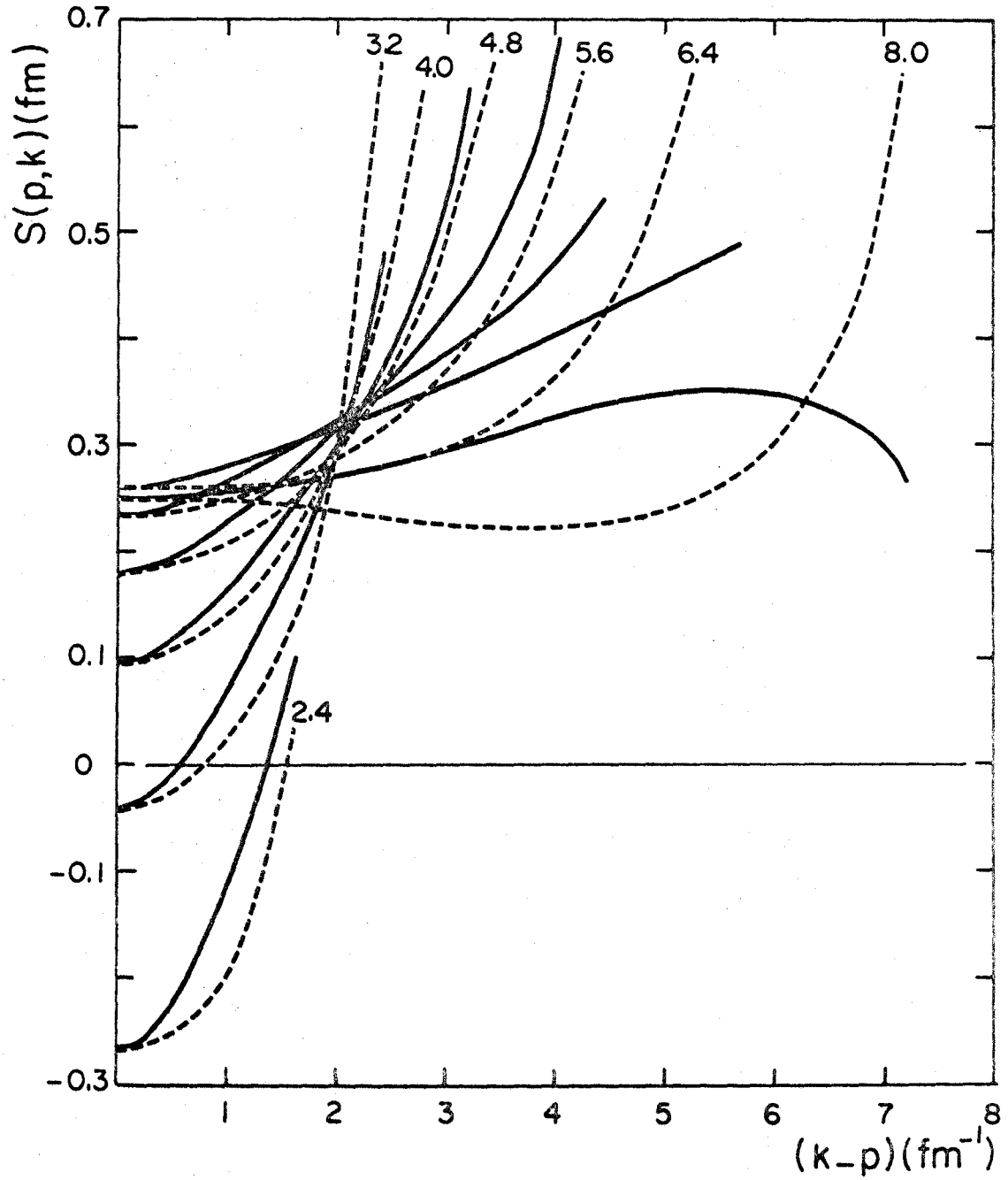

Figure 15

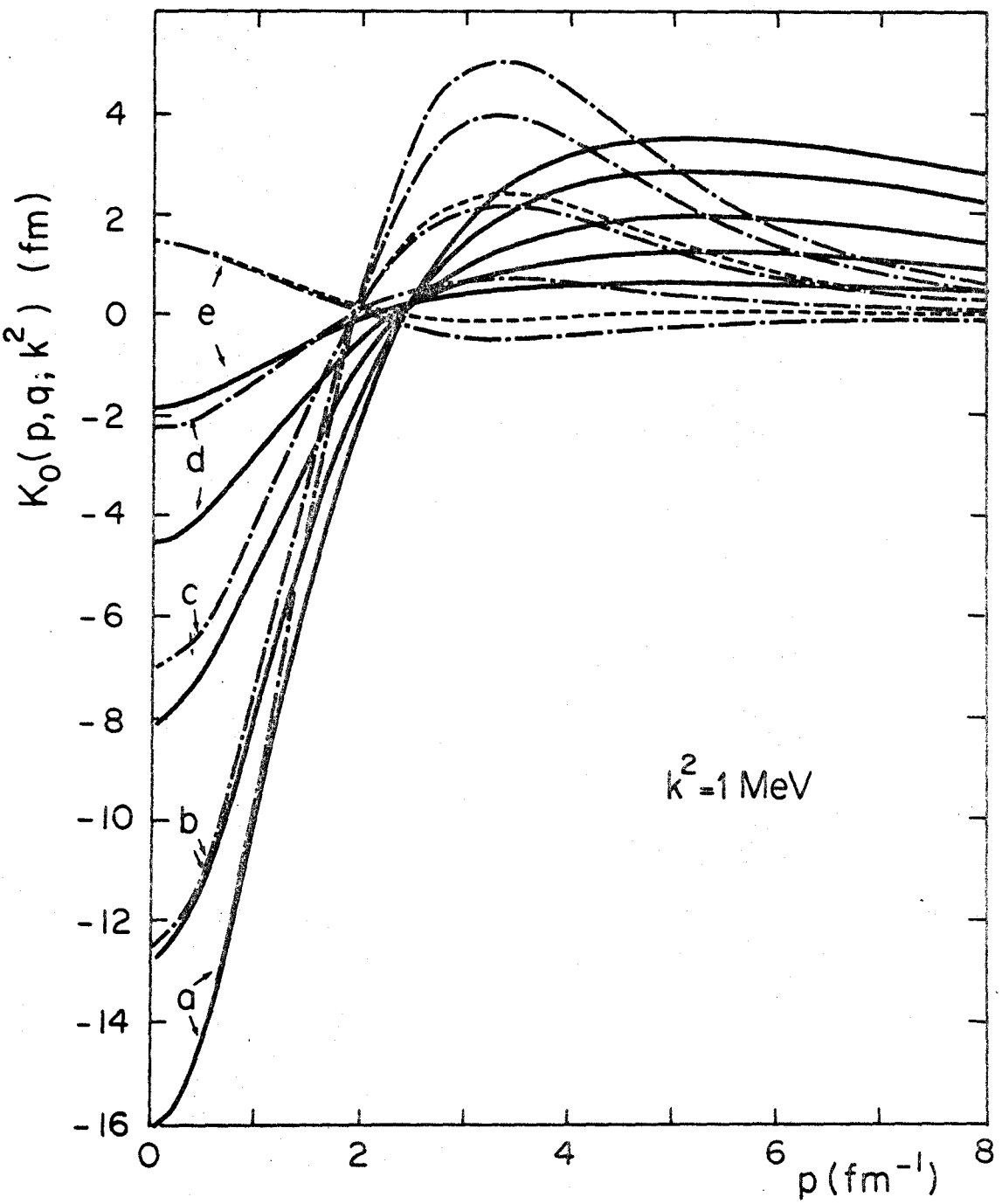

Figure 16(i)

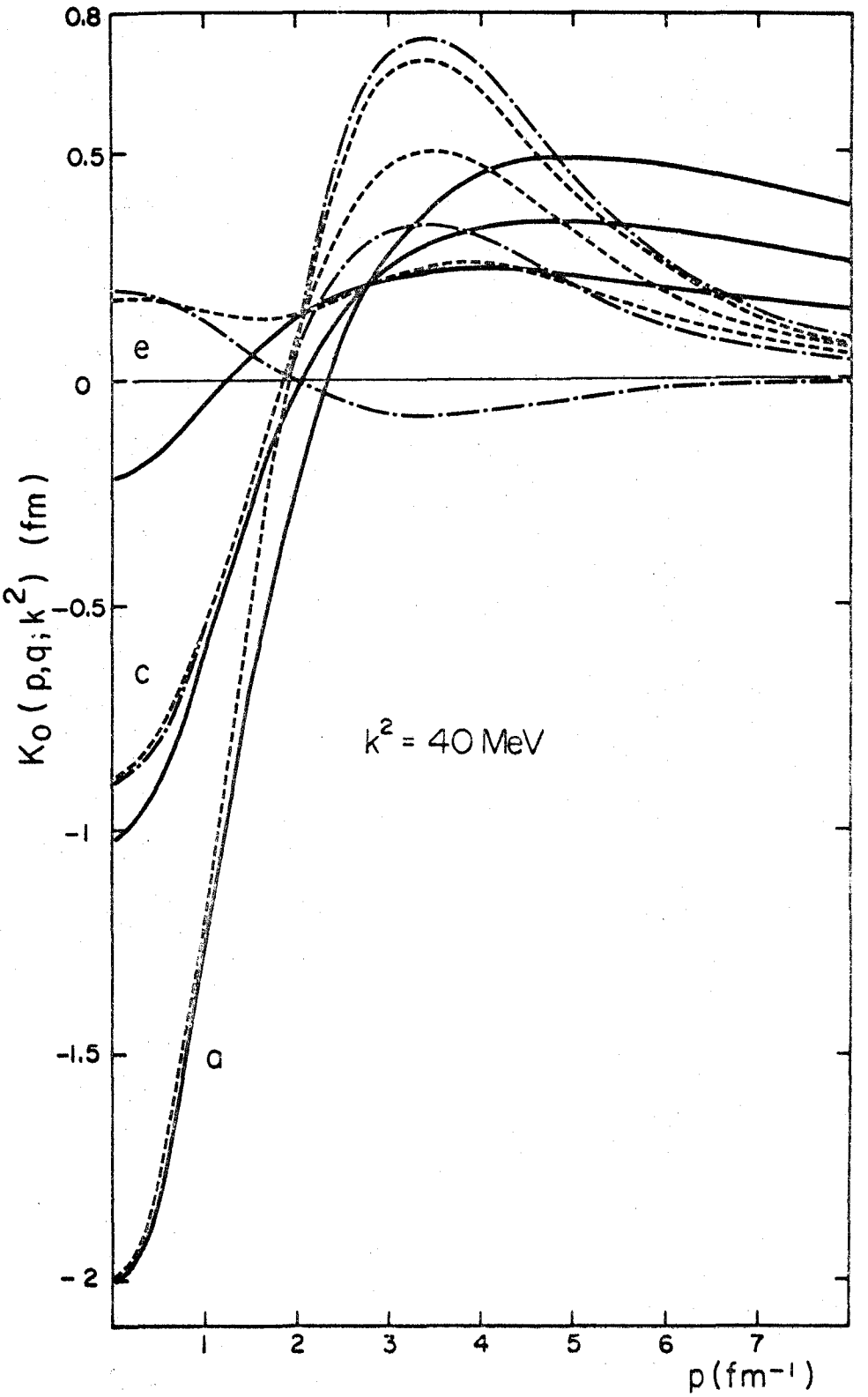

Figure 16(ii)

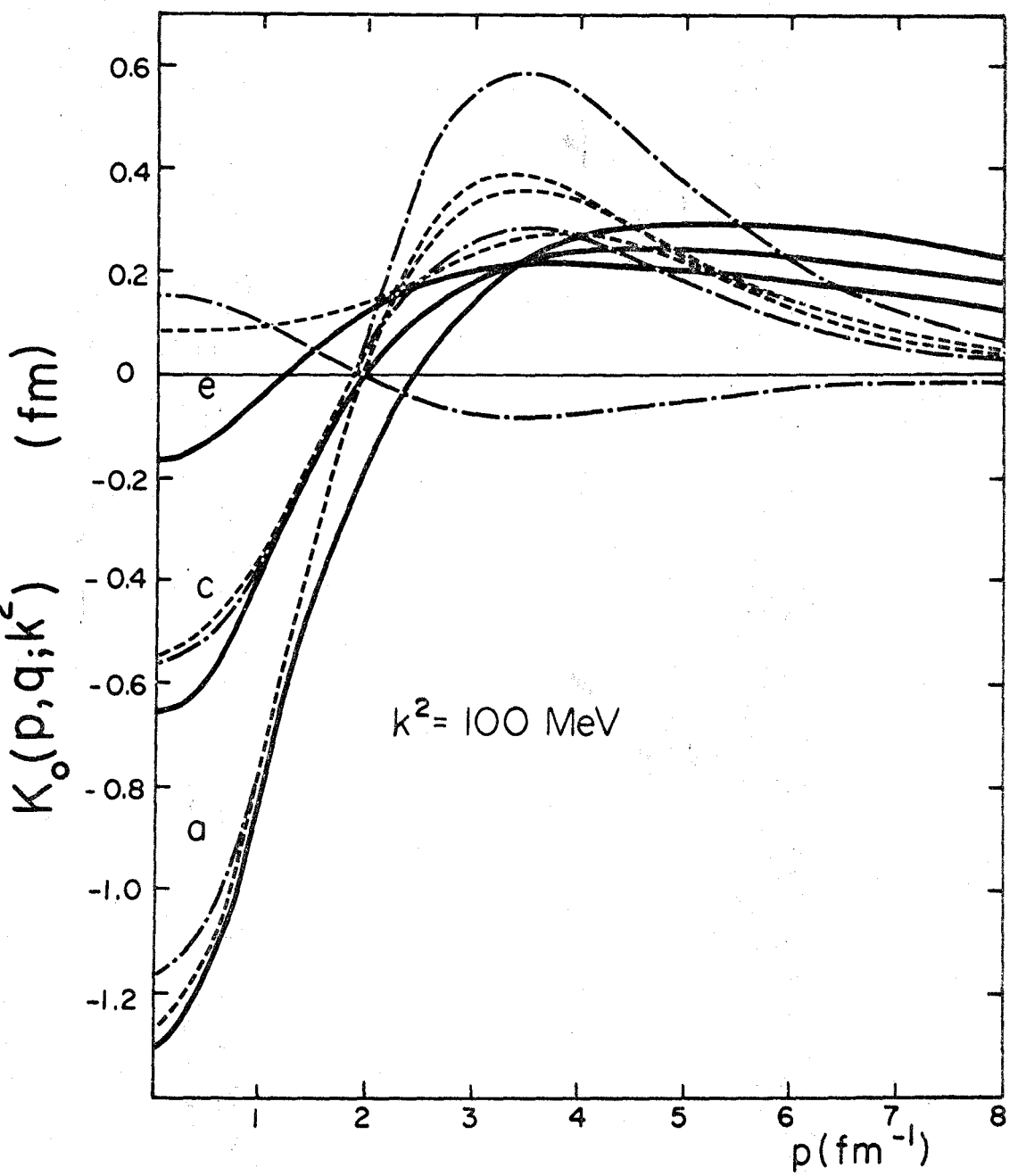

Figure 16(iii)

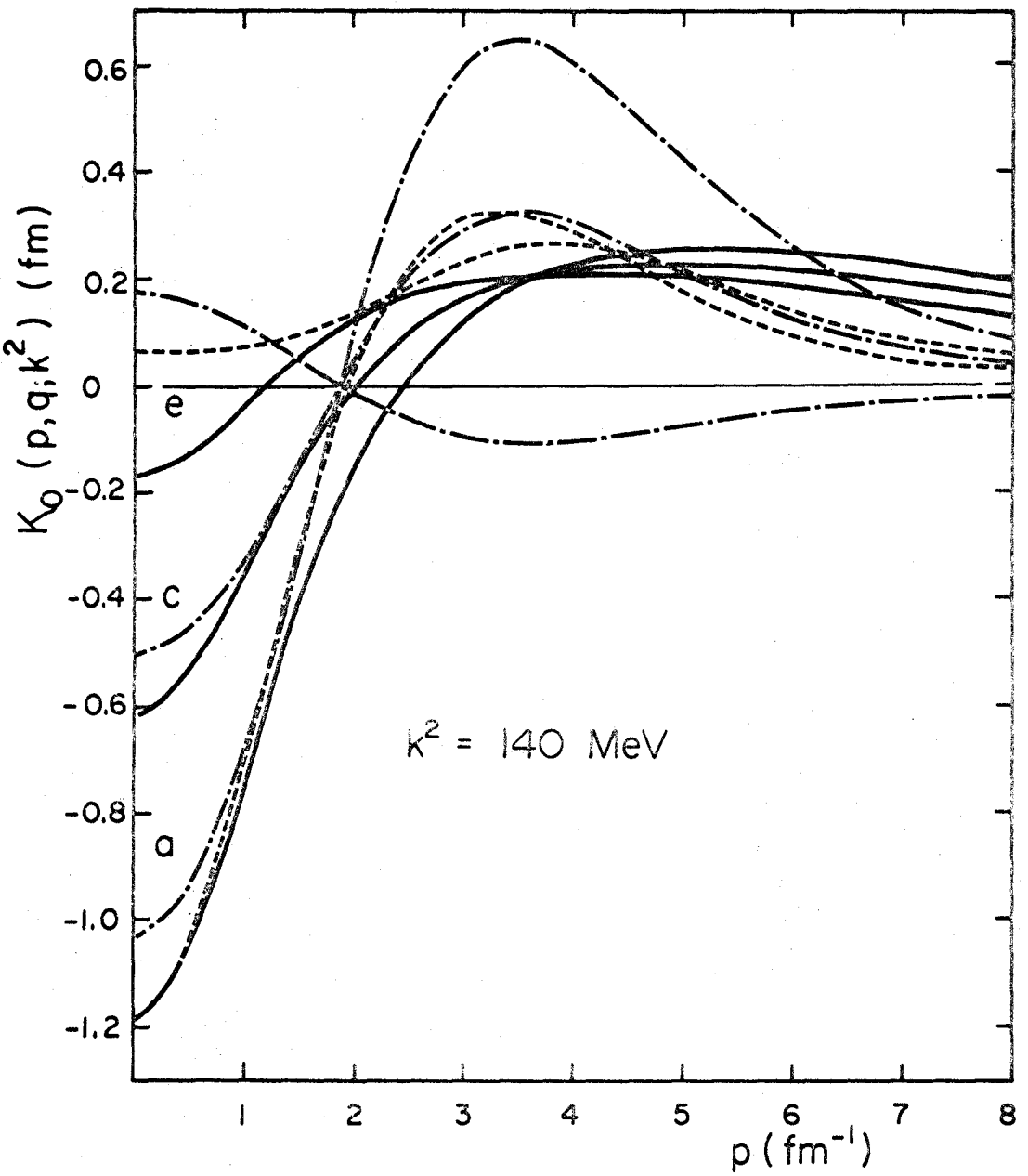
0.6
0.4
0.2
0
-0.2
-0.4
-0.6
-0.8
-1.0
-1.2
$K_0(p,q;k^2)$ (fm)
e
c
a
k^2 = 140 MeV
1
2
3
4
5
6
7
8
p (fm^{-1})

Figure 16(iv)

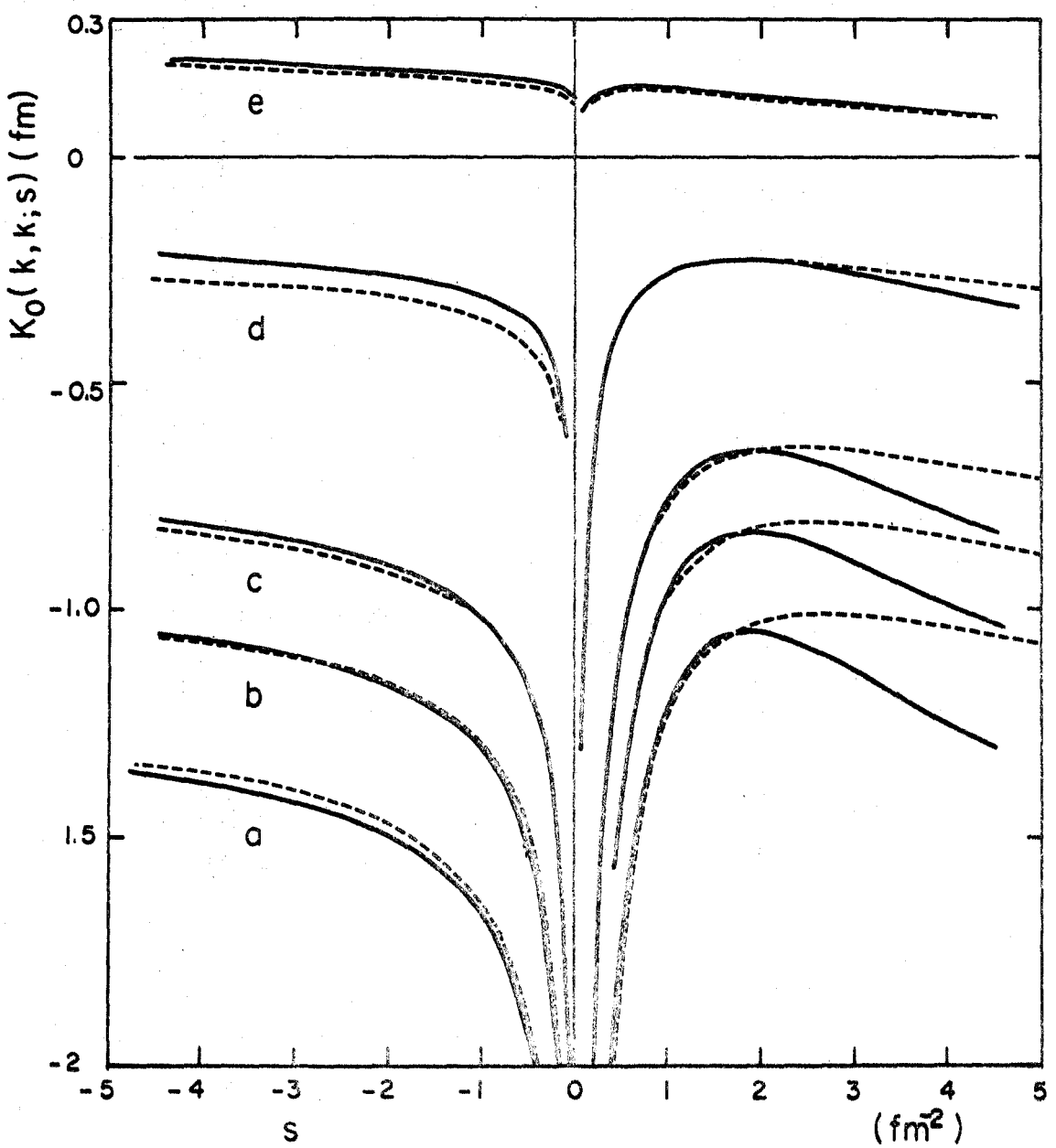

Figure 17

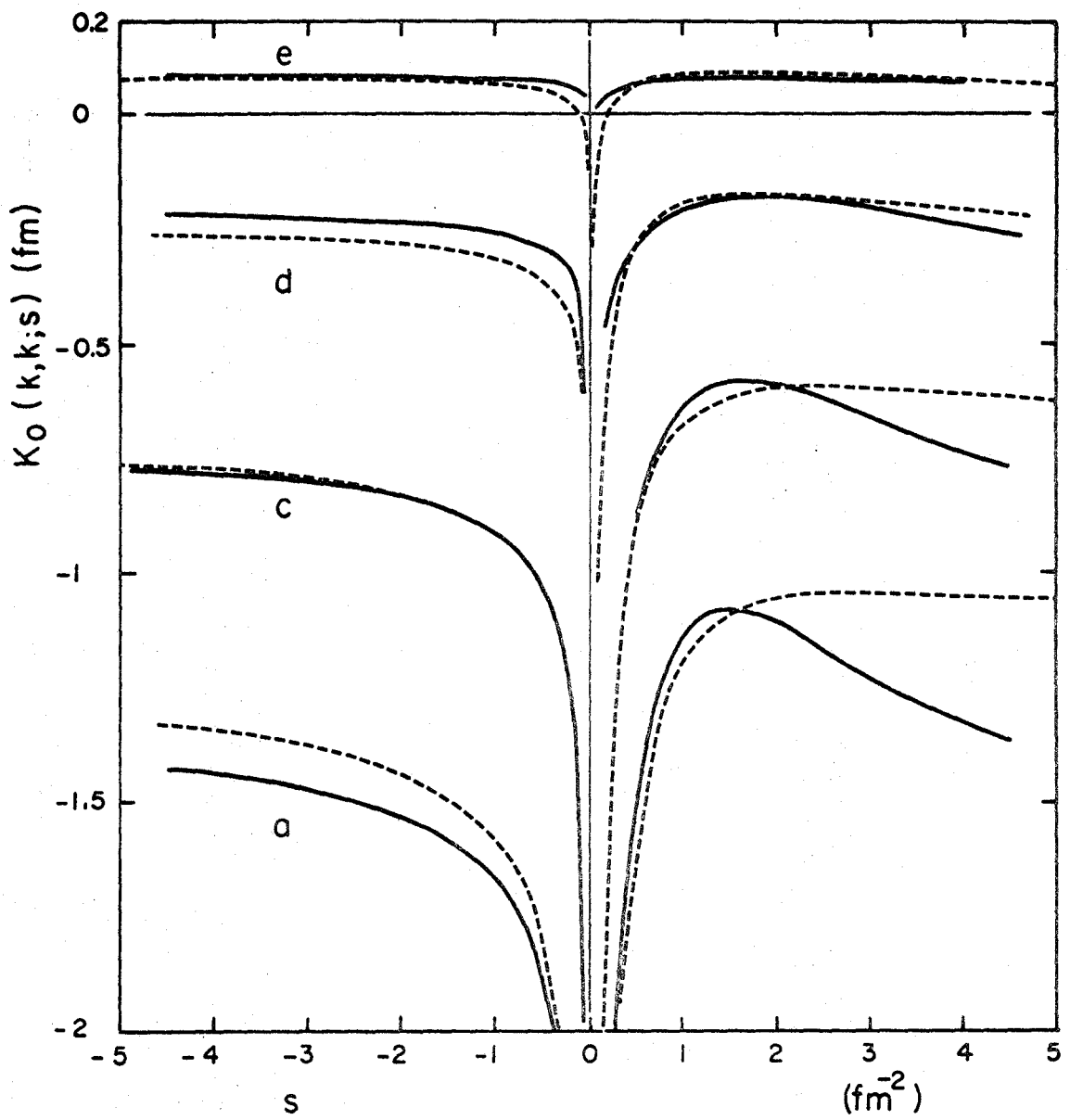

Figure 18

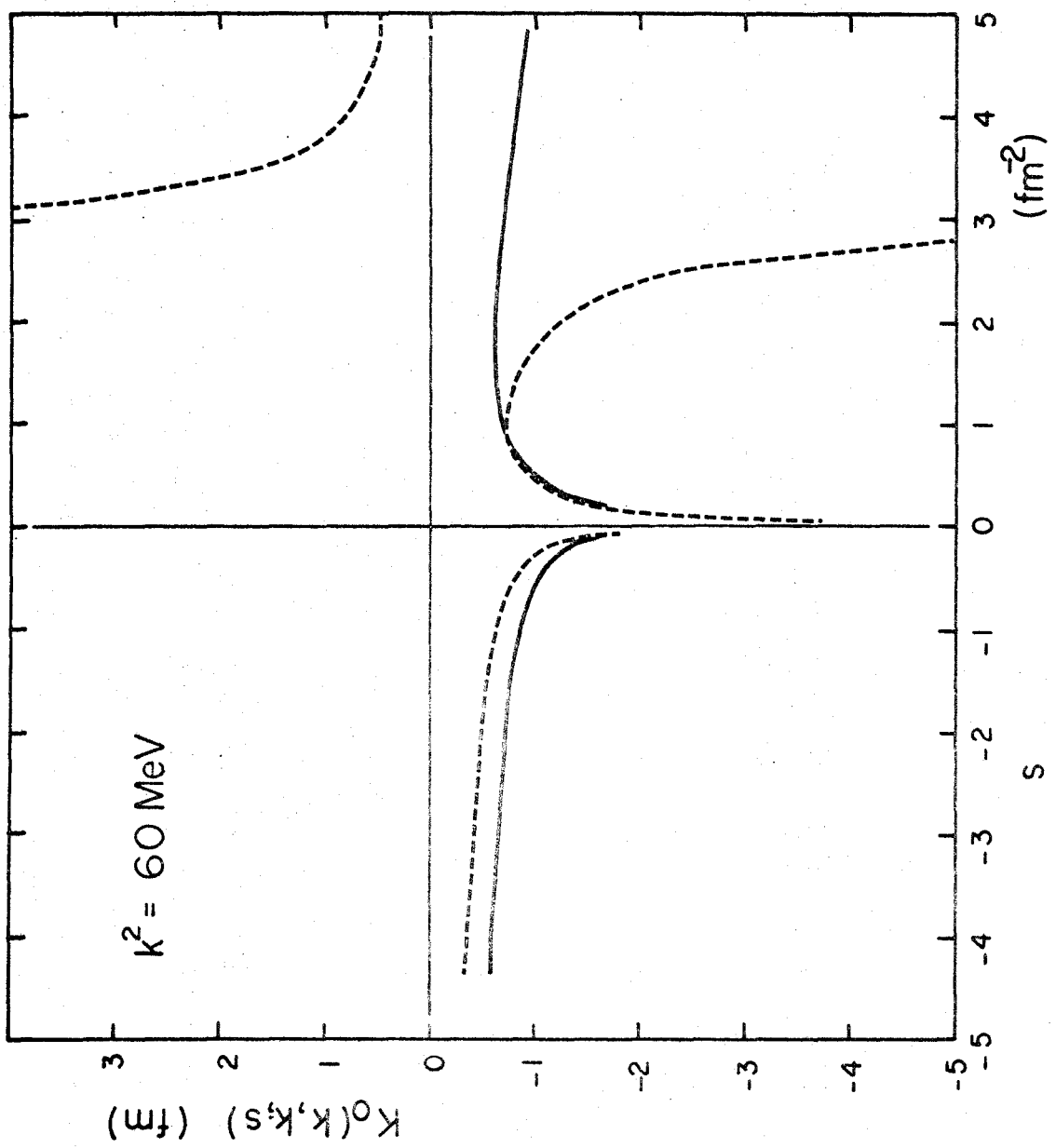

Figure 19

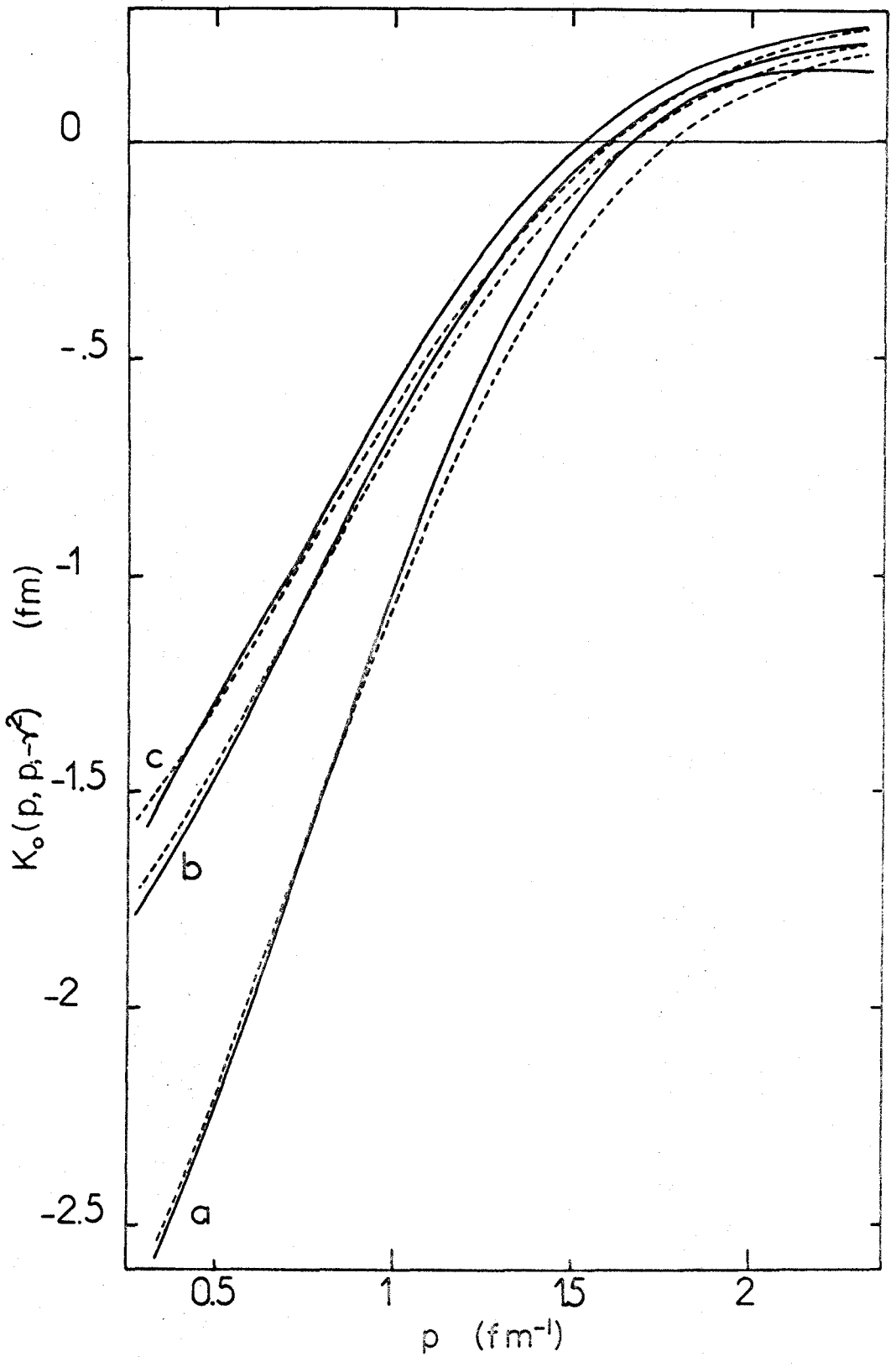

Figure 20

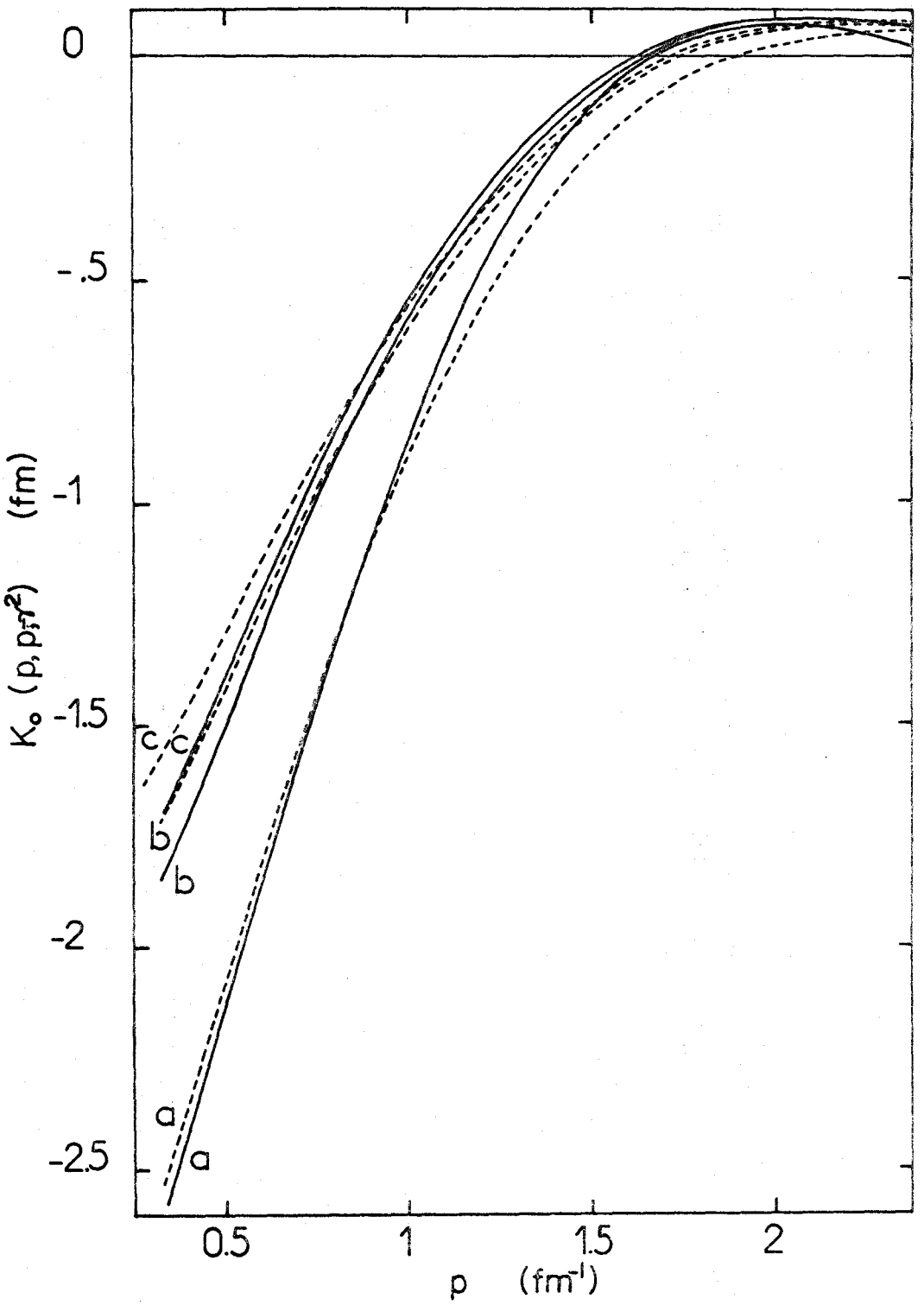

Figure 21

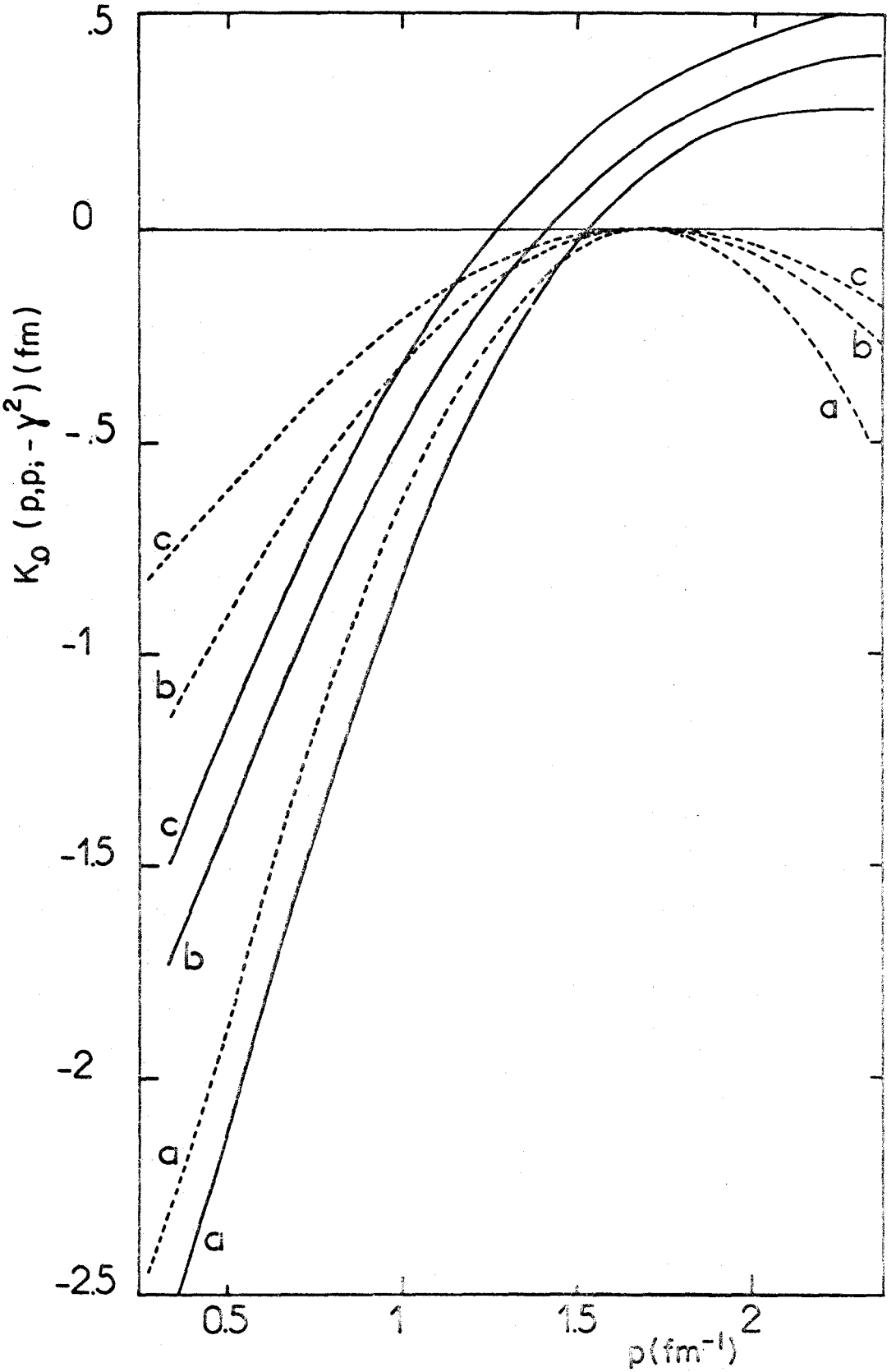

Figure 22

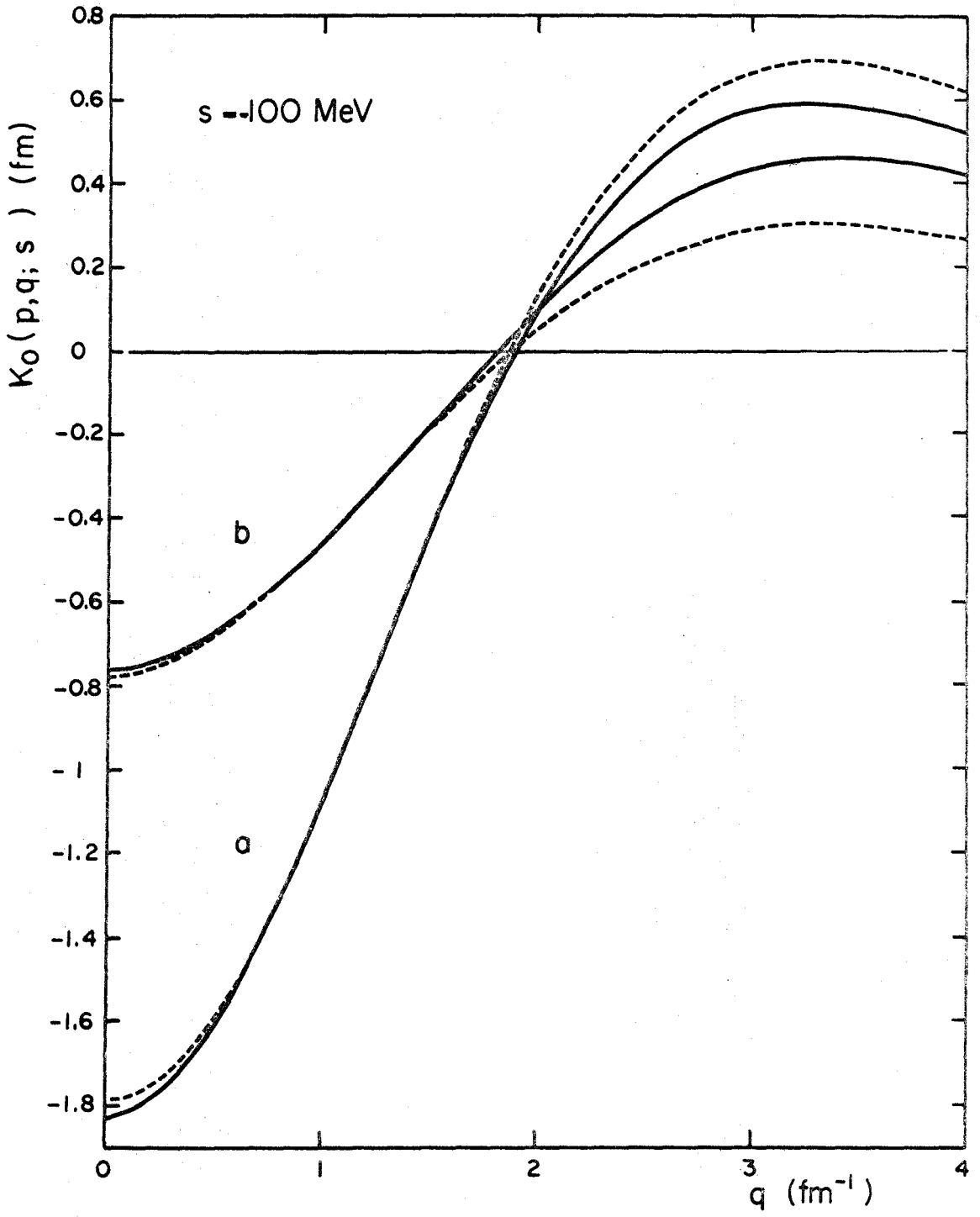
s = -100 MeV
b
a
$K_0(p,q;s)$ (fm)
q (fm^{-1})
0.8
0.6
0.4
0.2
0
-0.2
-0.4
-0.6
-0.8
-1
-1.2
-1.4
-1.6
-1.8
0
1
2
3
4

Figure 23

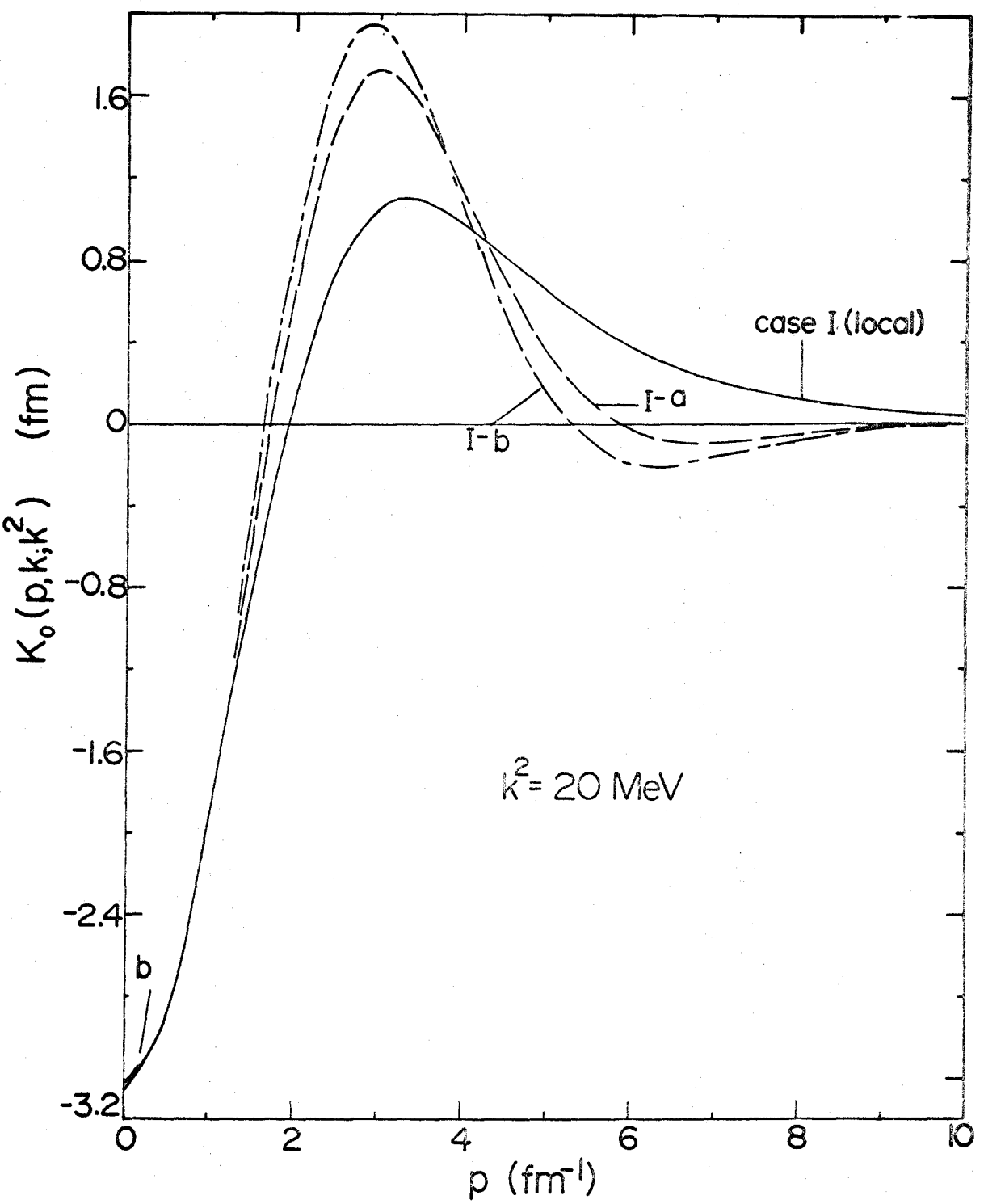
1.6
0.8
0
-0.8
-1.6
-2.4
-3.2
0
2
4
6
8
10
$K_0(p,k;k^2)$ (fm)
p (fm^{-1})
case I (local)
I-a
I-b
b
k^2= 20 MeV

Figure 24(i)

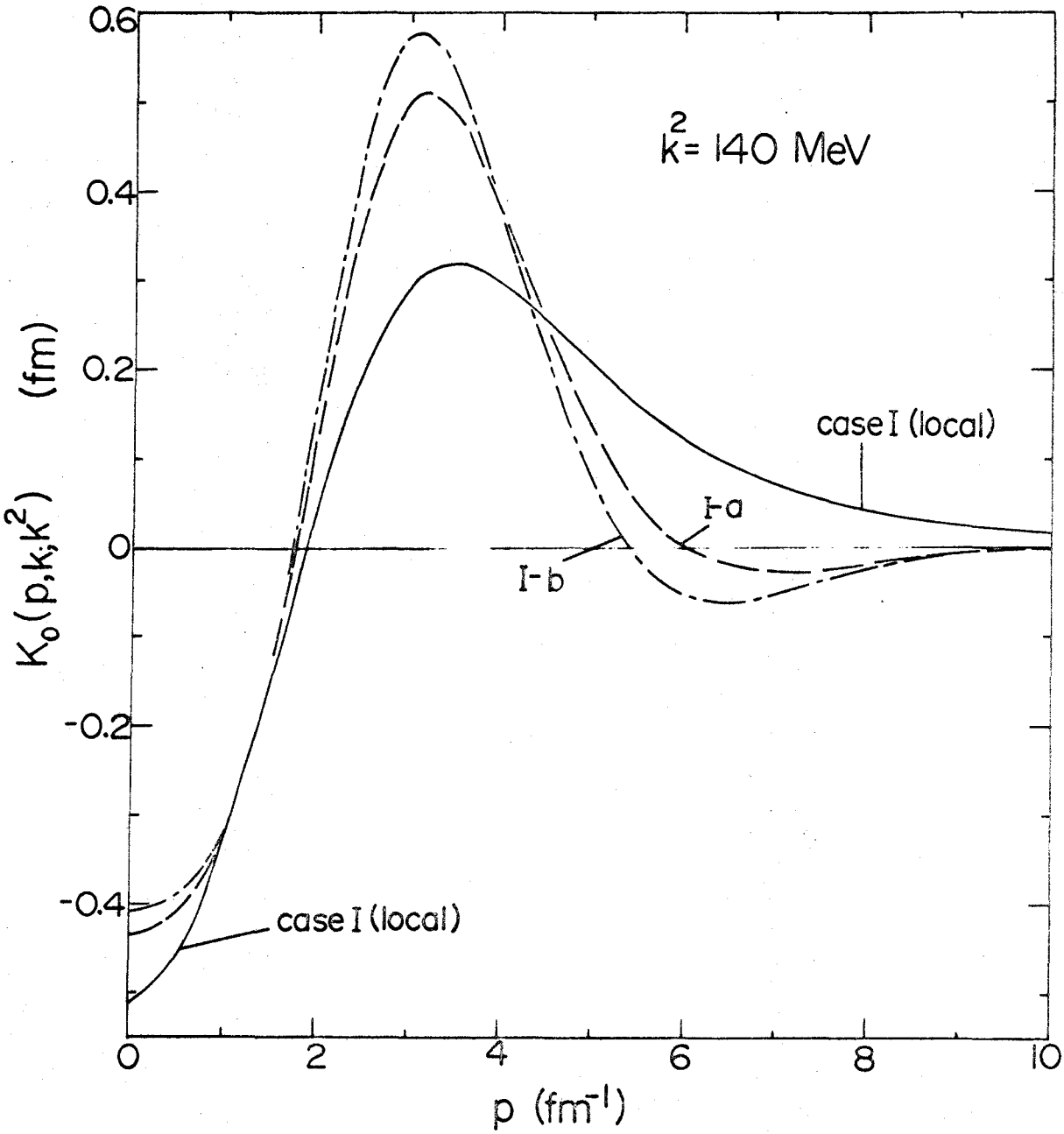
0.6
0.4
0.2
0
-0.2
-0.4
$K_0(p,k;k^2)$ (fm)
k^2= 140 MeV
case I (local)
I-a
I-b
case I (local)
0
2
4
6
8
10
p (fm^{-1})

Figure 24(ii)

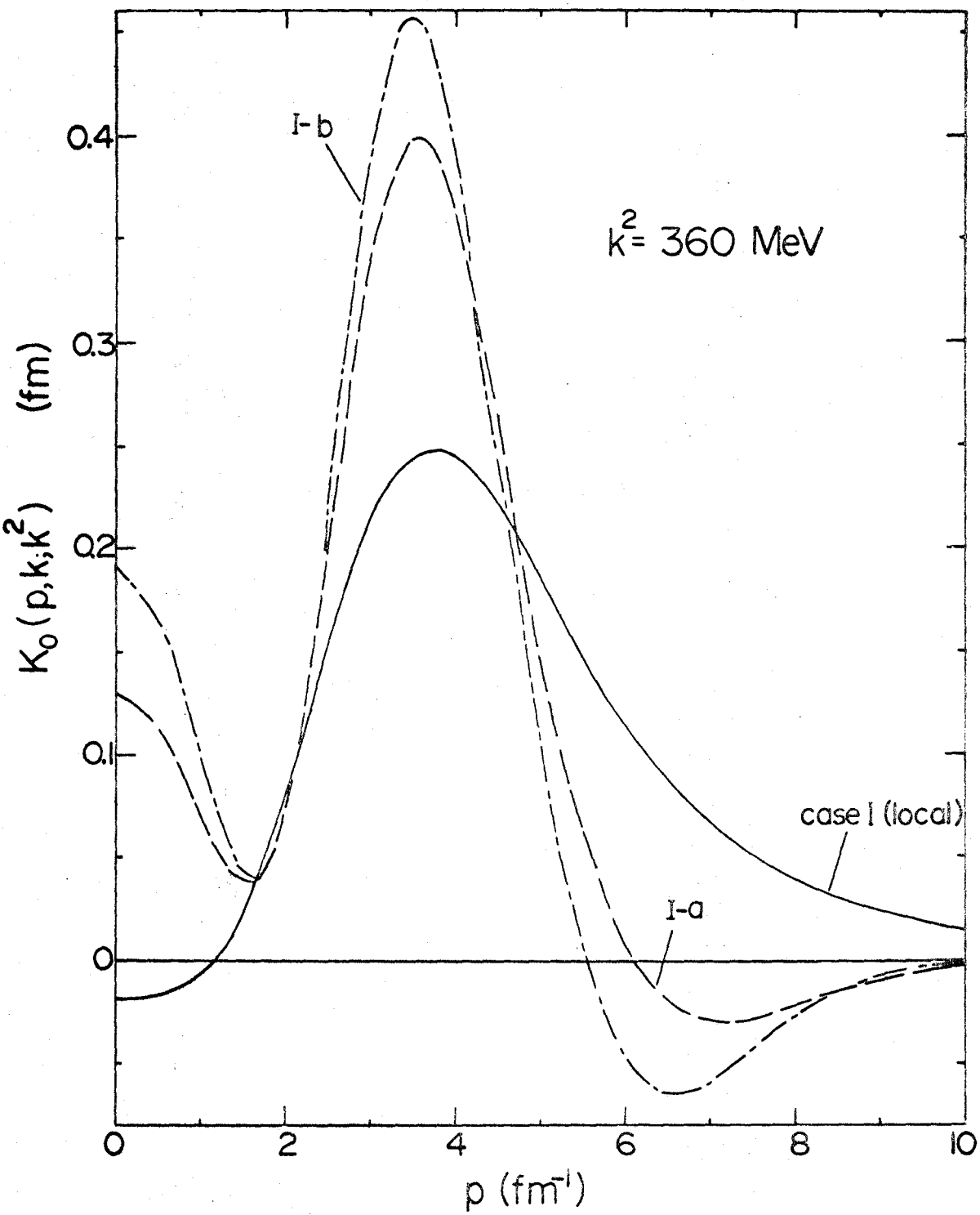

Figure 24(iii)

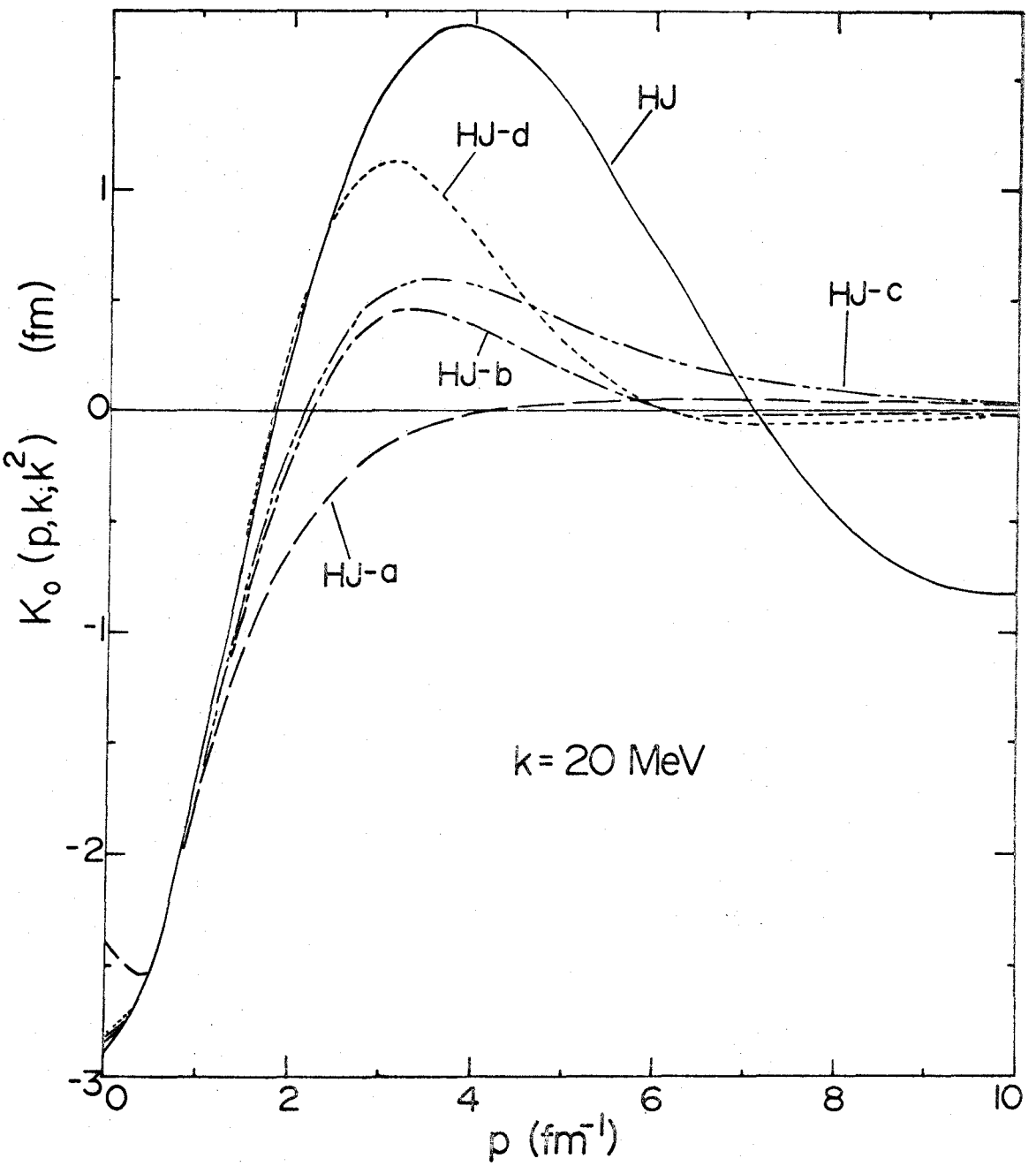

Figure 25(i)

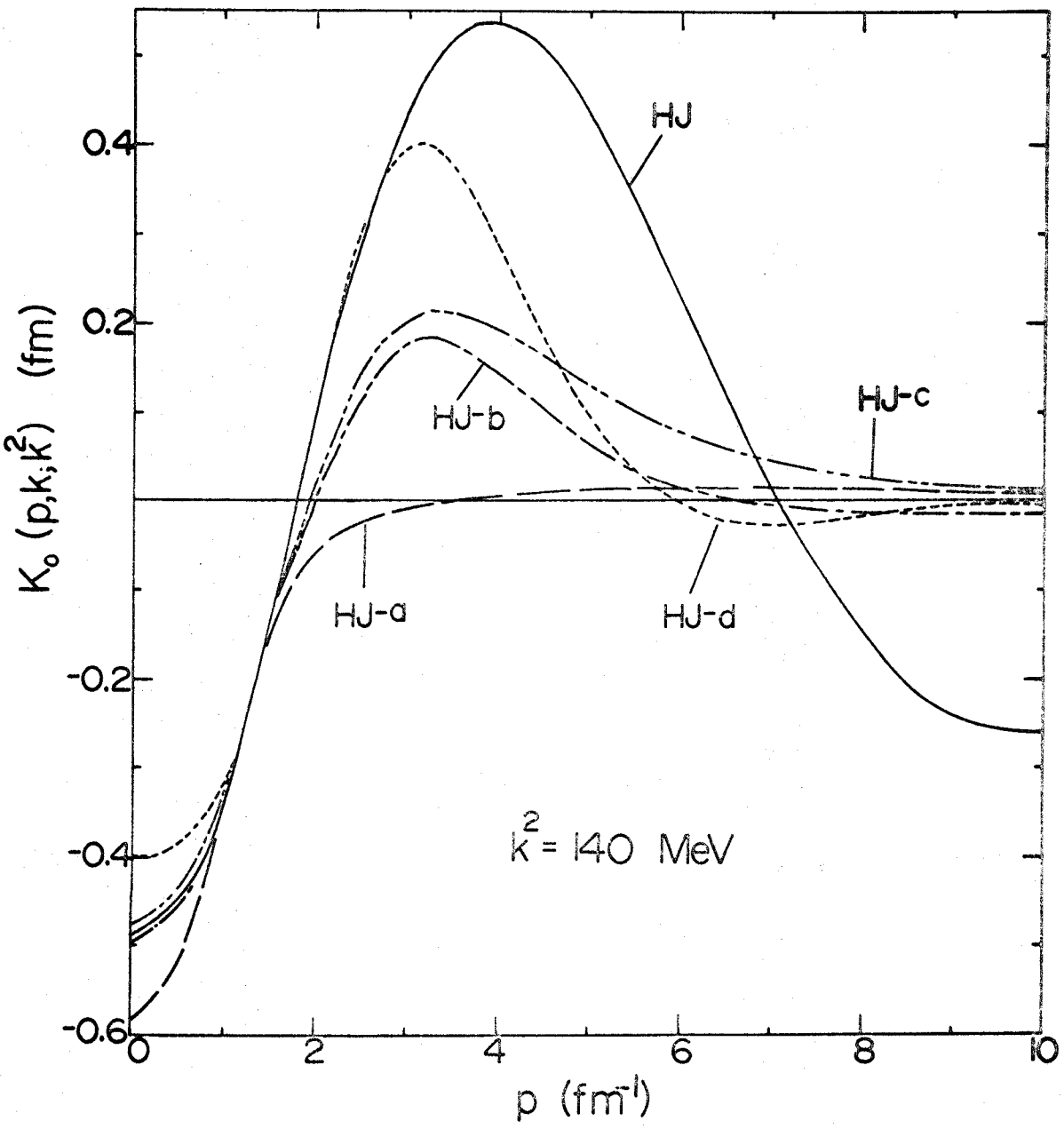
HJ
HJ-b
HJ-c
HJ-a
HJ-d
k^2 = 140 MeV
$K_o(p,k;k^2)$ (fm)
p (fm^{-1})
0.4
0.2
-0.2
-0.4
-0.6
0
2
4
6
8
10

Figure 25(ii)

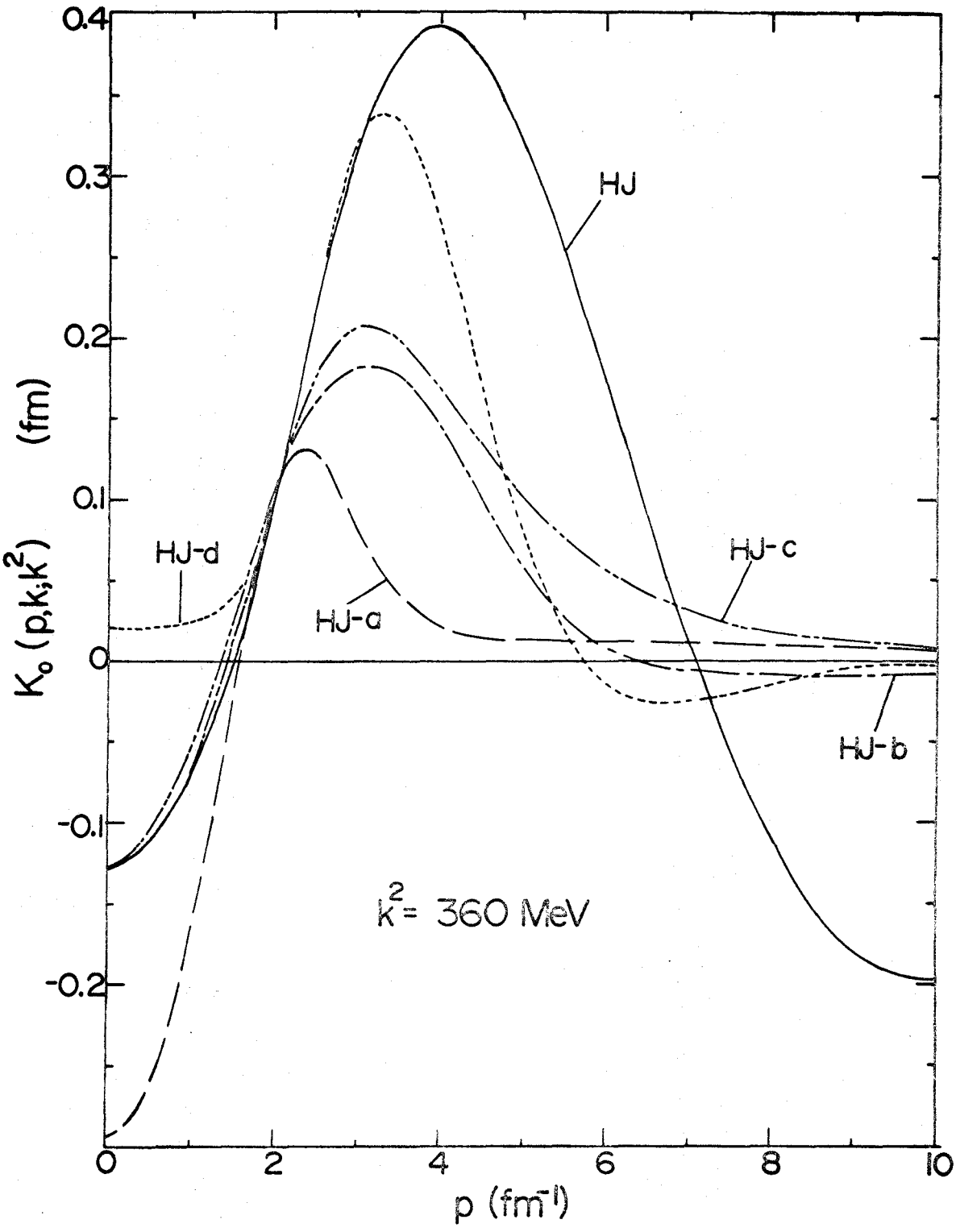

Figure 25(iii)

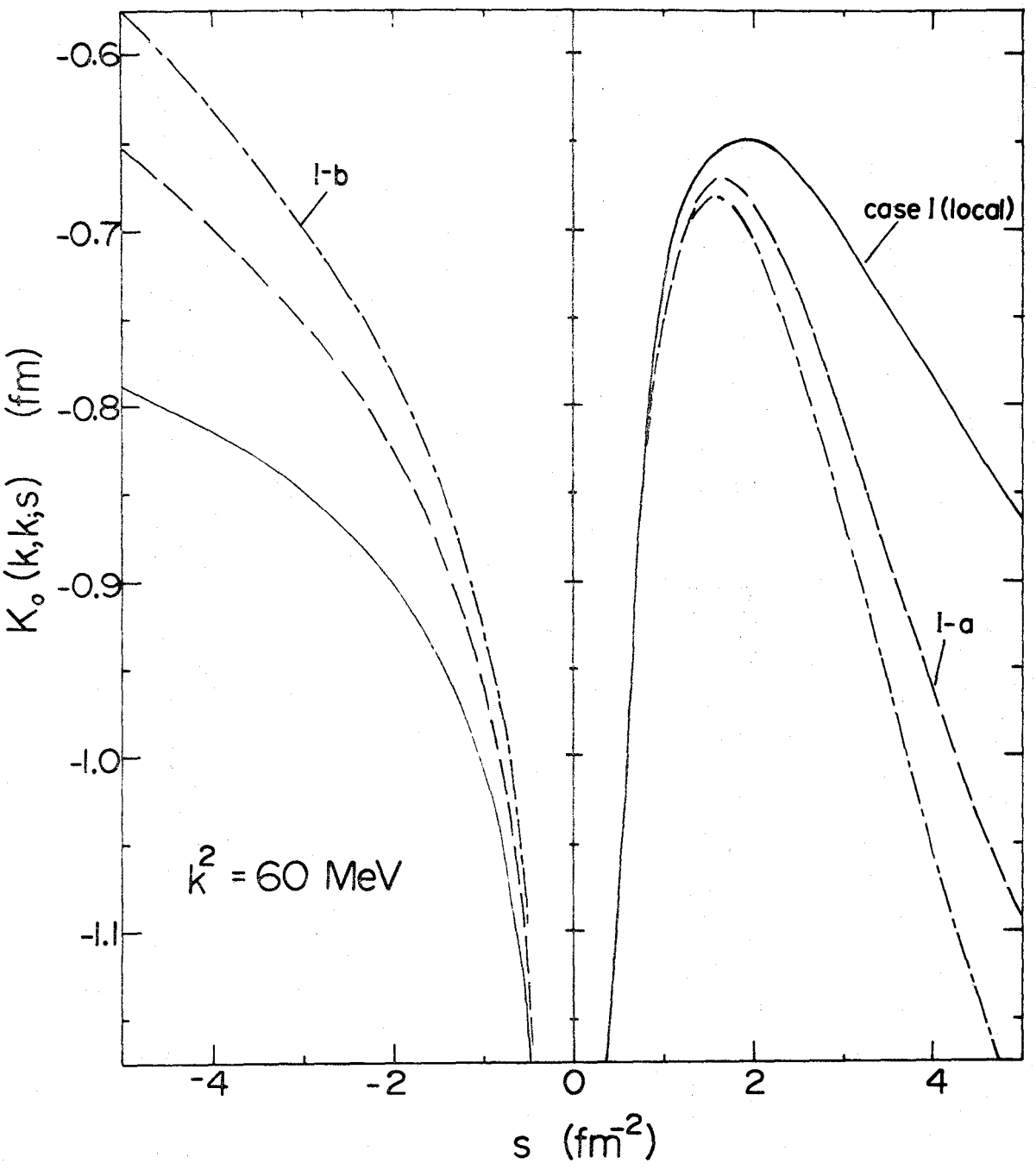

Figure 26

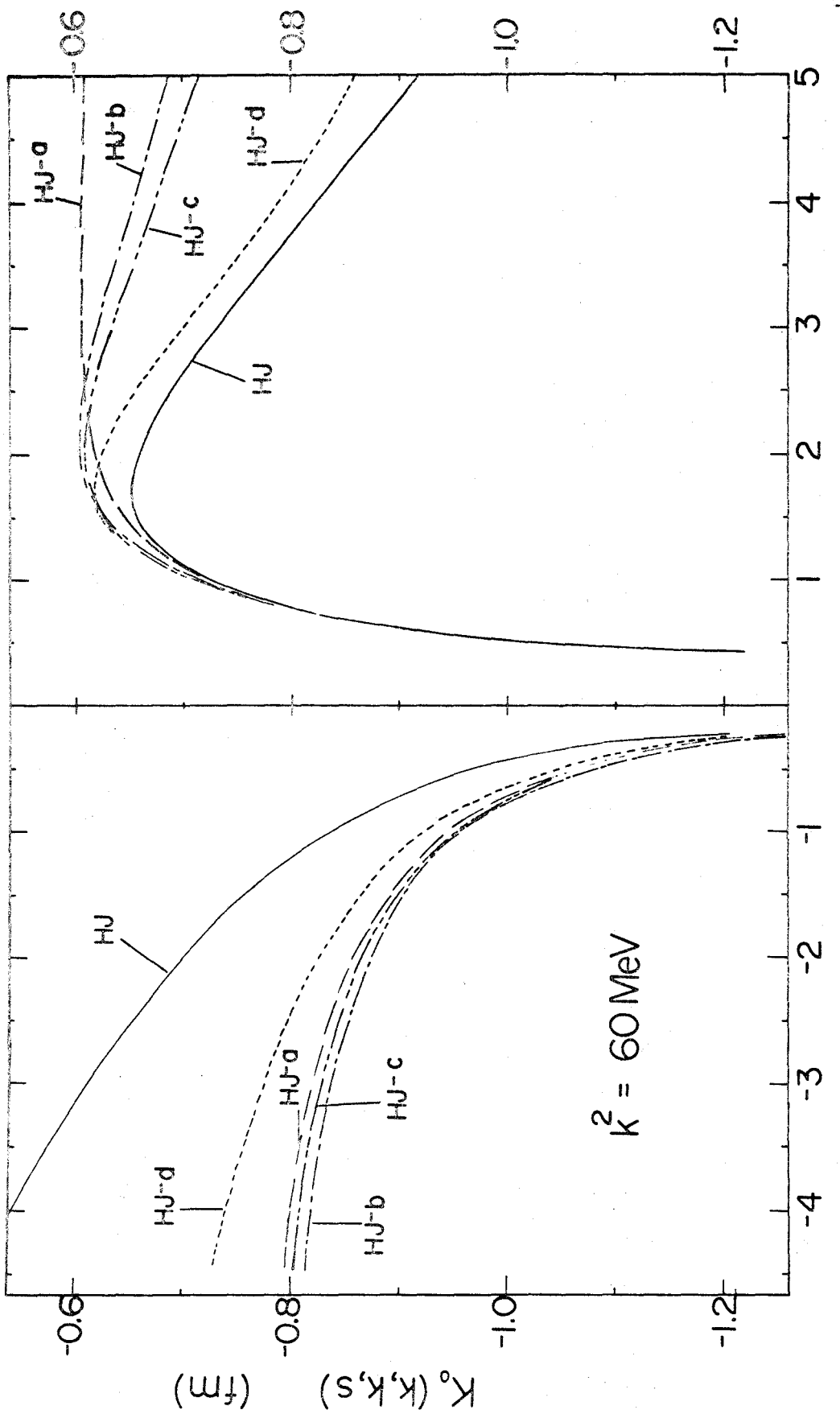
HJ-a
HJ-b
HJ-c
HJ-d
HJ
-0.6
-0.8
-1.0
-1.2
1
2
3
4
5
HJ
HJ-d
HJ-a
HJ-c
HJ-b
k^2 = 60 MeV
-1
-2
-3
-4
$K_0(k,k,s)$ (fm)
s (fm^{-2})

Figure 27

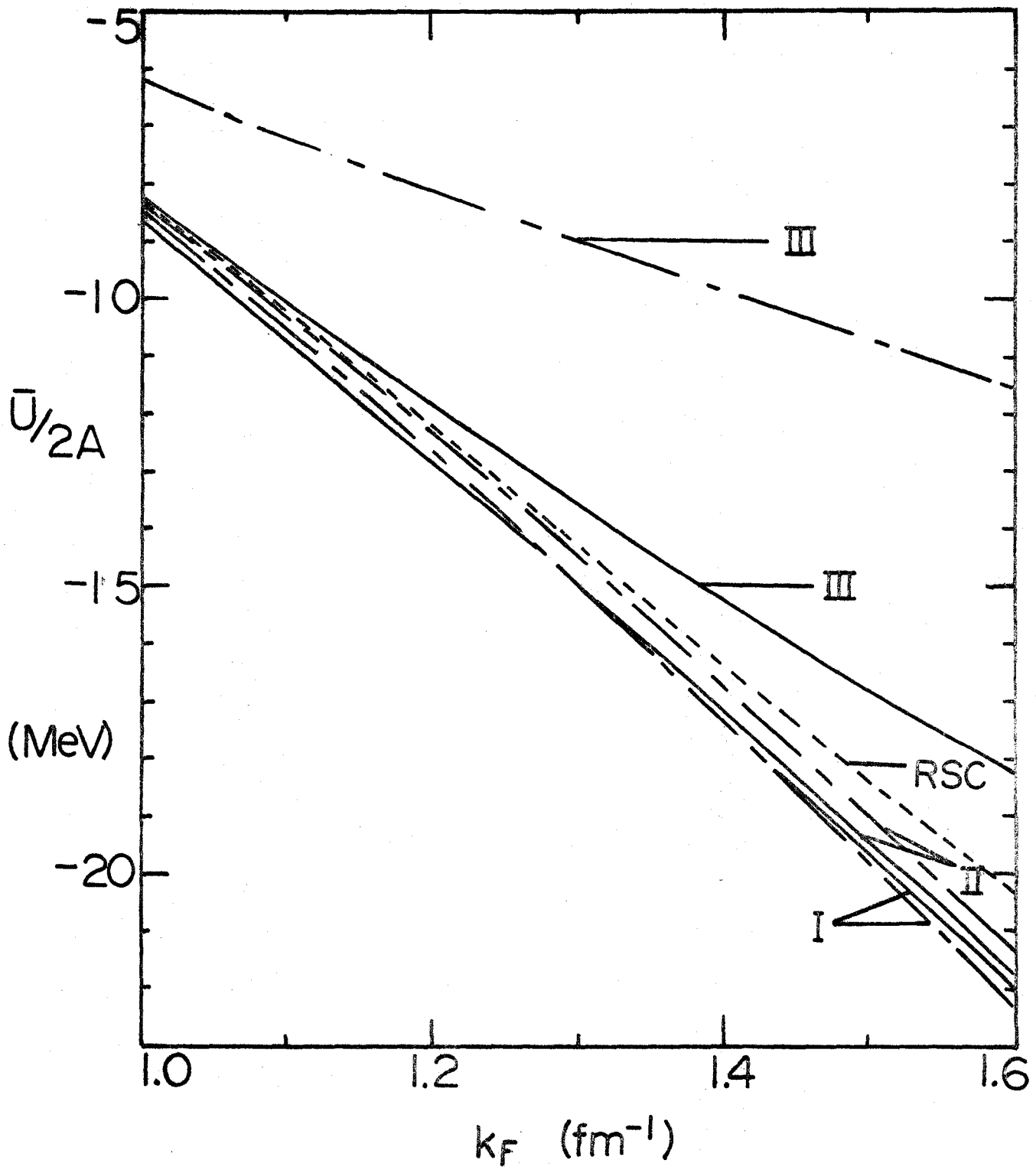

Figure 28

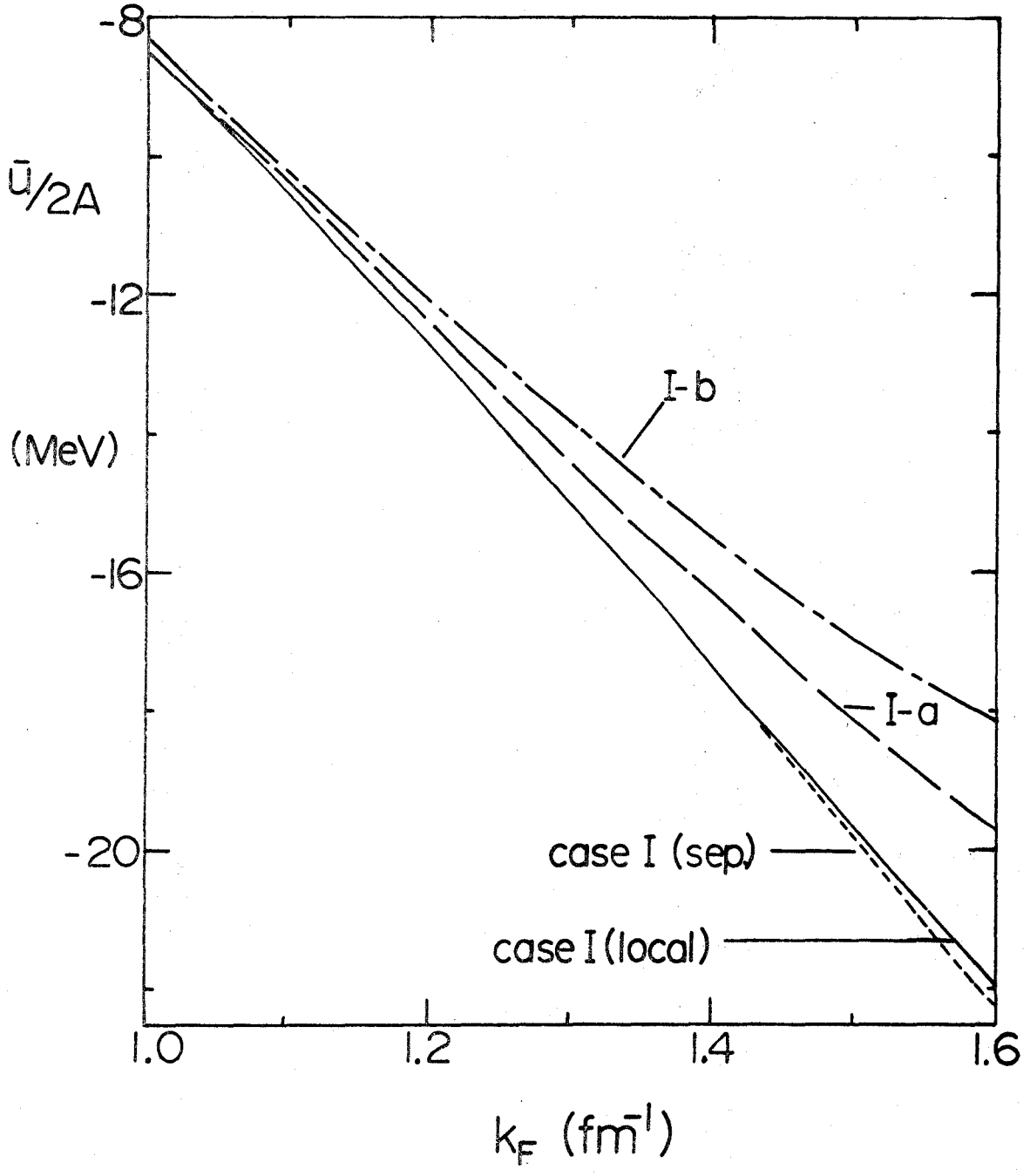

Figure 29

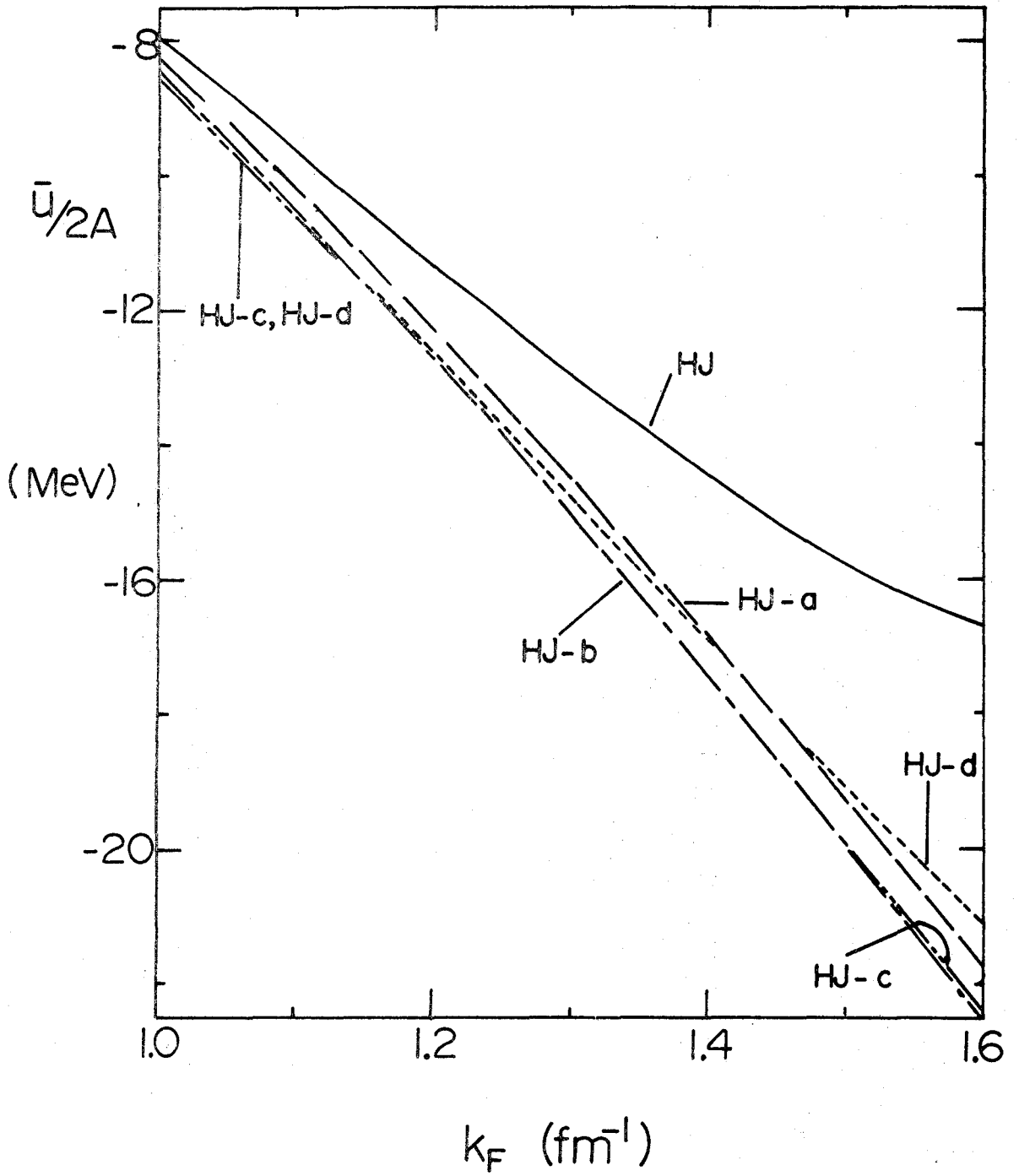

Figure 30

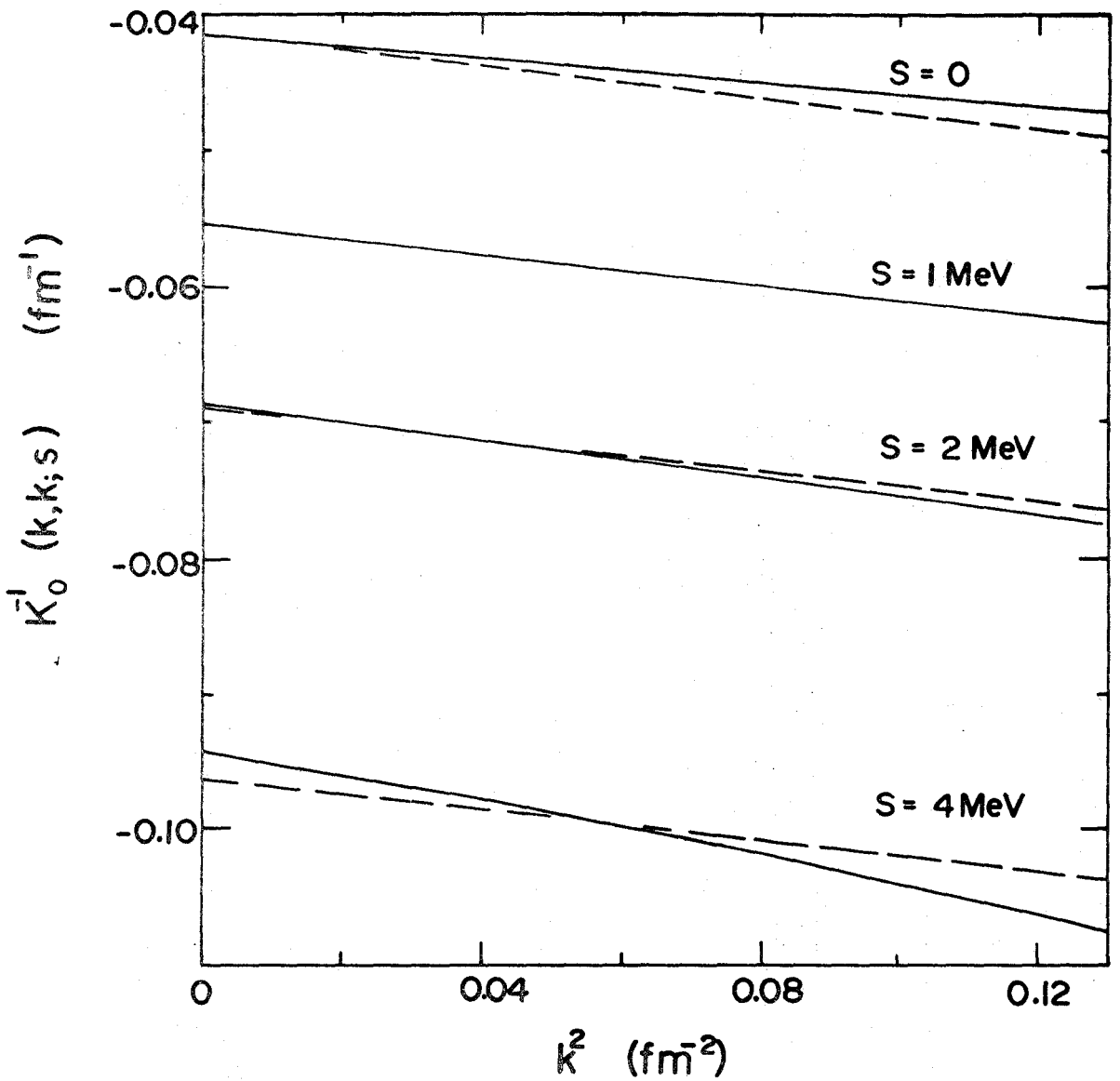
-0.04
-0.06
-0.08
-0.10
S = 0
S = 1 MeV
S = 2 MeV
S = 4 MeV
$K_0^{-1}(k,k;s)$ (fm^{-1})
0
0.04
0.08
0.12
k^2 (fm^{-2})

Figure 31

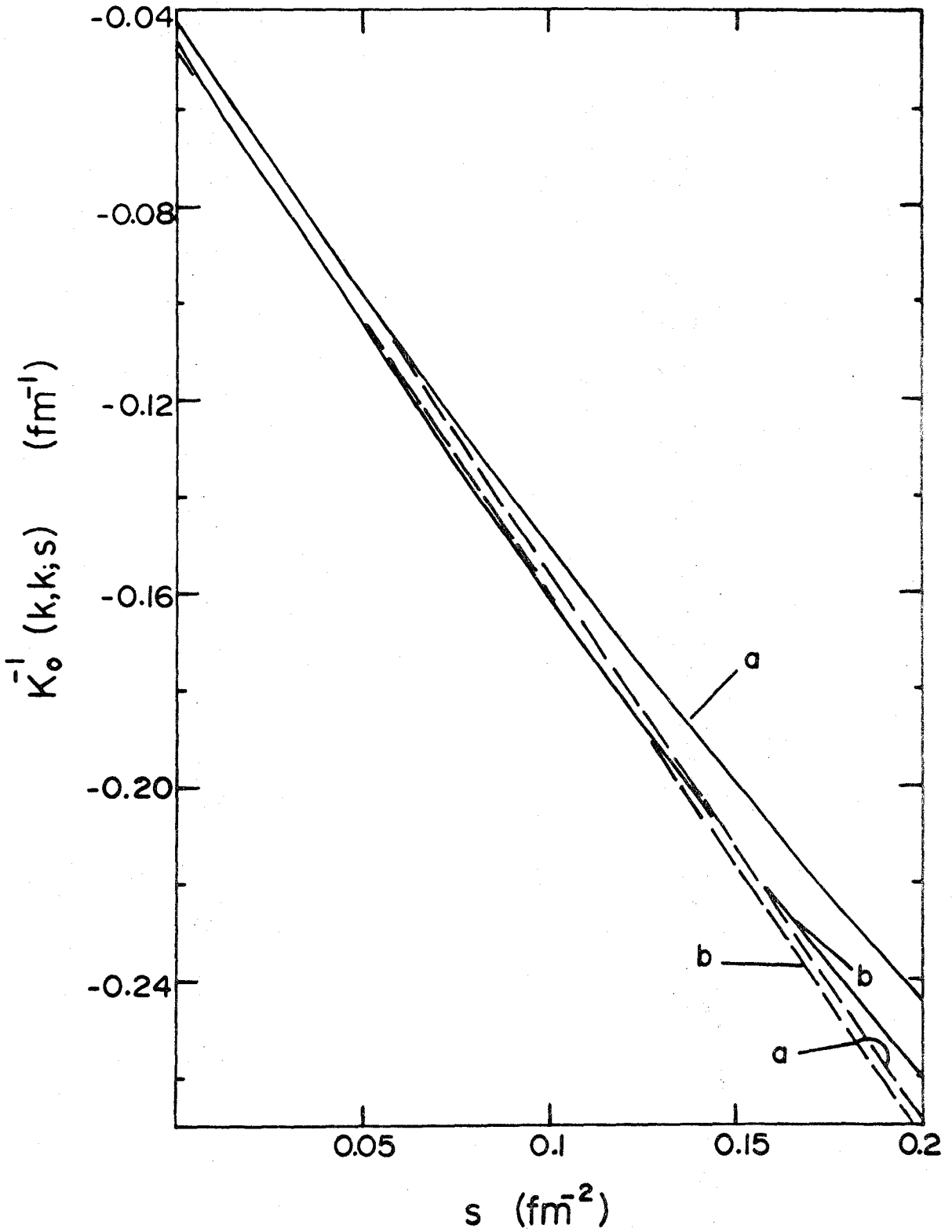

Figure 32

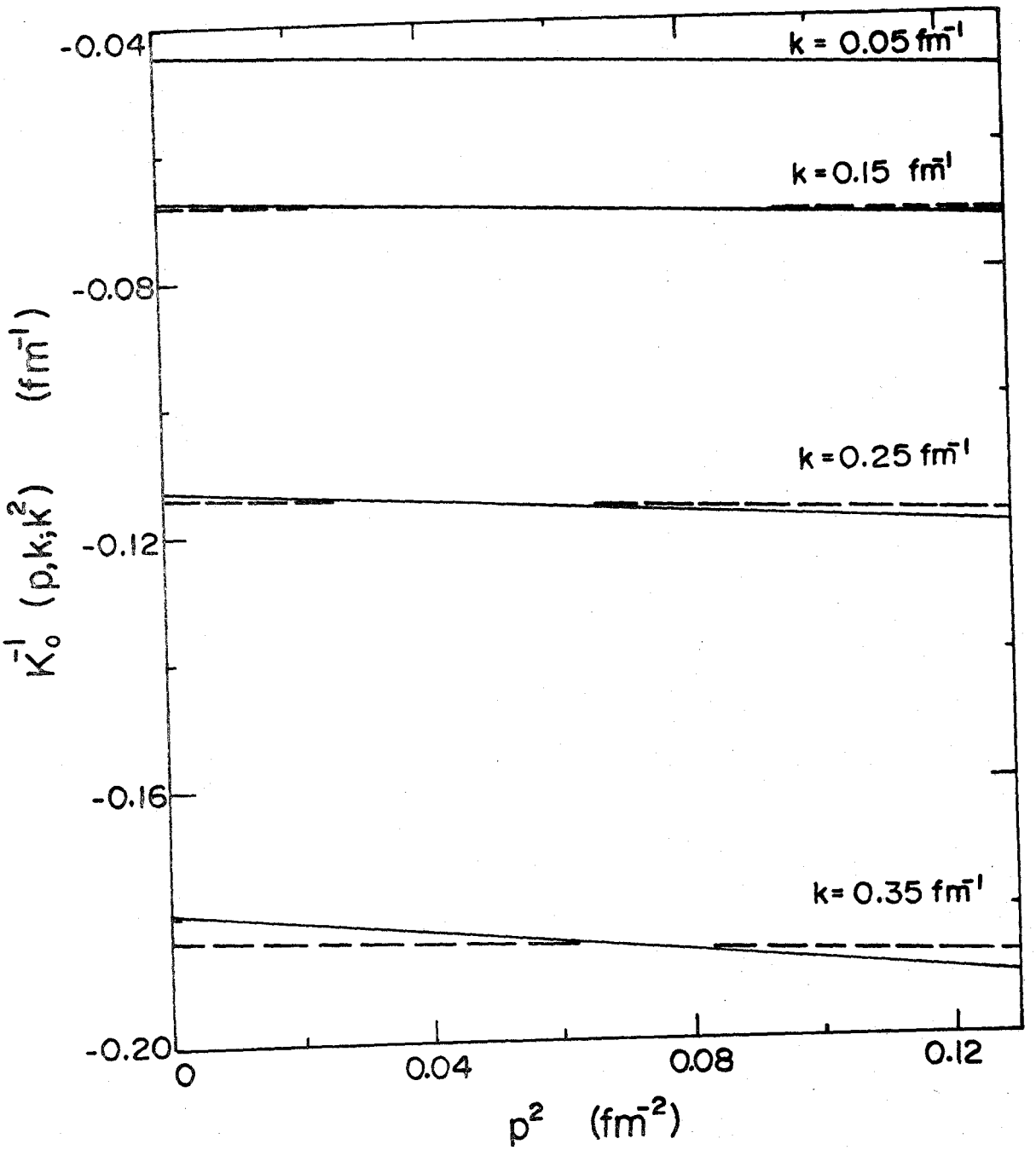
k = 0.05 fm⁻¹
k = 0.15 fm⁻¹
k = 0.25 fm⁻¹
k = 0.35 fm⁻¹
-0.04
-0.08
-0.12
-0.16
-0.20
0
0.04
0.08
0.12
$K_o^{-1}(p,k;k^2)$ (fm⁻¹)
p^2 (fm⁻²)

Figure 33